ISSN 2149-8695

www.oftalmoloji.org

TURKISH JOURNAL OF OPHTHALMOLOGY

TJO

Turkish Journal of Ophthalmology

Vol: 47 Issue: 5 September-October 2017 Page: 249-308

Original Articles

Review

Case Reports

galenos

September
October
2017
47 Volume
Issue 5

TURKISH JOURNAL OF OPHTHALMOLOGY

TJO

www.oftalmoloji.org

Publishing House
Molla Gürani Mah. Kaçamak Sokak No: 21,
34093 Fındıkzade-İstanbul-Turkey
Phone: +90 212 621 99 25 **Fax:** +90 212 621 99 27
E-mail: info@galenos.com.tr
Printed at: Bizim Basım Limited Şirketi
Litros yolu 2. Matbaacılar Sitesi ZD1 Topkapı -İstanbul
Phone: +90 212 709 75 25 **Fax:** +90 212 709 75 30
Date of printing: October 2017
International scientific journal published bimonthly.
ISSN: 2149-8695 **E-ISSN:** 2149-8709

The Turkish Journal of Ophthalmology is an official journal of the Turkish Ophthalmological Association.
On Behalf of Turkish Ophthalmological Association Owner
T. Reha Ersöz,
Çukurova University Faculty of Medicine, Department of Ophthalmology, Adana, Turkey

TURKISH JOURNAL OF OPHTHALMOLOGY

TJO

www.oftalmoloji.org

ABOUT US

The Turkish Journal of Ophthalmology (TJO) is the only scientific periodical publication of the Turkish Ophthalmological Association and has been published since January 1929. In its early years, the journal was published in Turkish and French. Although there were temporary interruptions in the publication of the journal due to various challenges, the Turkish Journal of Ophthalmology has been published continually from 1971 to the present.

The Turkish Journal of Ophthalmology is currently published in Turkish and English languages. TJO is an independent international periodical journal based on single-blind peer-review principle. TJO is regularly published six times a year and special issues are occasionally released. The aim of TJO is to publish original research papers of the highest scientific and clinical value at an international level. Furthermore, review articles, case reports, editorial comments, letters to the editor, educational contributions and congress/meeting announcements are released.

The target audience includes specialists and physicians in training in ophthalmology in all relevant disciplines.

The editorial policies are based on the "Recommendations for the Conduct, Reporting, Editing, and Publication of Scholarly Work in Medical Journals (ICMJE Recommendations)" by the International Committee of Medical Journal Editors (2013, archived at http://www.icmje.org/) rules.

The Turkish Journal of Ophthalmology is indexed in the **PubMed Central (PMC), Web of Science-Emerging Sources Citation Index (ESCI), Directory of Open Access Journals (DOAJ), Gale/Cengage Learning, Index Copernicus, EBSCO Database, Scopus, Turkish Medline-National Citation Index, Turk Medline, Cinahl, Proquest, TUBITAK/ULAKBIM and Turkish Citation Index** databases.

Open Access Policy

This journal provides immediate open access to its content on the principle that making research freely available to the public supports a greater global exchange of knowledge.

Open Access Policy is based on the rules of the Budapest Open Access Initiative (BOAI) http://www.budapestopenaccessinitiative.org/. By "open access" to peer-reviewed research literature, we mean its free availability on the public internet, permitting any users to read, download, copy, distribute, print, search, or link to the full texts of these articles, crawl them for indexing, pass them as data to software, or use them for any other lawful purpose, without financial, legal, or technical barriers other than those inseparable from gaining access to the internet itself. The only constraint on reproduction and distribution, and the only role for copyright in this domain, should be to give authors control over the integrity of their work and the right to be properly acknowledged and cited.

Subscription Information

TJO is sent free of charge to subscribers. Address changes should be immediately reported to the affiliates and to the managing editor. Subscribers who do not receive the journal in the relevant time period should contact the managing editor. All published volumes in full text can be reached free of charge through the website www.oftalmoloji.org. Requests for subscription should be addressed to the Turkish Ophthalmological Association.

Manuscripts can only be submitted electronically through the Journal Agent website (http://journalagent.com/tjo/) after creating an account. This system allows online submission and review.

Membership Procedures

Turkish Ophthalmological Association
Bank Account: Yapı Kredi Bankası, Şehremini Şubesi 65774842
IBAN: TR10 0006 7010 0000 0065 7748 42
Annual Subscription: Domestic: 100.-TL (Tax Incl)
Abroad: 100 USD (Tax Incl.)

Correspondence Address

Editor-in-Chief, Murat İrkeç, MD, Professor in Ophthalmology
Hacettepe University Faculty of Medicine, Department of Ophthalmology
06100 Sıhhiye-Ankara-Turkey
Phone: +90 212 801 44 36/37 Fax: +90 212 801 44 39
E-mail: mirkec@hacettepe.edu.tr

Secretary, Arzu Sevdasız

E-mail: dergi@oftalmoloji.org - sekreter@oftalmoloji.org
Address: Avrupa Konutları Kale, Maltepe Mah. Yedikule Çırpıcı Yolu Sk. 9. Blok No: 2 Kat:1 Ofis:1 Zeytinburnu-İstanbul-Turkey
Phone: +90 212 801 44 36/37 Fax: +90 212 801 44 39
Web Page: www.oftalmoloji.org

Permissions

Requests for permission to reproduce published material should be sent to the editorial office.
Editor-in-Chief: Murat İrkeç, MD, Professor in Ophthalmology
Address: Avrupa Konutları Kale, Maltepe Mah. Yedikule Çırpıcı Yolu Sk. 9. Blok No: 2 Kat:1 Ofis:1 Zeytinburnu-İstanbul-Turkey
Phone: +90 212 801 44 36/37 Fax: +90 212 801 44 39
Web Page: www.oftalmoloji.org
E-mail: dergi@oftalmoloji.org - sekreter@oftalmoloji.org

Advertisement

Applications for advertisement should be addressed to the editorial office.
Address: Avrupa Konutları Kale, Maltepe Mah. Yedikule Çırpıcı Yolu Sk. 9. Blok No: 2 Kat:1 Ofis:1 Zeytinburnu-İstanbul-Turkey
Phone: +90 212 801 44 36/37 Fax: +90 212 801 44 39
Web Page: www.oftalmoloji.org
E-mail: dergi@oftalmoloji.org - sekreter@oftalmoloji.org

Publisher Corresponding Address

Publisher: Erkan Mor
Galenos Yayınevi Tic. Ltd. Şti.
Address: Molla Gürani Mah. Kaçamak Sk. No: 21, 34093 Fındıkzade-İstanbul-Turkey
Phone: +90 212 621 99 25 Fax: +90 212 621 99 27
E-mail: info@galenos.com.tr

Instructions for Authors

Instructions for authors are published in the journal and on the website www.oftalmoloji.org

Material Disclaimer

The author(s) is (are) responsible for the articles published in the Turkish Journal of Ophthalmology.
The editor, editorial board and publisher do not accept any responsibility for the articles.

The journal is printed on acid-free paper.

TURKISH JOURNAL OF OPHTHALMOLOGY

TJO

www.oftalmoloji.org

INSTRUCTIONS TO AUTHORS

The Turkish Journal of Ophthalmology is an official peer-reviewed publication of the Turkish Ophthalmological Association. Accepted manuscripts are published in both Turkish and English languages.

Manuscripts written in Turkish should be in accordance with the Turkish Dictionary and Writing Guide ("Türkçe Sözlüğü ve Yazım Kılavuzu") of the Turkish Language Association. Turkish forms of ophthalmology-related terms should be checked in the TODNET Dictionary (http://www.todnet.org/sozluk/) and used accordingly.

The Turkish Journal of Ophthalmology does not charge any article submission or processing charges.

A manuscript will be considered only with the understanding that it is an original contribution that has not been published elsewhere.

Reviewed and accepted manuscripts are translated either from Turkish to English or from English to Turkish by the Journal through a professional translation service. Prior to printing, the translations are submitted to the authors for approval or correction requests, to be returned within 7 days. If no response is received from the corresponding author within this period, the translation is checked and approved by the editorial board.

The abbreviation of the Turkish Journal of Ophthalmology is TJO, however, it should be denoted as Turk J Ophthalmol when referenced. In the international index and database, the name of the journal has been registered as Turkish Journal of Ophthalmology and abbreviated as Turk J Ophthalmol.

The scientific and ethical liability of the manuscripts belongs to the authors and the copyright of the manuscripts belongs to the Turkish Journal of Ophthalmology. Authors are responsible for the contents of the manuscript and accuracy of the references.

All manuscripts submitted for publication must be accompanied by the Copyright Transfer Form. Once this form, signed by all the authors, has been submitted, it is understood that neither the manuscript nor the data it contains have been submitted elsewhere or previously published and authors declare the statement of scientific contributions and responsibilities of all authors.

All manuscripts submitted to the Turkish Journal of Ophthalmology are screened for plagiarism using the 'iThenticate' software. Results indicating plagiarism may result in manuscripts being returned or rejected.

Experimental, clinical and drug studies requiring approval by an ethics committee must be submitted to the Turkish Journal of Ophthalmology with an ethics committee approval report confirming that the study was conducted in accordance with international agreements and the Declaration of Helsinki (revised 2013) (https://www.wma.net/policies-post/wma-declaration-of-helsinki-ethical-principles-for-medical-research-involving-human-subjects/). The approval of the ethics committee and the fact that informed consent was given by the patients should be indicated in the Materials and Methods section. In experimental animal studies, the authors should indicate that the procedures followed were in accordance with animal rights as per the Guide for the Care and Use of Laboratory Animals (http://oacu.od.nih.gov/regs/guide/guide.pdf) and they should obtain animal ethics committee approval.

Authors must provide disclosure/acknowledgment of financial or material support, if any was received, for the current study.

If the article includes any direct or indirect commercial links or if any institution provided material support to the study, authors must state in the cover letter that they have no relationship with the commercial product, drug, pharmaceutical company, etc. concerned; or specify the type of relationship (consultant, other agreements), if any.

Authors must provide a statement on the absence of conflicts of interest among the authors and provide authorship contributions.

The Turkish Journal of Ophthalmology is an independent international journal based on single-blind peer-review principles. The manuscript is assigned to the Editor-in-Chief, who reviews the manuscript and makes an initial decision based on manuscript quality and editorial priorities. Manuscripts that pass initial evaluation are sent for external peer review, and the Editor-in-Chief assigns an Associate Editor. The Associate Editor sends the manuscript to three reviewers (internal and/or external reviewers). The reviewers must review the manuscript within 21 days. The Associate Editor recommends a decision based on the reviewers' recommendations and returns the manuscript to the Editor-in-Chief. The Editor-in-Chief makes a final decision based on editorial priorities, manuscript quality, and reviewer recommendations. If there are any conflicting recommendations from reviewers, the Editor-in-Chief can assign a new reviewer.

The scientific board guiding the selection of the papers to be published in the Journal consists of elected experts of the Journal and if necessary, selected from national and international authorities. The Editor-in-Chief, Associate Editors, biostatistics expert and English language consultant may make minor corrections to accepted manuscripts that do not change the main text of the paper.

In case of any suspicion or claim regarding scientific shortcomings or ethical infringement, the Journal reserves the right to submit the manuscript to the supporting institutions or other authorities for investigation. The Journal accepts the responsibility of initiating action but does not undertake any responsibility for an actual investigation or any power of decision.

The Editorial Policies and General Guidelines for manuscript preparation specified below are based on "Recommendations for the Conduct, Reporting, Editing, and Publication of Scholarly Work in Medical Journals (ICMJE Recommendations)" by the International Committee of Medical Journal Editors (2016, archived at http://www.icmje.org/).

Preparation of research articles, systematic reviews and meta-analyses must comply with study design guidelines:

CONSORT statement for randomized controlled trials (Moher D, Schultz KF, Altman D, for the CONSORT Group. The CONSORT statement revised recommendations for improving the quality of reports of parallel group randomized trials. JAMA 2001; 285: 1987-91) (http://www.consort-statement.org/);

PRISMA statement of preferred reporting items for systematic reviews and meta-analyses (Moher D, Liberati A, Tetzlaff J, Altman DG, The PRISMA Group. Preferred Reporting Items for Systematic Reviews and Meta-Analyses: The PRISMA Statement. PLoS Med 2009; 6(7): e1000097.) (http://www.prisma-statement.org/);

STARD checklist for the reporting of studies of diagnostic accuracy (Bossuyt PM, Reitsma JB, Bruns DE, Gatsonis CA, Glasziou PP, Irwig LM, et al., for the STARD Group. Towards complete and accurate reporting of studies of diagnostic accuracy: the STARD initiative. Ann Intern Med 2003;138:40-4.) (http://www.stard-statement.org/);

STROBE statement, a checklist of items that should be included in reports of observational studies (http://www.strobe-statement.org/);

MOOSE guidelines for meta-analysis and systemic reviews of observational studies (Stroup DF, Berlin JA, Morton SC, et al. Meta-analysis of observational studies in epidemiology: a proposal for reporting Meta-analysis of observational Studies in Epidemiology (MOOSE) group. JAMA 2000; 283: 2008-12).

GENERAL GUIDELINES

Manuscripts can only be submitted electronically through the Journal Agent website (http://journalagent.com/tjo/) after creating an account. This system allows online submission and review.

The manuscripts are archived according to ICMJE, Index Medicus (Medline/PubMed) and Ulakbim-Turkish Medicine Index Rules.

Format: Manuscripts should be prepared using Microsoft Word, size A4 with 2.5 cm margins on all sides, 12 pt Arial font and 1.5 line spacing.

Abbreviations: Abbreviations should be defined at first mention and used consistently thereafter. Internationally accepted abbreviations should be used; refer to scientific writing guides as necessary.

Cover letter: The cover letter should include statements about manuscript type, single-journal submission affirmation, conflict of interest statement, sources of outside funding, equipment (if applicable), approval of language for articles in English and approval of statistical analysis for original research articles.

REFERENCES

Authors are solely responsible for the accuracy of all references.

In-text citations: References should be indicated as a superscript immediately after the period/full stop of the relevant sentence. If the author(s) of a reference is/are indicated at the beginning of the sentence, this reference should be written as a superscript immediately after the author's name. If relevant research has been conducted in Turkey or by Turkish investigators, these studies should be given priority while citing the literature.

Presentations presented in congresses, unpublished manuscripts, theses, Internet addresses, and personal interviews or experiences should not be indicated as references. If such references are used, they should be indicated in parentheses at the end of the relevant sentence in the text, without reference number and written in full, in order to clarify their nature.

References section: References should be numbered consecutively in the order in which they are first mentioned in the text. All authors should be listed regardless of number. The titles of journals should be abbreviated according to the style used in the Index Medicus.

Reference Format

Journal: Last name(s) of the author(s) and initials, article title, publication title and its original abbreviation, publication date, volume, the inclusive page numbers. Example: Collin JR, Rathbun JE. Involutional entropion: a review with evaluation of

a procedure. Arch Ophthalmol. 1978;96:1058-1064.
Book: Last name(s) of the author(s) and initials, chapter title, book editors, book title, edition, place of publication, date of publication and inclusive page numbers of the extract cited.
Example: Herbert L. The Infectious Diseases (1st ed). Philadelphia; Mosby Harcourt; 1999:11;1-8.
Book Chapter: Last name(s) of the author(s) and initials, chapter title, book editors, book title, edition, place of publication, date of publication and inclusive page numbers of the cited piece.
Example: O'Brien TP, Green WR. Periocular Infections. In: Feigin RD, Cherry JD, eds. Textbook of Pediatric Infectious Diseases (4th ed). Philadelphia; W.B. Saunders Company;1998:1273-1278.
Books in which the editor and author are the same person: Last name(s) of the author(s) and initials, chapter title, book editors, book title, edition, place of publication, date of publication and inclusive page numbers of the cited piece.
Example: Solcia E, Capella C, Kloppel G. Tumors of the exocrine pancreas. In: Solcia E, Capella C, Kloppel G, eds. Tumors of the Pancreas. 2nd ed. Washington: Armed Forces Institute of Pathology; 1997:145-210.

TABLES, GRAPHICS, FIGURES, AND IMAGES

All visual materials together with their legends should be located on separate pages that follow the main text.
Images: Images (pictures) should be numbered and include a brief title. Permission to reproduce pictures that were published elsewhere must be included. All pictures should be of the highest quality possible, in
JPEG format, and at a minimum resolution of 300 dpi.
Tables, Graphics, Figures: All tables, graphics or figures should be enumerated according to their sequence within the text and a brief descriptive caption should be written. Any abbreviations used should be defined in the accompanying legend. Tables in particular should be explanatory and facilitate readers' understanding of the manuscript, and should not repeat data presented in the main text.

BIOSTATISTICS

To ensure controllability of the research findings, the study design, study sample, and the methodological approaches and applications should be explained and their sources should be presented.
The "P" value defined as the limit of significance along with appropriate indicators of measurement error and uncertainty (confidence interval, etc.) should be specified. Statistical terms, abbreviations and symbols used in the article should be described and the software used should be defined. Statistical terminology (random, significant, correlation, etc.) should not be used in non-statistical contexts.
All results of data and analysis should be presented in the Results section as tables, figures and graphics; biostatistical methods used and application details should be presented in the Materials and Methods section or under a separate title.

MANUSCRIPT TYPES

Original Articles

Clinical research should comprise clinical observation, new techniques or laboratories studies. Original research articles should include title, structured abstract, keywords relevant to the content of the article, introduction, materials and methods, results, discussion, study limitations, conclusion, references, tables/figures/images and acknowledgement sections. Title, abstract and key words should be written in both Turkish and English. The manuscript should be formatted in accordance with the above-mentioned guidelines and should not exceed sixteen A4 pages.
Title Page: This page should include the title of the manuscript, short title, name(s) of the authors and author information. The following descriptions should be stated in the given order:
1. Title of the manuscript (Turkish and English), as concise and explanatory as possible, including no abbreviations, up to 135 characters
2. Short title (Turkish and English), up to 60 characters
3. Name(s) and surname(s) of the author(s) (without abbreviations and academic titles) and affiliations
4. Name, address, e-mail, phone and fax number of the corresponding author
5. The place and date of scientific meeting in which the manuscript was presented and its abstract published in the abstract book, if applicable
Abstract: A summary of the manuscript should be written in both Turkish and English. References should not be cited in the abstract. Use of abbreviations should be avoided as much as possible; if any abbreviations are used, they must be taken into consideration independently of the abbreviations used in the text. For original articles, the structured abstract should include the following sub-headings:
Objectives: The aim of the study should be clearly stated.
Materials and Methods: The study and standard criteria used should be defined; it should also be indicated whether the study is randomized or not, whether it is retrospective or prospective, and the statistical methods applied should be indicated, if applicable.
Results: The detailed results of the study should be given and the statistical significance level should be indicated.
Conclusion: Should summarize the results of the study, the clinical applicability of the results should be defined, and the favorable and unfavorable aspects should be declared.
Keywords: A list of minimum 3, but no more than 5 key words must follow the abstract. Key words in English should be consistent with "Medical Subject Headings (MESH)" (www.nlm.nih.gov/mesh/MBrowser.html). Turkish key words should be direct translations of the terms in MESH.
Original research articles should have the following sections:
Introduction: Should consist of a brief explanation of the topic and indicate the objective of the study, supported by information from the literature.
Materials and Methods: The study plan should be clearly described, indicating whether the study is randomized or not, whether it is retrospective or prospective, the number of trials, the characteristics, and the statistical methods used.
Results: The results of the study should be stated, with tables/figures given in numerical order; the results should be evaluated according to the statistical analysis methods applied. See General Guidelines for details about the preparation of visual material.
Discussion: The study results should be discussed in terms of their favorable and unfavorable aspects and they should be compared with the literature. The conclusion of the study should be highlighted.
Study Limitations: Limitations of the study should be discussed. In addition, an evaluation of the implications of the obtained findings/results for future research should be outlined.
Conclusion: The conclusion of the study should be highlighted.
Acknowledgements: Any technical or financial support or editorial contributions (statistical analysis, English/Turkish evaluation) towards the study should appear at the end of the article.
References: Authors are responsible for the accuracy of the references. See General Guidelines for details about the usage and formatting required.

Case Reports

Case reports should present cases which are rarely seen, feature novelty in diagnosis and treatment, and contribute to our current knowledge. The first page should include the title in Turkish and English, an unstructured summary not exceeding 150 words, and key words. The main text should consist of introduction, case report, discussion and references. The entire text should not exceed 5 pages (A4, formatted as specified above).

Review Articles

Review articles can address any aspect of clinical or laboratory ophthalmology. Review articles must provide critical analyses of contemporary evidence and provide directions of current or future research. Most review articles are commissioned, but other review submissions are also welcome. Before sending a review, discussion with the editor is recommended.
Reviews articles analyze topics in depth, independently and objectively. The first chapter should include the title in Turkish and English, an unstructured summary and key words. Source of all citations should be indicated. The entire text should not exceed 25 pages (A4, formatted as specified above).

Letters to the Editor

Letters to the Editor should be short commentaries related to current developments in ophthalmology and their scientific and social aspects, or may be submitted to ask questions or offer further contributions in response to work that has been published in the Journal. Letters do not include a title or an abstract; they should not exceed 1,000 words and can have up to 5 references.

CORRESPONDENCE

All correspondence should be directed to the TJO editorial board:

Post: Turkish Ophthalmological Association
Adress: Avrupa Konutları Kale, Maltepe Mah. Yedikule Çırpıcı Yolu Sk. 9. Blok No: 2 Kat:1 Ofis:1 Zeytinburnu-İstanbul-Turkey
Phone: +90 212 801 44 36/37 Fax: +90 212 801 44 39
Web Page: www.oftalmoloji.org
E-mail: dergi@oftalmoloji.org / sekreter@oftalmoloji.org

TURKISH JOURNAL OF OPHTHALMOLOGY

TJO

www.oftalmoloji.org

CONTENTS

Original Articles

Review

Case Reports

TURKISH JOURNAL OF OPHTHALMOLOGY

TJO

www.oftalmoloji.org

EDITORIAL

2017 Issue 5 at a glance:

This issue of our journal features six original articles, one review, and five case reports representing the research being conducted by Turkish ophthalmologists in order to further global scientific knowledge.

Keratoconus is a corneal pathology characterized by progressive ectasia, generally exhibiting bilateral and asymmetrical involvement. Although the progressive disease course eventually affects both eyes, initially only one eye may be affected, or another possibility is that eyes with normal clinical findings and topographic patterns in fact have subclinical keratoconus. To investigate this possibility, Aksoy et al. compared quantitative topography indices (QTIs) and corneal higher-order aberration (HOA) data from the normal eyes of unilateral keratoconus patients to those of the fellow keratoconic eye and with the normal eyes of healthy individuals. They report that compared to healthy controls, the normal eyes of unilateral keratoconus patients had significantly higher QTI and HOA values except for spherical aberration. The authors concluded that these eyes may have an early form of the disease and that evaluating QTIs and HOA data together is more useful for diagnosing subclinical keratoconus (see pages 249-254).

The second article in this issue is also related to keratoconus and evaluates the disease from a different point of view, focusing on changes in endothelial cell count and morphology of the posterior surface. Previous studies have reported a tendency toward reduced endothelial cell density (ECD) and percentage of hexagonality with disease progression, but keratoconus stage has not been shown to significantly correlate with endothelial cell morphology or ECD changes. Believing that these conflicting findings may be a result of small numbers of keratoconus patients, Bozkurt et al. aimed to investigate changes in corneal endothelial cells in the different stages of keratoconus in a larger sample population. They determined that corneal endothelial cell count decreased with progression of keratoconus and emphasized that specular/confocal microscopic examination was required in eyes with advanced keratoconus (see pages 255-260).

Eser Öztürk et al. present a study in which they determine the prevalence of vitreomacular interface (VMI) pathologies and evaluate their association with clinical findings in patients with Behçet's uveitis. They retrospectively evaluated macular optical coherence tomography (OCT) images of 160 eyes of 96 patients diagnosed with Behçet's uveitis for VMI pathologies such as posterior vitreous detachment (PVD), epiretinal membrane (ERM), vitreomacular traction (VMT), vitreomacular adhesion (VMA), full-thickness macular hole (FTMH), lamellar macular hole (LMH), and pseudohole. They found that these conditions are common among uveitis patients and increase in frequency with longer duration of uveitis. They also report that OCT is more sensitive than fundus examination in the detection of VMI pathologies in uveitis patients (see pages 261-266).

In a study seeking to answer the question of whether all retinal nerve fiber layer (RNFL) defects are glaucomatous, Gür Güngör and Akman reassessed patients initially diagnosed with glaucoma based on RNFL damage detected on OCT and found that the ocular findings of some of those patients were actually due to different conditions such as ischemic optic neuropathy, optic neuritis associated with multiple sclerosis, optic disc drusen, and pseudotumor cerebri. The authors concluded that neuroophthalmologic diseases and optic disc anomalies could also cause RNFL thinning, and state that the differential diagnosis of glaucomatous and nonglaucomatous optic neuropathies should not depend only on OCT, but requires both RNFL measurements and disc topography parameters, as well as a thorough ophthalmic examination (see pages 267-273).

Akıncıoğlu et al. evaluated the efficacy and safety of an intravitreal dexamethasone implant (OZURDEX®, Allergan, Inc., Irvine, CA, USA) in the treatment of recalcitrant diabetic macular edema and reported that although the implants were fairly effective, they cannot be recommended instead of anti-VEGF agents as a first-line treatment due to steroid-related side effects (see pages 274-278).

In the final original research article of this issue, Nalcı et al. used both OCT angiography (OCTA) and spectral domain

DOI: 10.4274/tjo.45220
Turk J Ophthalmol 2017;47:249-254

Original Article

Topography and Higher Order Corneal Aberrations of the Fellow Eye in Unilateral Keratoconus

Sibel Aksoy*, Sezen Akkaya*, Yelda Özkurt*, Sevda Kurna*, Banu Açıkalın*, Tomris Şengör**
*Fatih Sultan Mehmet Training and Research Hospital, Ophthalmology Clinic, İstanbul, Turkey
**Bilim University Faculty of Medicine, Department of Ophthalmology, İstanbul, Turkey

Abstract

Objectives: Comparison of topography and corneal higher order aberrations (HOA) data of fellow normal eyes of unilateral keratoconus patients with keratoconus eyes and control group.

Materials and Methods: The records of 196 patients with keratoconus were reviewed. Twenty patients were identified as unilateral keratoconus. The best corrected visual acuity (BCVA), topography and aberration data of the unilateral keratoconus patients' normal eyes were compared with their contralateral keratoconus eyes and with control group eyes. For statistical analysis, flat and steep keratometry values, average corneal power, cylindrical power, surface regularity index (SRI), surface asymmetry index (SAI), inferior-superior ratio (I-S), keratoconus prediction index, and elevation-depression power (EDP) and diameter (EDD) topography indices were selected.

Results: Mean age of the unilateral keratoconus patients was 26.05±4.73 years and that of the control group was 23.6±8.53 years ($p>0.05$). There was no statistical difference in BCVA between normal and control eyes ($p=0.108$), whereas BCVA values were significantly lower in eyes with keratoconus ($p=0.001$). Comparison of quantitative topographic indices between the groups showed that all indices except the I-S ratio were significantly higher in the normal group than in the control group ($p<0.05$). The most obvious differences were in the SRI, SAI, EDP, and EDD values. All topographic indices were higher in the keratoconus eyes compared to the normal fellow eyes. There was no difference between normal eyes and the control group in terms of spherical aberration, while coma, trefoil, irregular astigmatism, and total HOA values were higher in the normal eyes of unilateral keratoconus patients ($p<0.05$). All HOA values were higher in keratoconus eyes than in the control group.

Conclusion: According to our study, SRI, SAI, EDP, EDD values, and HOA other than spherical aberration were higher in the clinically and topographically normal fellow eyes of unilateral keratoconus patients when compared to a control group. This finding may be due to the mild asymmetric and morphologic changes in the subclinical stage of keratoconus leading to deterioration in the indicators of corneal irregularity and elevation changes. Therefore, these eyes may be exhibiting the early form of the disease.

Keywords: Corneal aberrations, topography, unilateral keratoconus

Address for Correspondence: Sibel Aksoy MD, Fatih Sultan Mehmet Training and Research Hospital, Ophthalmology Clinic, İstanbul, Turkey
Phone: +90 544 381 98 25 E-mail: sibelaksoymd@gmail.com **ORCID-ID:** orcid.org/0000-0003-1395-6207
Received: 19.07.2016 **Accepted:** 23.02.2017

Introduction

Keratoconus is a noninflammatory corneal disease that generally exhibits bilateral and asymmetrical involvement. It results in thinning of the corneal stroma, corneal ectasia, irregular astigmatism, and reduced vision.[1,2] The progressive course of the disease ultimately affects both eyes, though only one eye may be affected initially. The prevalence of true unilateral keratoconus has been reported to range from 0.5-4% in studies using computerized videokeratography[3,4,5,6] and was 4.5% in a more recent study using slit scanning corneal topography (Orbscan 2).[7] Holland et al.[5] reported that patients with unilateral keratoconus developed signs of keratoconus in their apparently healthy fellow eyes 4 years later, while Li et al.[8] found that keratoconus developed in 50% of cases within 16 years. Therefore, it may be concluded that the fellow eyes of patients with unilateral keratoconus may seem normal with regard to clinical and topographical patterns yet have subclinical keratoconus. While it is easy to diagnose moderate and advanced keratoconus based on typical clinical and topographical findings, the lack of definitive criteria makes it difficult to diagnose subclinical keratoconus in patients who have normal visual acuity and do not exhibit clinical findings. This is particularly important in examinations prior to refractive surgery, as ectatic corneal disorders that have not been identified before refractive surgery may result in progressive keratectasia. Placido disk-based corneal topography is one of the methods commonly used to diagnose keratoconus. Many numerical topographic indices which identify abnormalities in keratoconic cornea topography have been developed, and these indices have high sensitivity and specificity in diagnosing keratoconus.[8,9,10,11]

The anterior surface of the cornea is the most important refractive component of the eye, and high-order corneal aberrations are seen significantly more in keratoconic corneas than in normal corneas. It has been reported that considering corneal topography in combination with corneal wavefront aberrations when diagnosing keratoconus may result in higher detection rates.[12,13]

The aim of this study was to analyze the quantitative topography indices and corneal high-order aberration (HOA) data from the normal eyes of unilateral keratoconus patients and to compare them with the fellow keratoconic eye and with the normal eyes of healthy individuals.

Materials and Methods

The records of 392 eyes of 196 patients diagnosed with keratoconus in the cornea and contact lens unit of our clinic between 2008 and 2015 were retrospectively reviewed. Twenty patients with clinical and topographical keratoconus in one eye and no clinical or topographical keratoconus findings in the fellow eye were included. The eyes were divided into the unilateral keratoconus group and a normal fellow eye group. Each of the patients was diagnosed with keratoconus based on a collective assessment of refraction examination, slit-lamp anterior segment examination, and corneal topography. The normal eyes of these patients had a keratometric astigmatism below 1.5 diopter (D), vertical keratometry value below 47 D, and no keratoconus patterns such as asymmetrical bow-tie pattern, skewed axis, or localized steepening on topography. The control group consisted of the right eyes of 20 age-matched healthy individuals without any ocular pathology except for refractive errors. Patients with ocular surgery history or accompanying ocular pathology were excluded from the study.

For all patients, best corrected visual acuity (BCVA) on Snellen chart, corneal topography and corneal HOA data were recorded. Corneal topography and cornea aberration measurement results were obtained from the database of the Placido-based NIDEK Magellan Mapper (NIDEK Technologies Srl, Padova-Italy) topography system. Flat (K1) and steep (K2) keratometry values, average corneal power (ACP), cylindrical power (CYL), surface regularity index (SRI), surface asymmetry index (SAI), inferior/superior ratio (I-S), keratoconus prediction index (KPI), elevation-depression power (EDP), and elevation/depression diameter (EDD) topography indices were selected for statistical analysis. BCVA, quantitative topography indices, and HOA root mean square (RMS) values of the normal fellow eyes were compared with those of the keratoconic eyes and the control eyes.

Statistical Analysis

Statistical analysis was carried out using NCSS (Number Cruncher Statistical System) 2007 & PASS (Power Analysis and Sample Size) 2008 Statistical Software (Utah, USA) software. The study data were evaluated using descriptive statistical methods (mean, standard deviation, median) as well as independent-samples test for intergroup comparison of parameters with normal distribution and the Mann-Whitney U test for intergroup comparisons of parameters with abnormal distribution. The results were assessed within a 95% confidence interval and significance was accepted at $p<0.05$.

Results

The prevalence of unilateral keratoconus among our patient group was 11.2%. The mean age of the 20 unilateral keratoconus patients was 26.05±4.73 years, and that of the 20 individuals in the control group was 23.60±8.53 years ($p>0.05$).

BCVA was 0.47 in the keratoconus eyes, 0.97 in the normal fellow eyes, and 1.0 in the control eyes. Although K1, K2, ACP, and CYL values were only slightly higher in the normal fellow eyes when compared to the control eyes, the difference was statistically significantly ($p<0.01$). The keratoconic eyes had significantly higher K1, K2, ACP, and CYL values compared to the normal fellow eyes ($p<0.01$).

Comparison of topography indices revealed no difference in I-S between the normal and control groups ($p=0.314$), whereas SRI, SAI, KPI, EDP, and EDD values were significantly higher in the normal group compared to the control group ($p<0.01$). All topographic indices of the keratoconic eyes were significantly higher than those of the normal fellow eyes ($p<0.01$). BCVA, K1, K2, ACP, CYL, I-S, SRI, SAI, KPI, EDP, and EDD values of

Table 1. Best corrected visual acuity, K1, K2, average corneal power, cylindrical power, inferior-superior ratio, surface irregularity, surface asymmetry index, keratoconus prediction index, elevation/depression power, and elevation/depression diameter values in the study groups

	Control (n=20)	Normal fellow (n=20)	Keratoconus (n=20)
	Mean ± SD (median)	Mean ± SD (median)	Mean ± SD (median)
BCVA	1.00±0.00 (1.00)	0.97±0.05 (1.00)	0.46±0.13 (0.45)
K1 (D)	43.44±1.01	44.78±1.60	50.78±3.97
K2 (D)	42.77±0.91	43.72±1.46	46.65±2.94
ACP (D)	43.06±0.96	44.23±1.56	48.20±3.44
CYL (D)	0.67±0.42 (0.53)	1.15±0.50 (1.12)	4.15±1.98 (3.92)
I-S	0.35±0.19 (0.33)	0.76±0.84 (0.52)	4.24±2.41 (3.32)
SRI	0.24±0.24 (0.22)	0.55±0.20 (0.57)	1.23±0.38 (1.32)
SAI	0.33±0.07 (0.31)	0.52±0.23 (0.48)	1.94±1.17 (1.58)
KPI	0.20±0.008	0.21±0.017	0.33±0.10
EDP (D)	0.11±0.33 (0.00)	0.97±0.63 (1.11)	2.78±1.21 (2.65)
EDD (mm)	0.003±0.015 (0.00)	0.77±1.23 (0.14)	11.06±6.02 (10.26)

SD: Standard deviation, BCVA: Best corrected visual acuity, K1: Flat keratometry, K2: Steep keratometry, D: Diopters, ACP: Average corneal power, CYL: Cylindrical power, I-S: Inferior-superior ratio, SRI: Surface irregularity index, SAI: Surface asymmetry index, KPI: Keratoconus prediction index, EDP: Elevation/depression power, EDD: Elevation/depression diameter

Table 2. Comparison of best corrected visual acuity, K1, K2, average corneal power, cylindrical power, inferior-superior ratio, surface irregularity, surface asymmetry index, keratoconus prediction index, elevation/depression power, and elevation/depression diameter values of the study groups

	Normal fellow-control	Normal fellow-keratoconus
	p value	p value
BCVA	[b]0.108	[b]0.001**
K1	[a]0.003**	[a]0.001**
K2	[a]0.019*	[a]0.001**
ACP	[a]0.007**	[a]0.001**
CYL	[b]0.006**	[b]0.001**
I-S	[b]0.314	[b]0.001**
SRI	[b]0.001**	[b]0.001**
SAI	[b]0.001**	[b]0.001**
KPI	[a]0.004**	[a]0.001**
EDP	[b]0.001**	[b]0.001**
EDD	[b]0.001**	[b]0.001**

[a]Student's t-test, [b]Mann-Whitney U test, **p<0.01
SD: Standard deviation, BCVA: Best corrected visual acuity, K1: Flat keratometry, K2: Steep keratometry, ACP: Average corneal power, CYL: Cylindrical power, I-S: Inferior-superior ratio, SRI: Surface irregularity index, SAI: Surface asymmetry index, KPI: Keratoconus prediction index, EDP: Elevation/depression power, EDD: Elevation/depression diameter

the groups are shown in Table 1, and the statistical significance levels are given in Table 2.

Evaluation of corneal aberrations showed no difference between the spherical aberration RMS values of the normal group and the control group (p=0.429), whereas coma, trefoil, irregular astigmatism, and total HOA-RMS values were significantly higher in the normal fellow eyes (p<0.01). However, all corneal aberrations in the keratoconic eyes were significantly greater than those of the normal fellow eyes (p<0.05). The HOA values of all patients are given in Table 3, with statistical significance levels in Table 4.

Discussion

Corneal topography is the gold standard in keratoconus diagnosis. There are various quantitative topography indices developed from computer-assisted videokeratoscopes which detect the topographic pattern of keratoconus. Some of these are the KPI, I-S index, KISA % index, and SARX (skewed radial axis) index, and these indices are highly sensitive in diagnosing keratoconus.[11,14] Each is generally associated with a topography instrument. Software of the NIDEK Magellan Mapper corneal topography equipment used in our study includes indices that provide information about surface asymmetry and elevation changes, as well as I-S index and KPI. As in many other studies in the literature, our study also demonstrates that keratoconus eyes have significantly higher mean values in all indices when compared with normal fellow eyes and the control group.[11,13]

The I-S index, developed by Rabinowitz and McDonnell[14], determines the dioptric power difference between the inferior and superior corneal zones. In the normal cornea, it is below 1.4. Patients with values above 1.4 are classified as suspected keratoconus, while values above 1.9, if accompanied by other clinical symptoms, are classified as keratoconus. Maximum I-S values are reached in decentralized cones, increasing relative to the displacement of the apex from the visual axis, and I-S values approach normal in centralized cones.[14] Although in the present study the average I-S value of the normal fellow eyes was twice that of the control group, it was below 1.4. In a study by Tummanapalli et al.,[15] the I-S value was 0.52 in the eyes with subclinical keratoconus, which was 2.6 times higher than in

Table 3. Distribution of high order aberrations by study group			
	Control (n=20)	**Normal fellow (n=20)**	**Keratoconus (n=20)**
	Mean ± SD (median)	**Mean ± SD (median)**	**Mean ± SD (median)**
Spherical (µm)	0.12±0.06 (0.14)	0.23±0.35 (0.15)	1.05±1.31 (0.77)
Coma (µm)	0.13±0.06 (0.11)	0.26±0.19 (0.20)	0.86±0.48 (0.76)
Trefoil (µm)	0.11±0.06 (0.10)	0.21±0.10 (0.21)	0.46±0.23 (0.36)
Irregular (µm)	0.11±0.04 (0.11)	0.27±0.13 (0.26)	1.75±1.58 (1.23)
Total (µm)	0.25±0.07 (0.24)	0.51±0.28 (0.41)	2.36±2.02 (1.76)
SD: Standard deviation			

Table 4. Comparison of high order aberrations of the study groups		
	Normal fellow-control	**Normal-keratoconus**
	p value	**p value**
Spherical	[b]0.429	[b]0.001**
Coma	[b]0.001**	[b]0.001**
Trefoil	[b]0.001**	[b]0.001**
Irregular	[b]0.001**	[a]0.001**
Total	[b]0.001**	[b]0.001**
[a]Student's t-test, [b]Mann-Whitney U test, **p<0.01		

normal eyes. The authors concluded that I-S had low specificity and sensitivity in differentiating between keratoconic and normal corneas. We believe that this was because the dioptric power differences between inferior and superior zones have not yet been determined in subclinical keratoconus. In contrast, Gordon-Shaag et al.[13] reported that the I-S ratio in subclinical keratoconus cases was 9.4 times higher than the normal cases, while Rabinowitz et al.[16] found it to be 5.4 times higher. The former study included 21 subclinical keratoconus patients having astigmatism with symmetrical bow-tie pattern and a KCI over 35% without any other keratoconus symptoms, while the latter study included 16 subclinical keratoconus patients with a K value below 47 D and without inferior steepening. These cases exhibited more pronounced asymmetric characteristics compared to the cases in our study.

SRI indicates local fluctuations in central corneal power and is correlated with potential visual acuity. If SRI values are high, it may be attributable to corneal surface irregularities along the entrance pupil. Normal values are in the 0-0.56 range.[9,14,17] Although in our study the mean SRI value in the normal fellow eyes was 0.55, it was significantly higher than that of the control eyes. SAI measures differences in corneal power within each ring along the entire corneal surface, and it increases as irregular astigmatism increases and the decentralized cone becomes steeper. Normal values are in the range of 0.10-0.42.[9,14,17] In our study, the mean SAI value was 0.52 in the normal group and 0.33 in the control group. No research was found in the literature which used Placido-based topography to compare SRI and SAI in subclinical keratoconus and normal eyes. Lim et al.[11] compared topographic indices in keratoconus and subclinical keratoconus cases using Placido-based topography (Tomey TMS-2) and reported a mean SRI of 0.7 and mean SAI of 1.04 in patients with subclinical keratoconus. In the same study, comparison of subclinical keratoconus cases and normal cases using slit-scanning topography (Orbscan 2) showed that 3-mm and 5-mm SRI values were significantly higher in the subclinical keratoconus group. In that study, the subclinical keratoconus group included patients who exhibited central, inferior, or superior steepening on topography in addition to over 1.5 D of oblique astigmatism, central corneal thickness less than 500 µm, and a steep keratometry value of 47 D without any biomicroscopic signs, whereas our group of normal fellow eyes had an average keratometry value of 44.23 D with no topographic signs that might indicate keratoconus. Similarly, Tummanapalli et al.[15] used the Orbscan 2 to show that the anterior and posterior 3-mm and 5-mm SRI values were significantly higher in the subclinical keratoconus group than in the normal cases. Based on the findings of these studies, we can state that SRI and SAI are important indicators in the diagnosis of subclinical keratoconus.

The KPI was developed via multivariate analysis encompassing the SimK1, SimK2, OSI, CSI, DSI, SAI, IAI, and AA indices in order to improve diagnostic potential. As a composite index, it may be considered the most sensitive indicator for identifying cornea asymmetry. KPI values are below 0.225 in normal corneas.[14] Smolek and Klyce[10] reported that KPI values are not sufficient for distinguishing between moderate and severe keratoconus, and have limited value in determining the degree of asymmetric disease. In our study, the mean KPI value was within normal limits in the normal fellow eyes, but was significantly higher than that of the control group. Lim et al.[11] reported a mean KPI of 0.27 in subclinical keratoconus, but the patients included in their study had topographic findings suggesting early stage keratoconus. In our patient group, the KPI values, like the I-S value, did not have any asymmetric features that may lead to the threshold value being exceeded. In that sense, the I-S and KPI indices are not sufficient by themselves to distinguish between subclinical keratoconus and normal eyes.

EDP calculates the average power of apparent islands and valleys for those areas of the cornea that are within the demarcated pupil. The unit is D. It can be used to estimate the size of so-called central islands after excimer laser photorefractive

keratectomies. EDD is twice the square root of this zone divided by pi, is an equivalent diameter. The unit is mm. Abnormal EPD and EDD values can be seen in keratoconus, corneal grafts, and astigmatic normal corneas.[9] In our study, the normal fellow eyes exhibited significantly higher EDP and EDD values compared to the control group. Our topography device provides only anterior elevation data and derives them from curvature maps. However, keratoconus affects not only the anterior surface of the cornea, but also the posterior surface. Uçakhan et al.[18] reported that posterior elevation data were more definitive than anterior elevation data in distinguishing subclinical keratoconus from normal corneas. A study using Pentacam showed that 88% of the normal eyes of patients classified as unilateral keratoconus according to standard Rabinowitz criteria exhibited posterior corneal surface changes.[19] It has also been determined that the posterior corneal surface shows changes before the anterior surface in ectatic corneal diseases.[20] Rao et al.[21] developed a keratoconus identification algorithm using posterior elevation values (Orbscan 2, cut-off 40 µm) in combination with videokeratography data (Rabinowitz or Klyce/Maeda method) and suggested that elevation and pachymetry data be combined with curvature data in cases of suspected keratoconus. Elevation-based topography systems provide both anterior and posterior cornea curvature and elevation maps, corneal thickness, and anterior segment data. Because the topography device used in the present study provides data about only the anterior surface of the cornea, it may not have been adequate to diagnose keratoconus.

Various studies have demonstrated that keratoconic corneas exhibit increased wavefront aberrations as compared to normal corneas.[22,23,24,25] Zernike polynomials enable the rendering of complex corneal shapes and human eye wavefront aberrations to identifiable shapes and mathematical formulas such as defocus, astigmatism, and spherical aberration. RMS value shows the overall size of the aberration relative to pupil diameter; an optically perfect eye has an RMS value of 0. Our finding is consistent with the literature in that the RMS values of all HOAs in keratoconic patients were significantly higher than those of the normal fellow eyes and the control group. In the group of normal fellow eyes, all HOA-RMS values except spherical aberration were found to be higher than in the control group. Bühren et al.[26] found that the coma, trefoil, total HOA-RMS values, and Z_3^{-1}, Z_5^{-1} vertical coma coefficients were higher in the subclinical keratoconus group than in the normal cases, with the biggest difference being in the vertical coma coefficients. Accordingly, vertical asymmetry was interpreted to be the earliest symptom of keratoconus. Coma aberration results from the decentration of the optic system, clinically known as the kappa angle, and this natural condition manifests itself as a decentralized spherical aberration. In eyes with keratoconus, the cone with higher dioptric power than the other corneal surfaces causes deformation in wavefront, shifting of the visual axis and associated significant increase in coma aberration. Alio and Shabayek.[22] determined that coma aberration was a good indicator in identifying and grading keratoconus; they observed a significant positive correlation between increasing K values and coma aberration, and developed a modified Amsler-Krumeich keratoconus grading system using coma aberration. Our study supported the results of Gordon-Shaag et al.,[13] who showed that all HOAs other than total tetrafoil and spherical aberration were significantly higher in eyes with suspected keratoconus when compared with normal fellow eyes.

In our study, the unilateral keratoconus ratio was found to be 11.2%. The prevalence of true unilateral keratoconus is reported in the international literature as ranging between 0.5% and 4.5%. In a study conducted in Turkey, a unilateral keratoconus prevalence of 14.9% was determined using Pentacam.[27] The main limitation of our study was that the elevation data provided by our topography device was not adequate and not able to evaluate the posterior corneal surface. Another limitation is that long-term patient follow-up data was not available. The suspected keratoconus eyes that we determined to be normal may exhibit signs that would lead to a keratoconus diagnosis if examined using more advanced topography systems.

Conclusion

In summary, the present study demonstrates that in keratoconus cases, sometimes one of the eyes does not exhibit the clinical and topographical findings to diagnose keratoconus, but may be in a subclinical and subtopographical phase and have significantly different values compared to the eyes of normal people, particularly with regard to surface regularity indices, elevation values, and corneal HOAs. Therefore, we believe that the corneal curvature map, elevation map, and corneal HOAs should be evaluated collectively when diagnosing subclinical keratoconus and selecting eligible patients prior to refractive surgery.

Ethics

Ethics Committee Approval: University of Healty Sciences (2017/28).

Informed Consent: Retrospective study.

Peer-review: Externally and internally peer-reviewed.

Authorship Contributions

Surgical and Medical Practices: Sibel Aksoy, Sezen Akkaya, Yelda Özkurt, Sevda Kurna, Banu Açıkalın, Tomris Şengör, Concept: Sibel Aksoy, Design: Sibel Aksoy, Data Collection or Processing: Sibel Aksoy, Analysis or interpretation: Sibel Aksoy, Banu Açıkalın, Tomris Şengör, Literature Search: Sibel Aksoy, Writing: Sibel Aksoy.

Conflict of Interest: No conflict of interest was declared by the authors.

Financial Disclosure: The authors declared that this study received no financial support.

References

1. Krachmer JH, Feder RS, Belin MW. Keratoconus and related noninflammatory corneal thinning disorders. Surv Ophthalmol. 1984;28:293-322.
2. Rabinowitz YS. Keratoconus. Surv Ophthalmol. 1998;42:297-319.
3. Wilson SE, Lin DTC, Klyce SD. Corneal topography of keratoconus. Cornea. 1991;10:2-8.

4. Rabinowitz YS, Nesburn AB, McDonnell PJ. Videokeratography of the fellow eye in unilateral keratoconus. Ophthalmology. 1993;100:181-186.
5. Holland DR, Maeda N, Hannush SB, Riveroll LH, Green MT, Klyce SD, Wilson SE. Unilateral keratoconus; incidence and quantitative topographic analysis. Ophthalmology. 1997;104:1409-1413.
6. Lee LR, Hirst LW, Readshaw G. Clinical detection of unilateral keratoconus. Aust N Z J Ophthalmol. 1995;23:129-133.
7. Wei RH, Zhao SZ, Lim L, Tan DT. Incidence and characteristics of unilateral keratoconus classified on corneal topography. J Refract Surg 2011;27:745-751.
8. Li X, Rabinowitz YS, Rasheed K, Yang H. Longitudinal study of the normal eyes in unilateral keratoconus patients. Ophthalmology. 2004;111:440-446.
9. Maeda N, Klyce SD, Smolek MK, Thompson HW. Automated keratoconus screening with corneal topography analysis. Invest Ophthalmol Vis Sci. 1994;35:2749-2757.
10. Smolek MK, Klyce SD. Current keratoconus detection methods compared with a neural network approach. Invest Ophthalmol Vis Sci. 1997;38:2290-2299.
11. Lim L, Wei RH, Chan WK, Tan DT. Evaluation of keratoconus in Asians: role of Orbscan II and Tomey TMS-2 corneal topography. Am J Ophthalmol. 2007;143:390-400.
12. Gobbe M, Guillon M. Corneal wavefront aberration measurements to detect keratoconus patients. Cont Lens Anterior Eye. 2005;28:57- 66.
13. Gordon-Shaag A, Millodot M, Ifrah R, Shneor E. Aberrations and topography in normal, keratoconus-suspect, and keratoconic eyes. Optom Vis Sci. 2012;89:411-418.
14. Rabinowitz YS, McDonnell PJ. Computer-assisted corneal topography in keratoconus. Refract Corneal Surg. 1989;6:400-408.
15. Tummanapalli SS, Potluri H, Vaddavalli PK, Sangwan VS. Efficacy of axial and tangential corneal topography maps in detecting subclinical keratoconus. J Cataract Refract Surg. 2015;41:2205-2214.
16. Rabinowitz YS, Li X, Canedo ALC, Ambrosio R Jr, Bykhovskaya Y. Optical coherence tomography combined with videokeratography to differentiate mild keratoconus subtypes. J Refract Surg. 2014;30:80-87.
17. Wilson SE, Klyce SD. Advances in the analysis of corneal topography. Surv Ophthalmol. 1991;35:269-277.
18. Uçakhan ÖÖ, Cetinkor V, Özkan M, Kanpolat A. Evaluation of Scheimpflug imaging parameters in subclinical keratoconus, keratoconus, and normal eyes. J Cataract Refract Surg. 2011;37:1116-1124.
19. Carvalho MQ, Viteri E, Salgado-Borges J, Oliveira C, Ambrosio R. "Corneal tomographic study of contralateral normal eyes of patients with very asymmetric keratoconus," paper presented at the ASCRS Symposium on Cataract, IOL and Refractive Surgery. Chicago, IL, USA; April 2008.
20. Auffarth GU, Wang L, Volcker HE. Keratoconus evaluation using the Orbscan Topography System. J Cataract Refract Surg. 2000;26:222-228.
21. Rao SN, Raviv T, Majmudar PA, Epstein RJ. Role of Orbscan II in screening keratoconus suspects before refractive corneal surgery. Ophthalmology. 2002;109:1642-1646.
22. Alio JL, Shabayek MH. Corneal higher order aberrations: a method to grade keratoconus. J Refract Surg. 2006;22:539-545.
23. Barbero S, Marcos S, Merayo Lloves J, Moreno-Barriuso E. Validation of the estimation of corneal aberrations from videokeratography in keratoconus. J Refract Surg. 2002;18:263-270.
24. Jafri B, Li X, Yang H, Rabinowitz YS. Higher order wavefront aberrations and topography in early and suspected keratoconus. J Refract Surg. 2007;23:774-781.
25. Schlegel Z, Lteif Y, Bains HS, Gatinel D. Total, corneal, and internal ocular optical aberrations in patients with keratoconus. J Refract Surg. 2009;25(10 Suppl):951-957.
26. Bühren J, Kook D, Yoon G, Kohnen T. Detection of subclinical keratoconus by using corneal anterior and posterior surface aberrations and thickness spatial profiles. Invest Ophthalmol Vis Sci. 2010;51:3424-3432.
27. Faik Oruçoğlu. Unilateral keratokonuslarda insidans ve tomografik değerlendirme. Turk J Ophthalmol. 2013;43:83-86.

DOI: 10.4274/tjo.22800
Turk J Ophthalmol 2017;47:255-260

Original Article

Correlation of Corneal Endothelial Cell Density with Corneal Tomographic Parameters in Eyes with Keratoconus

Banu Bozkurt*, Mevlüt Yılmaz**, Ali Meşen*, Ümit Kamış***, Bengü Ekinci Köktekir*, Süleyman Okudan*
*Selçuk University Faculty of Medicine, Department of Ophthalmology, Konya, Turkey
**Dr. Munif İslamoğlu State Hospital, Ophthalmology Clinic, Kastamonu, Turkey
***Dünyagöz Hospital, Ophthalmology Clinic, Konya, Turkey

Abstract

Objectives: To examine changes in corneal endothelial cell density (ECD) in different stages of keratoconus and evaluate its correlation with corneal tomographic parameters.

Materials and Methods: Two hundred six patients with keratoconus were enrolled in the study. Corneal topography was performed by Sirius (CSO, Italy), which has a rotating Scheimpflug camera and a Placido disc topographer. Automatic endothelial analysis was done with the non-contact endothelial microscope (20x probe) of Confoscan-4 (NIDEK, Japan). The eyes were classified into stages based on steepest keratometric value as follows: mild <45 D; moderate 45-52 D; severe >52 D and according to thinnest cornea thickness (TCT) as <400 µm, 400-450 µm, and >450 µm. Tomographic and endothelial cell parameters were compared among the groups using Kruskal-Wallis test and the correlations between them were analyzed using Spearman correlation.

Results: The study included 391 eyes of 100 male (24.29±7.7 years, range 11-47 years) and 106 female (26.26±7.5 years, range 13-45 years) patients (p=0.07). Mean ECD values were 2628±262 cells/mm^2, 2541.9±260.4 cells/mm^2, and 2414.6±384.3 cells/mm^2 in mild, moderate, and severe keratoconus, respectively (p<0.001) and 2592.3±277 cells/mm^2, 2502±307 cells/mm^2 and 2348±296 cells/mm^2 in corneas with TCT values >450 µm, 400-450 µm, and <400 µm, respectively (p<0.001). ECD showed significant negative correlation with keratometric and elevation parameters and positive correlation with pachymetric parameters (p<0.05).

Conclusion: As endothelial cell numbers seem to decrease with the progression of keratoconus, specular/confocal microscopy screening should be carried out, especially in eyes with advanced stages and corneas with TCT <400 µm.

Keywords: Keratoconus, cornea endothelial cell density, corneal tomography, specular microscopy, morphological changes

Introduction

Keratoconus is an ectatic corneal disorder characterized by progressive localized thinning and protrusion of the cornea, resulting in irregular astigmatism and decreased vision. Its annual incidence ranges between 50 and 230 per 100,000.[1] Placido disc-based corneal topographies and measurement of corneal thickness are widely used methods in identifying cases of keratoconus. However, Placido-based corneal topographies evaluate only the anterior surface of the cornea and do not show corneal curvature and elevation of the posterior corneal surface.[2,3,4] One of the most recent advances in corneal topography is the introduction of slit-scanning and Scheimpflug imaging systems, which take measurements both from anterior and posterior corneal surfaces. These systems provide more accurate, reliable, three-dimensional information about the shape of the cornea, including anterior and posterior corneal surface elevation data measurement and pachymetry map.[3,4,5,6,7] Elevation measurements obtained by Orbscan and Pentacam have shown that corneal deformation also occurs in the posterior surface in eyes with keratoconus

Address for Correspondence: Banu Bozkurt MD, Selçuk University Faculty of Medicine, Department of Ophthalmology, Samsun, Turkey
Phone: +90 530 849 19 49 E-mail: drbanubozkurt@yahoo.com **ORCID-ID:** orcid.org/0000-0002-9847-3521
Received: 22.12.2016 **Accepted:** 24.03.2017

and that posterior elevation is the most sensitive parameter in discriminating keratoconus from normal corneas.[7,8,9,10,11] Sirius (CSO, Italy) is a corneal tomography device which combines Scheimpflug photography analysis with the classic Placido disc technology. This provides highly consistent anterior and posterior corneal curvature measurements.[12,13,14]

Since keratoconus is an ectatic disease affecting both the anterior and posterior corneal surfaces, there might be changes in corneal endothelial cell number and morphology, especially in advanced stages of the disease. In keratoconus, evaluation of the corneal endothelium may be important since theoretically these cells may be damaged as a result of microscopic ruptures in Descemet's membrane in ectatic areas, ultraviolet radiation damage due to stromal thinning, chronic eye rubbing, long-term contact lens wear, and oxidative stress.[15] Keratoconus can also be associated with Fuchs' corneal endothelial dystrophy.[16] The status of cornea endothelial cells might alter the choice of keratoplasty technique (e.g. penetrating keratoplasty or Descemet stripping endothelial keratoplasty rather than deep anterior lamellar keratoplasty in eyes with low endothelial cell count) and is important in the decision to perform crosslinking (CXL) procedure or the selection of CXL protocols (transepithelial/hypotonic riboflavin solutions vs. isotonic dextran riboflavin solutions) to avoid endothelial cell toxicity in eyes with reduced endothelial cell count. However, our understanding of corneal endothelial changes in keratoconus remains incomplete. Histopathological evaluation of the corneal buttons of keratoconic eyes removed during penetrating keratoplasty has revealed deterioration in endothelial cell morphology and number.[17,18] The findings of *in-vivo* confocal studies are conflicting.[19,20,21,22,23,24,25,26,27] Specular microscopic examinations showed an increased variation in endothelial cell size (polymegathism) and shape (pleomorphism) in eyes with keratoconus.[28,29] In a recent study, a trend toward lower endothelial cell density (ECD) and percentage of hexagonality, and a higher coefficient of variation was detected with advancing disease. However, there was no statistically significant correlation between the stage of keratoconus and changes in endothelial cell morphology and density.[30] The conflicting results and the lack of significance in the correlation between ECD and topographic parameters might be due small number of keratoconus subjects within those studies.

In this study, our aim was to examine changes in corneal endothelial cells in different stages of keratoconus and evaluate the correlation of ECD with keratometric, pachymetric, and elevation parameters in eyes with keratoconus. Among studies evaluating the ECD and morphology in keratoconus, this study has the largest number of eyes with different stages of keratoconus.

Materials and Methods

The prospective cross-sectional study was performed in the Ophthalmology Department of Selçuk University Hospital. The study was approved by the Selçuk University Research Ethics Committee and followed the tenets of the Declaration of Helsinki. Written informed consent was obtained from all patients and the parents of those younger than 18 years.

Two hundred six patients with keratoconus were enrolled into the study. Each participant underwent a comprehensive ophthalmic examination including determination of uncorrected and best-corrected visual acuity, slit-lamp biomicroscopy, intraocular pressure measurement, and fundus examination. Eyes were diagnosed with keratoconus if they had at least one slit-lamp finding of anterior corneal bulging, stromal thinning, conical protrusion of the cornea at the apex, Fleischer ring, or Vogt striae and/or corneal topography findings characteristic of keratoconus such as asymmetric bow-tie pattern with or without skewed axes and inferior-superior power asymmetry. Exclusion criteria were past ocular surgery, contact lens wear, central corneal scarring, history of hydrops, or associated corneal dystrophies.

Corneal topography was performed using the Sirius corneal tomographer (CSO, Italy), which has a 360°-rotating Scheimpflug camera and a Placido disc topographer. Scheimpflug photography enables the acquisition and processing of 25 radial sections of the cornea and anterior chamber within a few seconds. Sirius takes measurements from 35,632 points for the anterior corneal surface and 30,000 for the posterior corneal surface in high-resolution mode in approximately 1 s or less and provides tangential and axial curvature data of the anterior and posterior corneal surfaces, refractive power of the cornea, and corneal pachymetry maps. A second camera checks that the alignment of the eye is maintained during measurement. Measurements were performed according to the manufacturer's guidelines. The patients were seated in front of the machine and placed their chin on a chinrest and their forehead against the forehead strap. They were instructed to fixate on an internal fixation target and permitted to blink just before each measurement to spread an optically smooth tear film over the cornea and keep the eye open during image acquisition. Images with "OK" signal, which means that Scheimpflug acquisitions were above the required quality specifications for coverage and centration, were included in statistical analysis. Keratometry values in the flat (K1) and steep (K2) meridian, mean keratometry, thinnest corneal thickness (TCT), pachymetry at the apex of the cone (pachymetry apex), and highest anterior and posterior elevation values were recorded for each eye.

Measurements of corneal ECD and morphology were performed using the non-contact specular mode of Confoscan 4 (NIDEK, Japan). Non-contact endothelial microscope with 20x probe with a wider field of view was used for the measurement. The patient's head was positioned similar to slit-lamp examination, and the patient was instructed to look straight ahead into the built-in fixation targets. Automatic focusing was used to ensure the image of the pupil on the monitor was in clear focus and within the aiming circle visible on the monitor. Three successive images were selected for the analysis. The central or paracentral area was determined by the operator and the automated cell analysis detected overall density, number

of sides, and area of each cell as well as overall pleomorphism and polymegathism indices. Mean ECD, polymegatism, and pleomorphism of three images were calculated and recorded for statistical analysis.

Eyes were grouped into stages according to the collaborative longitudinal evaluation of keratoconus (CLEK) study group recommendation with respect to the curvature of the steepest corneal meridian (K2) as mild (<45 D), moderate (45-52 D), and severe (>52 D),[31] and according to TCT as corneas less than 400 mm, 400-450 mm, and greater than 450 mm.

Statistical Analysis

All statistical calculations were performed using SPSS (Statistical Package for the Social Science, version 16; SPSS Inc, Chicago, IL, USA) for Microsoft Windows. Data were statistically described in terms of mean ± SD and range. The normality of all data distributions was checked using the Shapiro-Wilk test. As the parameters were not normally distributed, tomographic and endothelial cell parameters were compared among the groups using Kruskall-Wallis test. In case of significance, Mann-Whitney-U test with Bonferroni's adjustment for post-hoc analysis was used to analyze the differences between the two groups. The correlations between corneal tomographic parameters and endothelial cell parameters were analyzed using Spearman correlation. A p value <0.05 was accepted as statistically significant.

Results

The study included 391 eyes of 100 male (age: 24.29±7.7 years, range 11-47 years) and 106 female (age: 26.26±7.5 years, range 13-45 years), with no statistically significant differences in age or sex ratio (p=0.07).

According to the CLEK criteria, 39 eyes (10%) had mild keratoconus, 252 eyes (64.4%) had moderate, and 100 eyes (25.6%) had severe keratoconus. There were no significant differences in age among the 3 groups (p=0.07). Mean values of corneal tomographic parameters and endothelial cell parameters according to different stages of keratoconus are shown in Table 1. There was a statistically significant difference in ECD values according to stage of keratoconus, with the lowest value being in severe keratoconus (2628±262 cells/mm^2, 2541.9±260.4 cells/mm^2 and 2414.6±384.3 cells/mm^2 in mild, moderate, and severe stages, respectively) (p<0.001).

There were 170 eyes with TCT >450 mm, 161 eyes with TCT between 400-450 mm, and 60 eyes with TCT <400 mm, with no statistically significant difference in respect to age (p=0.09) (Table 2). Mean values of corneal tomographic parameters and endothelial cell parameters according to TCT are presented in Table 2. Mean ECD values were 2592.3±277 cells/mm^2, 2502±307 cells/mm^2, and 2348±296 cells/mm^2 in corneas with TCT values >450 µm, 400-450 µm, and <400 µm, respectively (p<0.001).

Overall pleomorphism and polymegathism indices did not differ among keratoconic eyes with different stages and thickness values (p>0.05) (Tables 2 and 3).

The correlations between ECD and keratometric values, anterior and posterior elevation parameters, and thickness parameters were statistically significant, but weak (r=0.17-0.26) (p<0.05) (Table 3).

Discussion

Despite the numerous studies in the literature evaluating corneal endothelial changes in keratoconus, there is still no consensus regarding whether endothelial cell count and morphology change in keratoconus and deteriorate with the progression of the disease. Among confocal studies which showed a decrease in ECD in keratoconus, Uçakhan et al.[19] compared ECD in 48 eyes of 24 patients with keratoconus with 44 eyes of 22 healthy subjects and also among different stages of keratoconus using Confoscan 2.0 (NIDEK, Japan). Although they found lower ECD in keratoconic eyes (2754±312 cells/mm^2) than control eyes (2900±354 cells/mm^2), this difference

Table 1. Corneal topographic and endothelial cell parameters according to keratoconus stage

	Whole group n=391 eyes	Mild (K2<45 D) n=39 eyes	Moderate (K2 45-52 D) n=252 eyes	Severe (K2>52 D) n=100 eyes	p
Age (years)	25.31±7.7	25.6±9	25.2±7.6	25.8±7.1	0.7
K1 (D)	46.23±3.56	42.68±1.2	45.21±2	50.2±4	<0.001
K2 (D)	49.85±3.97	44.3±0.85	48.6±1.8	55.2±2.9	<0.001
TCT (µm)	443.1±48.7	483.5±37.6	451.4±39.1	406.4±52.6	<0.001
Pachymetry apex (µm)	462.31±50.75	508.7±32.5	468.7±43.5	428.1±53.1	<0.001
Posterior elevation (µm)	48.3±30.7	27.8±16.2	44.2±26.6	66.7±35.6	<0.001
Anterior elevation (µm)	28.6±16.8	14.9±8.2	26.1±13.9	40.2±19.1	<0.001
ECD (cells/mm^2)	2517.92±303.6	2628±262	2541.9±260.4	2414.6±384.3	<0.001
Pleomorphism (%)	37.5±9.7	39.04±8.4	37.8±9.7	36.4±10.3	0.3
Polymegathism (%)	52.01±11.1	52.9±9.2	51.5±10.7	52.9±12.8	0.5

Non-parametric Kruskal-Wallis test

D: Diopter, K1: Flat keratometry value, K2: Steep keratometry value, TCT: Thinnest corneal thickness, ECD: Endothelial cell density

Table 2. Corneal topographic and endothelial cell parameters according to thinnest cornea thickness				
Parameters	**TCT>450 µm n=170 eyes**	**TCT 400-450 µm n=161 eyes**	**TCT<400 µm n=60 eyes**	**p**
Age (years)	25.05±8.1	25.1±7.3	27.2±7.1	0.09
K1 (D)	44.6±2.1	46.31±2.6	50.8±4.8	<0.001
K2 (D)	47.96±2.9	49.95±2.9	54.9±4.5	<0.001
TCT (µm)	486.2±25.2	427.4±14.5	363.4±28.8	<0.001
Pachymetry apex (µm)	503.1±28.1	445.9±28.3	390.7±43.2	<0.001
Posterior elevation (µm)	37.1±26.5	50.7±27.3	73.6±34.3	<0.001
Anterior elevation (µm)	22.2±14.6	30.3±14.8	42.3±18.3	<0.001
ECD (cells/mm^2)	2592.3±277	2502±307	2348±296	<0.001
Pleomorphism (%)	38.5±9.5	37.1±9.9	35.9±9.9	0.1
Polymegathism (%)	51.5±10.2	52.8±11.4	51.4±12.9	0.4
Non-parametric Kruskal-Wallis test K1: Flat keratometry value, K2: Steep keratometry value, D: Diopter, TCT: Thinnest corneal thickness, ECD: Endothelial cell density				

Table 3. Correlations between endothelial cell density and corneal thickness and topographic parameters		
Spearman's rho coefficient	**ECD (cells/mm^2)**	**p**
K1 (D)	-0.21	<0.001
K2 (D)	-0.21	<0.001
TCT (µm)	0.26	<0.001
Pachymetry apex (µm)	0.19	<0.001
Posterior elevation (µm)	-0.17	<0.001
Anterior elevation (µm)	-0.17	<0.001
ECD: Endothelial cell density, K1: Flat keratometry value, K2: Steep keratometry value, D: Diopter, TCT: Thinnest corneal thickness		

did not reach clinical significance. Mean ECD in eyes with severe keratoconus [mean K>55 diopter (D), n=26] was statistically significantly lower than in eyes with moderate (mean 47-55 D, n=17) (p<0.05) or mild (mean K<47 D, n=5) (p<0.05) keratoconus. The mean endothelial cell hexagonality percentage was statistically significantly lower in eyes with keratoconus compared to controls (p<0.05) and in eyes with severe keratoconus compared to mild or moderate keratoconus (p>0.05). Consistent with these findings, Mocan et al.[20] found decreased endothelial cell count in eyes with keratoconus (2719±279 cells/mm^2) compared to controls (2924±300 cells/mm^2) with Confoscan 3.0 (NIDEK, Japan). In a study by Niederer et al.[21] using laser scanning confocal microscopy (HRT, Heidelberg, Germany), ECD was found to be significantly reduced in eyes with keratoconus compared to controls (2412.2±339.5 cells/mm^2 and 2845.6±313.0 cells/mm^2, respectively), but the difference did not reach statistical significance between mild to moderate (steepest K<45 D and 45-52 D) keratoconus (21 eyes) and severe keratoconus (steepest K>52 D) (31 eyes) (2510.6±334.4 cells/mm^2 and 2345.5±331.8 cells/mm^2, respectively) (p=0.09). Bitirgen et al.[22] found lower ECD in 78 keratoconic subjects with no history of contact lens use (2686±265 cells/mm^2) compared to 36 age-matched control subjects (2875±223 cells/mm^2) (p<0.001). El-Agha et al.[30] evaluated the correlation between disease stage and corneal ECD and morphology in 40 eyes with keratoconus (11 eyes with stage 1, 17 eyes with stage 2, and 12 eyes with stage 3). They found lower ECD in eyes with stage 3 (2214.8±748 cells/mm^2) compared to stage 1 (2404.5±345 cells/mm^2) and stage 2 (2455.4±331 cells/mm^2) (p=0.91). Advanced stage was also associated with higher coefficient of variation and lower percentage of hexagonal endothelial cells, although there was no statistically significant correlation. The lack of significant results may be explained by the small number of eyes within each group.

Some studies reported no endothelial changes associated with keratoconus.[21,22,23,24] Using Confoscan, Weed et al.[23] found no differences in ECD between keratoconus (n=19) (2888 cells/mm^2 vs. 2941 cells/mm^2 in moderate and severe cases, respectively) and healthy eyes (n=38) (3043 cells/mm^2). Yeniad et al.[24] used Confoscan 2.0 and observed no differences in ECD values among eyes with mild/moderate keratoconus and controls, even when the eyes were further subgrouped according to contact lens wear history. In a study by Timucin et al.[25] no significant difference was found in ECD measured by laser scanning confocal microscopy in eyes with keratoconus (2731.6±303.2 cells/mm^2) compared with controls (2664.9±319.5 cells/mm^2) (p=0.4). They also could not show a significant difference according to disease stage when the eyes were classified as mild (steepest K<45 D, n=19), moderate (45-52 D, n=21), and severe (>52 D, n=25) (p=0.17). Ozgurhan et al.[26] detected no differences in mean ECD among patients with manifest keratoconus (n=30), subclinical keratoconus (n=32), relatives of keratoconus patients, and a control group (p=0.592).

Interestingly, Hollingsworth et al.[27] examined 29 keratoconus eyes and 29 age-matched healthy eyes using tandem scanning confocal microscopy (Tomey Confoscan) and showed increased endothelial cell count in eyes with keratoconus (3250±352 cells/mm^2) compared to healthy eyes (3056±365 cells/mm^2). The level of polymegathism did not differ between keratoconic subjects (0.35±0.05) and matched controls (0.38±0.07).

Conflicting results among studies might be due to inadequate number of eyes within the different stages of keratoconus, differences in exclusion criteria (current or previous contact lens wear), measurement devices (slit scanning or laser scanning confocal microscopy), techniques for image acquisition and cell density calculation (image size, image location, automated or manual cell counting), and classification of disease severity (Krumleich-Amsler, CLEK, etc). A central single assessment of less than 1/400 of the total number of endothelial cells in an eye with keratoconus may miss polymegathism, pleomorphism, and endothelial cell damage in the region of eccentric cone since the sample observed might not be representative.[15] Furthermore, the accuracy of calculations decreases with lower image quality.

Most of the studies in the literature included a limited number of keratoconic eyes (less than 70), mostly in early and moderate stages, in which endothelial changes were not expected. Some studies showed decreased ECD in eyes with keratoconus but could not detect a statistically significant difference among the different stages of keratoconus, which might also be explained by small numbers of eyes within each stage. We think that a larger number of patients could have yielded statistically significant results in most of those studies. Therefore, we included a large number of keratoconic eyes (391 eyes) and classified eyes according to disease stage based on the CLEK recommendation and according to TCT. We used Sirius corneal tomographer (CSO, Italy), one of the latest corneal topography devices that combines Scheimpflug imaging with Placido-disc topography, and Confoscan-4 (Tokyo, Japan) with 20x probe, which images a wider field of view compared to other confocal systems and counts up to 1000 cells per exam. The automatic endothelial analysis gives the density plus polymegathism and pleomorphism indices, which makes Confoscan-4 a more objective device in the evaluation of corneal endothelium than other confocal microscopes. We found lower ECD in advanced stages of keratoconus and in thinner corneas, and the correlations between ECD and topographic parameters were significant ($p<0.05$). We excluded subjects who wear contact lenses or had a history of contact lens in the past, since wearing contact lenses was reported to cause a decrease in basal epithelial cell density, loss of keratocytes, and endothelial cell damage.[24,26,32] In a study by Edmonds et al.[32], after controlling for age and keratoconus severity, patients who wore SoftPerm contact lenses had 18% lower endothelial cell counts (2157±442 cells/mm^2) than patients without contact lenses (2538±398 cells/mm^2) and 15% lower than patients who wore soft toric disposable contact lenses (2483±292 cells/mm^2). The large number of subjects, proper selection of cases, and use of the latest technologies make the results of our study more reliable and significant in terms of statistical analysis.

Conclusion

In conclusion, as endothelial cell numbers seem to decrease with the progression of keratoconus, specular/confocal microscopy screening should be carried out, especially in eyes with advanced disease stage and corneas with TCT<400 µm.

Ethics

Ethics Committee Approval: Selçuk University Medical Faculty Ethics Committee (2013/236).

Informed Consent: It was taken.

Peer-review: Externally and internally peer-reviewed.

Authorship Contributions

Surgical and Medical Practices: Banu Bozkurt, Ümit Kamış, Concept: Banu Bozkurt, Design: Banu Bozkurt, Data Collection or Processing: Mevlüt Yılmaz, Ali Meşen, Analysis or Interpretation: Banu Bozkurt, Ümit Kamış, Süleyman Okudan, Bengü Ekinci Köktekir, Literature Search: Banu Bozkurt, Mevlüt Yılmaz, Ali Meşen, Writing: Banu Bozkurt.

Conflict of Interest: No conflict of interest was declared by the authors.

Financial Disclosure: The authors declared that this study received no financial support.

References

1. Rabinowitz YS. Keratoconus. Surv Ophthalmol. 1998;42:297-319.
2. Swartz T, Marten L, Wang M. Measuring the cornea: the latest developments in corneal topography. Curr Opin Ophthalmol. 2007;18:325-333.
3. Matalia H, Swarup R. Imaging modalities in keratoconus. Indian J Ophthalmol. 2013;61:394-400.
4. Belin MW, Kachikian SS. An introduction to understanding elevation-based topography: how elevation data are displayed-a review. Clin Exp Ophthalmol. 2009;37:14-29.
5. Ho JD, Tsai CY, Tsai RJ, Kuo LL, Tsai IL, Liou SW. Validity of the keratometric index: evaluation by the Pentacam rotating Scheimpflug camera. J Cataract Refract Surg. 2008;34:137-145.
6. Orucoglu F. Incidence and Tomographic Evaluation of Unilateral Keratoconus. Turk J Ophthalmol. 2013;43:83-86.
7. Quisling S, Sjoberg S, Zimmerman B, Goins K, Sutphin J. Comparison of Pentacam and Orbscan II on posterior curvature topography measurements in keratoconus eyes. Ophthalmology. 2006;113:1629-1632.
8. Tomidokoro A, Oshika T, Amano S, Higaki S, Maeda N, Miyata K. Changes in anterior and posterior corneal curvatures in keratoconus. Ophthalmology. 2000;107:1328-1332.
9. De Sanctis U, Loiacono C, Richiardi L, Turco D, Mutani B, Grignolo FM. Sensitivity and specificity of posterior corneal elevation measured by Pentacam in discriminating keratoconus/subclinical keratoconus. Ophthalmology. 2008;115:1534-1539.
10. Mihaltz K, Kovács I, Takács A, Nagy ZZ. Evaluation of Keratometric, Pachymetric, and Elevation Parameters of Keratoconic Corneas With Pentacam. Cornea. 2009;28:976-980.
11. Kamiya K, Ishii R, Shimizu K, Igarashi A. Evaluation of corneal elevation, pachymetry and keratometry in keratoconic eyes with respect to the stage of Amsler-Krumeich classification. Br J Ophthalmol. 2014;98:459-463.
12. Montalbán R, Piñero DP, Javaloy J, Alió JL. Intrasubject repeatability of corneal morphology measurements obtained with a new Scheimpflug photography-based system. J Cataract Refract Surg. 2012;38:971-977.
13. Savini G, Barboni P, Carbonelli M, Hoffer KJ. Repeatability of automatic measurements by a new Scheimpflug camera combined with Placido topography. J Cataract Refract Surg. 2011;37:1809-1816.

14. Montalban R, Alio JL, Javaloy J, Piñero DP. Comparative analysis of the relationship between anterior and posterior corneal shape analyzed by Scheimpflug photography in normal and keratoconus eyes. Graefes Arch Clin Exp Ophthalmol. 2013;251:1547-1555.
15. McMonnies CW. Corneal endothelial assessment with special references to keratoconus. Optom Vis Sci. 2014;91:124-134.
16. Vira S, Abugo U, Shih CY, Udell IJ, Sperling B, Hannush SB, Basti S, Bouchard CS. Descemet stripping endothelial keratoplasty for the treatment of combined fuchs corneal endothelial dystrophy and keratoconus. Cornea. 2014;33:1-5.
17. Fernandes BF, Logan P, Zajdenweber ME, Santos LN, Cheema DP, Burnier MN Jr. Histopathological study of 49 cases of keratoconus. Pathology. 2008;40:623-626.
18. Sturbaum CW, Peiffer RL Jr. Pathology of corneal endothelium in keratoconus. Ophthalmologica. 1993;206:192-208.
19. Uçakhan O, Kanpolat A, Ylmaz N, Ozkan M. In vivo confocal microscopy findings in keratoconus. Eye Contact Lens. 2006;32:183-191.
20. Mocan MC, Yilmaz PT, Irkec M, Orhan M. In vivo confocal microscopy for the evaluation of corneal microstructure in keratoconus. Curr Eye Res. 2008;33:933-939.
21. Niederer RL, Perumal D, Sherwin T, McGhee CN. Laser scanning in vivo confocal microscopy reveals reduced innervation and reduction in cell density in all layers of the keratoconic cornea. Invest Ophthalmol Vis Sci. 2008;49: 2964-2970.
22. Bitirgen G, Ozkagnici A, Bozkurt B, Malik RA. In vivo corneal confocal microscopic analysis in patients with keratoconus. Int J Ophthalmol. 2015;8:534-539.
23. Weed KH, MacEwen CJ, Cox A, McGhee CN. Quantitative analysis of corneal microstructure in keratoconus utilising in vivo confocal microscopy. Eye (Lond). 2007;21:614-623.
24. Yeniad B, Yilmaz S, Bilgin LK. Evaluation of the microstructure of cornea by in vivo confocal microscopy in contact lens wearing and non-contact lens wearing keratoconus patients. Cont Lens Anterior Eye. 2010;33:167-170.
25. Timucin OB, Karadag MF, Cinal A, Asker M, Asker S, Timucin D. Assessment of corneal endothelial cell density in patients with keratoconus not using contact lenses. Cont Lens Anterior Eye. 2013;36:80-85.
26. Ozgurhan EB, Kara N, Yildirim A, Bozkurt E, Uslu H, Demirok A. Evaluation of corneal microstructure in keratoconus: a confocal microscopy study. Am J Ophthalmol. 2013;156:885-893.
27. Hollingsworth JG, Efron N, Tullo AB. In vivo corneal confocal microscopy in keratoconus. Ophthalmic Physiol Opt. 2005;25:254-260.
28. Matsuda M, Suda T, Manabe R. Quantitative analysis of endothelial mosaic pattern changes in anterior keratoconus. Am J Ophthalmol. 1984;98:43-49.
29. Laing RA, Sandstrom MM, Berrospi AR, Leibowitz HM. The human corneal endothelium in keratoconus: a specular microscopic study. Arch Ophthalmol. 1979;97:1867-1869.
30. El-Agha MS, El Sayed YM, Harhara RM, Essam HM. Correlation of Corneal Endothelial Changes With Different Stages of Keratoconus. Cornea. 2014;33:707-711.
31. Zadnik K, Barr JT, Gordon MO, Edrington TB. Biomicroscopic signs and disease severity in keratoconus. Collaborative longitudinal evaluation of keratoconus (CLEK) Study Group. Cornea. 1996;15:139-146.
32. Edmonds CR, Wung SF, Husz MJ, Pemberton B. Corneal endothelial cell count in keratoconus patients after contact lens wear. Eye Contact Lens. 2004;30:54-58.

DOI: 10.4274/tjo.77632
Turk J Ophthalmol 2017;47:261-266

Original Article

Vitreomacular Interface Disorders in Behçet's Uveitis

Hilal Eser Öztürk, Özlem Eşki Yücel, Yüksel Süllü
Ondokuz Mayıs University Faculty of Medicine, Department of Ophthalmology, Samsun, Turkey

Abstract

Objectives: To determine the prevalence of vitreomacular interface (VMI) disorders in patients with Behçet's uveitis and assess the relationship between VMI disorders and clinical characteristics.

Materials and Methods: The macular optical coherence tomography (OCT) images of 160 eyes of 96 patients with Behçet's uveitis who were being followed in the Uvea-Behçet's clinic were assessed retrospectively for VMI disorders including posterior vitreous detachment (PVD), epiretinal membrane (ERM), vitreomacular adhesion (VMA), vitreomacular traction (VMT), full-thickness macular hole (FTMH), lamellar hole (LH) and pseudohole.

Results: Twenty-four patients (25%) with unilateral and 72 patients with bilateral uveitis were included in the study. Six (30%) of 20 eyes with anterior uveitis and 57 (40.7%) of 140 eyes with posterior uveitis, in total 63 (39.4%) eyes of 160 eyes had at least one VMI disorder. PVD was detected in 4 eyes (2.5%), ERM in 48 eyes (30%), VMA in 12 eyes (7.5%), and LH in 1 eye (0.6%). None of the eyes had VMT, FTMH, or pseudohole. ERM was detected in 13 eyes (8.1%) on fundus examination and 48 (30%) eyes by OCT (p=0.001). VMI was detected in 12 (50%) of 24 eyes with prior intraocular surgery and 51 (37.5%) of 136 eyes without. The mean duration of uveitis was 7.3±5.8 years in patients with VMI disorders and 5.8±7.7 years in patients without (p=0.04). There was no relation between VMI disorders and anatomic location of uveitis, history of past ocular surgery, number of ocular/periocular steroid injections, or visual acuity.

Conclusion: VMI disorders are common in patients with Behçet's uveitis. Their frequency increases with the duration of uveitis. OCT is more sensitive than fundus examination in the detection of VMI disorders.

Keywords: Behçet's uveitis, vitreomacular interface, optical coherence tomography

Introduction

The vitreous is responsible for globe stabilization, and its relationship to the retinal surface is extremely complex. With aging, the vitreous starts to separate from the retina due to vitreous liquefaction and the weakening of vitreoretinal connections. This separation culminates in total posterior vitreous detachment (PVD) unless it is complicated by one of the vitreomacular interface (VMI) pathologies such as epiretinal membrane (ERM), vitreomacular adhesion (VMA), vitreomacular traction (VMT), full-thickness macular hole (FTMH), lamellar macular hole (LMH), or pseudohole. These pathologies can either occur idiopathically with advancing age or be triggered by intraocular inflammation such as uveitis. They may be completely asymptomatic or cause vision disorders including decreased visual acuity, photopsia, or metamorphopsia.[1,2] Moreover, they have been shown to impact treatment success when treating complications such as uveitic macular edema.[3]

Optical coherence tomography (OCT) is considered the gold standard in identifying these pathologies, determining prognosis, and in treatment and follow-up.[2,4,5]

Address for Correspondence: Hilal Eser Öztürk MD, Ondokuz Mayıs University Faculty of Medicine, Department of Ophthalmology, Samsun, Turkey
Phone: +90 532 573 70 25 E-mail: hilaleser@yahoo.com **ORCID-ID:** orcid.org/0000-0002-0050-7894
Received: 14.10.2016 **Accepted:** 06.02.2017

The aim of this study was to evaluate the frequency of VMI pathologies in patients with Behçet's uveitis as measured by OCT and determine their relation with uveitis duration and clinical findings.

Materials and Methods

The study included 160 eyes of 96 Behçet's uveitis patients, comprising 26 females (27.1%) and 70 males (72.9%), who were followed in the Uvea-Behçet's unit of the Ophthalmology Department of Ondokuz Mayıs University Faculty of Medicine between March 2015 and June 2016. Approval for the study was obtained from the Clinical Research Ethics Committee of Ondokuz Mayıs University and the Declaration of Helsinki was observed.

Data from the patients' most recent examination and OCT images obtained on the same date were reviewed retrospectively. Eyes that could not be imaged with OCT or yielded images with a signal strength of 6/10 or below were excluded from the study. The patients' age, duration of uveitis, site of involvement, presence of cataract, and any previous treatments and intraocular surgeries were recorded.

The Cirrus 512x128 macular cube measurements of all patients obtained by Cirrus Spectral Domain OCT (Carl Zeiss Meditec, Jena, Germany) were reviewed. The images were evaluated with regard to the presence of VMI pathologies such as PVD, ERM, VMT, VMA, FTMH, LMH, and pseudohole. The classification criteria of the International Vitreomacular Traction Study Group were used for defining these VMI pathologies (Table 1).[2] The definitions are summarized in Table 1. Macular thickness measurements were recorded for all patients.

We assessed the correlations between presence of VMI pathologies and age, duration and location of uveitis, average best corrected visual acuity, lens status, average number of posterior sub-Tenon's steroid injections, number of intraocular steroid injections, and clinical findings such as macular thickness. The correlation between those same parameters and ERM, one of the interface pathologies, was analyzed separately. Data related to the interface pathologies identified by OCT were used in the statistical analyses. In addition, we determined the extent to which PVD and ERM can be identified by fundus examination and/or OCT.

Statistical Analysis

The data obtained during the research was analysed using SPSS version 21.0 (SPSS, Chicago, IL, USA) software package. T-test was used in intergroup comparisons of continuous quantitative data with normal distribution; Mann-Whitney U test was used for comparisons of those that did not have normal distribution. Chi-square test was used in comparisons of discrete data. P values below 0.05 were accepted as statistically significant.

Results

The analysis included the medical records and macular OCT data of 96 patients with Behçet's uveitis, 12 (12.5%) with anterior segment involvement and 84 (87.55%) with posterior segment involvement, who presented between March 2015 and June 2016. Uveitic involvement was unilateral in 24 patients (25%) and bilateral in 72 patients (75%).

The OCT images of 160 eyes met the inclusion criteria and were evaluated. Sixty-three (39.4%) of the 160 eyes exhibited at least one VMI pathology on OCT (Figure 1). Furthermore, macular edema was detected in 15 eyes (9.4%) and macular atrophy in 41 eyes (25.6%). Although no FTMH was evident on OCT, 3 (3.1%) of the patients had previously undergone surgery for FTMH and achieved anatomic success. Including these 3 eyes, there were a total of 93 eyes (58.1%) with at least one macular pathology.

Assessment of the correlations between VMI pathology and age, duration and location of uveitis, average best corrected visual acuity, lens status, average number of posterior sub-Tenon's steroid injections, number of intraocular steroid injections, and macular thickness revealed significant correlation only between VMI pathology and duration of uveitis (p=0.045). The other data are shown in Table 2. The correlation between number of attacks per year and the presence of VMI pathology was examined but the result was nonsignificant (p=0.973). The correlation between average number of attacks and the presence of VMI pathology was also evaluated. The average number of attacks was 3.55±3.32 in the VMI pathology group and 3.49±4.56 in the non-VMI pathology group, which was not a statistically significant difference (p=0.107). ERM, which is the most common VMI pathology and has the greatest effect on vision, showed statistically significant correlations with duration of uveitis (p=0.041), visual acuity (p=0.009), and previous cataract surgery (p=0.005). The other data are shown in Table 3. While number of attacks per year was not significantly correlated with the presence of ERM (p=0.745), the average number of attacks was 4.00±3.6 in the ERM group and 3.30±4.30 in the non-ERM group, which was a statistically significant difference (p=0.008). Although OCT revealed PVD in only 4 (2.5%) of the eyes, the patients' medical records indicated that

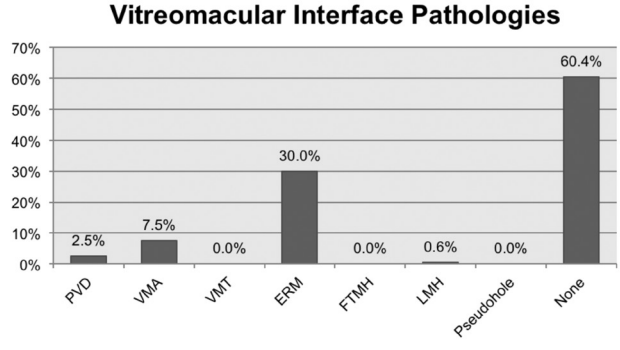

Figure 1. Prevalence of vitreomacular interface disorders detected with optical coherence tomography

PVD: Posterior vitreous detachment, VMA: Vitreomacular adhesion, VMT: Vitreomacular traction, ERM: Epiretinal membrane, FTMH: Full-thickness macular hole, LMH: Lamellar macular hole, VMID: Vitreomacular interface disorder

PVD was detected in 12 eyes (7.5%) on fundus examination (p=0.071). In contrast, ERM was detected in 13 eyes (8.1%) on fundus examination and 48 eyes (30%) on OCT, which was a statistically significant difference (p<0.05).

Discussion

While VMI pathologies can adversely affect visual acuity and quality, they may also manifest as clinically asymptomatic conditions detectable only by OCT. In particular, VMA without traction and localized PVD without posterior hyaloid thickening do not cause visual symptoms. However, studies conducted among patients with age-related macular degeneration (AMD) have shown that VMI pathologies strongly impact the efficacy of intravitreal anti-VEGF (vascular endothelial growth factor) therapy.[6,7] Consequently, Munk et al.[3] examined the effects of VMI pathology in the treatment of uveitis-related macular edema and demonstrated a larger and faster reduction in central retinal thickness in the PVD group as compared to the group with VMA but no PVD; however, they did not observe significant differences in visual acuity improvement or retinal volume. They reported that the detection of VMI pathology may be important in monitoring the treatment of uveitis complications and determining visual prognosis.

In our evaluation of VMI pathologies in patients with Behçet's uveitis, we identified at least one of these pathologies in 39.4% of the eyes, with PVD in 4 eyes (2.5%), ERM in 48 (30%), VMA in 12 (7.5%), and LMH in 1 eye (0.6%). Three eyes (3.1%) had previously undergone surgery for FTMH. This is consistent with two major studies in the literature, in which Tugal-Tutkun et al.[8] reported this rate as 2.6% and Benchekroun et al.[9] as 3.4%. Munk et al.[3] reported prevalences of 44.1% for VMA, 40.7% for PVD, and 39% for ERM in patients

Table 1. Definitions of vitreomacular interface pathologies

	OCT findings
PVD	Separation of the posterior vitreous from the retina with no adhesions
ERM	Presence of a hyperreflective signal at the inner retinal surface with evidence of contractility
VMA	Vitreous adhesion to the central macula with no distortion of foveal contour
VMT	Vitreous adhesion to the central macula causing distortion of foveal contour
FTMH	Disruption of retinal integrity including all neural retinal layers from the ILM to the RPE
LMH	Defect of the inner neural retinal layers with intact photoreceptor layer
Pseudohole	Presence of ERM with central opening and invaginated foveal edges without retinal tissue loss

OCT: Optical coherence tomography, PVD: Posterior vitreous detachment, ERM: Epiretinal membrane, VMA: Vitreomacular adhesion, VMT: Vitreomacular traction, FTMH: Full-thickness macular hole, LMH: Lamellar macular hole, ILM: Internal limiting membrane, RPE: Retinal pigment epithelium

Table 2. Demographic and clinical characteristics of Behçet's uveitis patients with and without vitreomacular interface disorders

	VMID (+)	**VMID (-)**	**p**
Number of patients/Eyes	49/63	47/97	
Mean age (years)	36.8±10.6	33.3±11.6	0.101
Sex Female Male	 12 (24.5%) 37 (75.5%)	 13 (27.7%) 34 (72.3%)	0.904
Uveitis duration (years)	7.3±5.8 (mean) 5.5 (median)	5.8±7.0 (mean) 3.0 (median)	**0.045**
Involvement Anterior uveitis Posterior uveitis	 6 (9.5%) 57 (90.5%)	 14 (14.4%) 83 (85.6%)	0.501
Visual acuity	0.6±0.3	0.7±0.3	0.268
Lens status Phakic Pseudophakic	 52 (82.5%) 11 (17.5%)	 90 (92.8%) 7 (7.2%)	0.081
Mean number of periocular steroid injections	0.6±1.52	0.6±1.13	0.612
Mean number of intraocular steroid injections	0.05±0.20	0.04±0.21	0.848
History of intraocular surgery other than cataract (+) (-)	 12 (19%) 51 (81%)	 12 (12.4%) 85 (87.6%)	0.353
Macular thickness	255.0±69.0	243.5±66.7	0.183

VMID: Vitreomacular interface disorder

Table 3. Demographic and clinical characteristics of Behçet's uveitis patients with and without epiretinal membrane			
	ERM +	**ERM -**	**p**
Number of patients/Eyes	38/48	58/112	
Age (years)	37.3±10.6	33.5±11.4	0.094
Sex Female Male	 7 (18.4%) 31 (81.6%)	 18 (31%) 40 (69%)	 0.255
Uveitis duration (years)	7.8±6.2 (mean)	6.0±6.5 (mean)	**0.041**
Involvement Anterior uveitis Posterior uveitis	 3 (6.3%) 45 (93.8%)	 17 (15.2%) 95 (84.4%)	 0.192
Visual acuity	0.60±0.3	0.74±0.3	**0.009**
Lens status Phakic Pseudophakic	 37 (77.1%) 11 (22.9%)	 105 (93.8%) 7 (6.3%)	 **0.005**
Mean number of posterior sub-Tenon injections	0.7±1.6	0.5±1.1	0.269
Number of intraocular injections	0.06±0.25	0.04±0.19	0.449
History of intraocular surgery other than cataract (+) (-)	 11 (22.9%) 37 (77.1%)	 13 (11.6%) 99 (88.4%)	 0.111
Macular thickness	249.7±75.8	247.4±64.2	0.955
ERM: Epiretinal membrane			

with uveitic cystoid macular edema. These percentages seem very high compared to the data we obtained in our study. This may be because our study was based on the data of all Behçet's uveitis patients, with or without complications, while Munk et al.[3] included only cases complicated by cystoid macular edema. In addition, because we used only OCT data to determine PVD prevalence, some cases of PVD may have been overlooked because they were not within the field of the acquired image. Munk et al.[3] used clinical examination findings as well as OCT to diagnose PVD. They described the OCT appearance of incomplete PVD as a preretinal, thin, hyperreflective band not connected to the macula. To diagnose complete PVD, they examined the medical records of patients whose vitreous margin was not visible on OCT scans and based their decision on the presence of Weiss ring and other signs of complete PVD in the examination findings. Although we mentioned the number of PVDs we detected during examination, these examination findings were not included in the analysis because the focus of our study was identifying VMI pathologies using OCT. PVD was determined to be the most common interface pathology in a study conducted on patients with neovascular AMD.[7] However, PVD is seen less frequently than VMA in uveitic patients. Munk et al.[3] have attributed this to the difference in age between patients in the AMD and uveitis groups. While age-related liquefaction of the vitreous leads to PVD, intraocular inflammation may contribute to the formation of VMA in younger uveitis patients.[3] There are also differences between age-related and uveitic VMI pathologies with regard to their mechanisms of formation. It was reported that the formation of idiopathic ERM occurs secondary to glial cell migration from the retinal nerve fiber layer, and requires retinal pigment epithelial (RPE) cells.[10] However, uveitic ERMs are different from idiopathic ERMs in that their mechanism of formation does not involve RPE and they contain a large number of inflammatory cells.[11]

In the present study, we identified at least one VMI pathology, macular edema, or macular atrophy in 65% of the eyes. Liu et al.[12] found this ratio to be 58.6% in their study on the uveitic population living in China. A particularly remarkable aspect of their study was that the rates of ERM (12.6%) and foveal atrophy (8.9%) were lower than in our study. A possible explanation for this discrepancy is that our study included patients with Behçet's uveitis, which is a specific uveitis group in which posterior segment involvement is more common.

The present study did not reveal statistically significant correlations between the presence of any of the VMI pathologies and any of the demographic or clinical data except for duration of uveitis. Analysis of the association between VMI pathologies and attack frequency revealed no significant correlation with the patients' average number of attacks or number of attacks per year. This may be due to our failure to determine the actual attack rate because we could not access patients' medical records before their presentation and/or because patients may not have visited the hospital for every attack. Although there was no significant association between presence of ERM and number of attacks per year, a correlation was observed between ERM and number of average attacks. We also found that presence of ERM was statistically correlated with longer duration of uveitis and pseudophakia. In addition, mean visual acuity was significantly lower in eyes with ERM compared to eyes without ERM. In

their study of the relationship between visual acuity and the morphologic characteristics of ERM, Nazari et al.[13] reported that central foveal involvement, presence of focal adherence, and foveal internal segment/external segment junction damage were correlated with low visual acuity. They also demonstrated that thick ERMs reduce vision more than thin ERMs, and that the thickness of ERMs is associated with their duration. In an epidemiologic study of uveitic patients, Nicholson et al.[14] reported that the presence of ERM is correlated with advanced age, duration of uveitis, male gender, cataract surgery history, and intermediate and posterior segment involvement. In our study, 3 (6.3%) of the patients with ERM had anterior segment involvement and 45 (93.8%) had posterior segment involvement. The lack of a statistically significant correlation between the site of involvement and the presence of ERM may be attributable to the low number of anterior uveitis patients.

Our evaluation of the effects of all previous injections and surgical procedures on the development of any of the VMI pathologies and ERM formation specifically revealed no statistically significant correlations with intraocular and posterior sub-Tenon's steroid injections or surgical procedures other than cataract surgery. Nicholson et al.[14] compared the eyes of patients with unilateral ERM and reported that a significantly higher proportion of the ERM eyes underwent vitrectomy, retinal laser, and intraocular injection, while there were no significant correlations with the other ophthalmologic surgeries and periocular steroid injections.

Only a third of the ERMs identified on OCT in our study were visible on fundus examination. Other studies comparing fundus photographs and fundoscopic examination with OCT indicated that 37-38% of membranes identified by OCT are overlooked in those methods. Therefore, OCT is currently considered the gold standard in ERM detection.[14,15] It is nearly impossible to detect localized, shallow PVD or VMA by fundus examination, and it is also difficult to detect VMT and examine macular hole characteristics. OCT plays an important role in the follow-up of VMI pathologies and evaluation of treatment efficacy, as well as determination of visual prognosis.[16]

Study Limitations

The main limitation of our study was its retrospective design. No data were available regarding patient follow-up prior to their presentation to our clinic.

Conclusion

Identifying the presence of VMI pathologies in uveitic patients can assist in predicting visual prognosis and managing complications. OCT is considered the gold standard in the detection and follow-up of these pathologies. Therefore, it is important to carefully evaluate the VMI in OCT images when following uveitic patients.

Acknowledgements

We would like to thank Assistant Professor Özlem Terzi from the Public Health Department of Ondokuz Mayıs University for her assistance with the statistical analyses.

Ethics

Ethics Committee Approval: Clinical Research Ethics Committee of Ondokuz Mayıs University (KAEK 2016/210).

Informed Consent: Retrospective study.

Peer-Review: Externally and internally peer-reviewed.

Authorship Contributions

Surgical and Medical Practices: Hilal Eser Öztürk, Özlem Eşki Yücel, Yüksel Süllü, Concept: Hilal Eser Öztürk, Özlem Eşki Yücel, Yüksel Süllü, Design: Hilal Eser Öztürk, Özlem Eşki Yücel, Yüksel Süllü, Data Collection or Processing: Hilal Eser Öztürk, Özlem Eşki Yücel, Analysis or Interpretation: Hilal Eser Öztürk, Özlem Eşki Yücel, Yüksel Süllü, Literature Search: Hilal Eser Öztürk, Özlem Eşki Yücel, Writing: Hilal Eser Öztürk, Özlem Eşki Yücel, Yüksel Süllü.

Conflict of Interest: No conflict of interest was declared by the authors.

Financial Disclosure: The authors declared that this study received no financial support.

References

1. Steel DH, Lotery AJ. Idiopathic vitreomacular traction and macular hole: a comprehensive review of pathophysiology, diagnosis, and treatment. Eye (Lond). 2013;27(Suppl 1):1-21.
2. Duker JS, Kaiser PK, Binder S, de Smet MD, Gaudric A, Reichel E, Sadda SR, Sebag J, Spaide RF, Stalmans P. The International Vitreomacular Traction Study Group classification of vitreomacular adhesion, traction, and macular hole. Ophthalmology. 2013;120:2611-2619.
3. Munk MR, Ram R, Rademaker A, Liu D, Setlur V, Chau F, Schmidt-Erfurth U, Goldstein DA. Influence of the vitreomacular interface on the efficacy of intravitreal therapy for uveitis-associated cystoid macular oedema. Acta Ophthalmol. 2015;93:561-567.
4. Onal S, Tugal-Tutkun I, Neri P, P Herbort C. Optical coherence tomography imaging in uveitis. Int Ophthalmol. 2014;34:401-435.
5. Erdem E, Sekeroglu HT, Soylu M, Ciloglu E. The Correlation of Clinical Findings and Macular Changes Detected by Optical Coherence Tomography in Patients with Uveitis. Turk J Ophthalmol. 2011;41:396-400.
6. Üney GÖ, Ünlü N, Acar MA, Hazirolan D, Altiparmak UE, Yalniz-Akkaya Z, Örnek F. Role of posterior vitreous detachment on outcome of anti-vascular endothelial growth factor treatment in age-related macular degeneration. Retina. 2014;34:32-37.
7. Mayr-Sponer U, Waldstein SM, Kundi M, Ritter M, Golbaz I, Heiling U, Papp A, Simader C, Schmidt-Erfurth U. Influence of the vitreomacular interface on outcomes of ranibizumab therapy in neovascular age-related macular degeneration. Ophthalmology. 2013;120:2620-2629.
8. Tugal-Tutkun I, Onal S, Altan-Yaycioglu R, Huseyin Altunbas H, Urgancioglu M. Uveitis in Behcet disease: an analysis of 880 patients. Am J Ophthalmol. 2004;138:373-380.
9. Benchekroun O, Lahbil D, Lamari H, Rachid R, El Belhadji M, Laouissi N, Zaghloul K, Benamour S, Amraoui A. Macular damage in Behcet's disease. J Fr Ophtalmol. 2004;27:154-159.

10. Snead DR, James S, Snead MP. Pathological changes in the vitreoretinal junction 1: epiretinal membrane formation. Eye (Lond). 2008;22:1310-1317.
11. Sheybani A, Harocopos GJ, Rao PK. Immunohistochemical study of epiretinal membranes in patients with uveitis. J Ophthalmic Inflamm Infect. 2012;2:243-248.
12. Liu T, Bi H, Wang X, Gao Y, Wang G, Ma W. Macular Abnormalities in Chinese Patients with Uveitis. Optom Vis Sci. 2015;92:858-862.
13. Nazari H, Dustin L, Heussen FM, Sadda S, Rao NA. Morphometric spectral-domain optical coherence tomography features of epiretinal membrane correlate with visual acuity in patients with uveitis. Am J Ophthalmol. 2012;154:78-86.
14. Nicholson BP, Zhou M, Rostamizadeh M, Mehta P, Agron E, Wong W, Wiley H, Nussenblatt R, Sen HN. Epidemiology of epiretinal membrane in a large cohort of patients with uveitis. Ophthalmology. 2014;121:2393-2398.
15. Milani P, Raimondi G, Morale D, Scialdone A. Biomicroscopy versus optical coherence tomography screening of epiretinal membranes in patients undergoing cataract surgery. Retina. 2012;32:897-904.
16. Barak Y, Ihnen MA, Schaal S. Spectral domain optical coherence tomography in the diagnosis and management of vitreoretinal interface pathologies. J Ophthalmol. 2012;2012:876472.

DOI: 10.4274/tjo.86461
Turk J Ophthalmol 2017;47:267-273

Original Article

Are All Retinal Nerve Fiber Layer Defects on Optic Coherence Tomography Glaucomatous?

Sirel Gür Güngör, Ahmet Akman
Başkent University Faculty of Medicine Department of Ophthalmolgy, Ankara, Turkey

Abstract

Objectives: In this study, we investigated the patients who were referred to our clinic with a prediagnosis of glaucoma based on retinal nerve fiber layer (RNFL) defects on optic coherence tomography (OCT) but were determined to have nonglaucomatous RNLF defects upon detailed examination.

Materials and Methods: The ophthalmic examination notes, OCT images, Heidelberg retinal tomography (HRT) II and fundus photographs of 357 patients were retrospectively evaluated. Final diagnoses of these patients were investigated.

Results: Of the 357 patients, 216 (60.5%) were diagnosed as open angle glaucoma, 33 (9.2%) as low-tension glaucoma, 39 (10.9%) as pre-perimetric glaucoma. The ophthalmic examinations of 14 patients (3.9%) were normal and there were no RNFL defects in OCT examinations after dilatation. In 39 patients (10.9%), the ophthalmic and optic disc examinations were completely normal and no etiologic factor explaining RNFL defects was found. Twenty-two eyes of 16 patients (4.5%) were included in this study (the mean age was 53.8±11.5 years; 9 men and 7 women). After detailed questioning of the medical history and systemic and neurologic examinations, a diagnosis of ischemic optic neuropathy was made in 11 eyes (10 patients) (2.8%), optic neuritis in 3 eyes (2 patients) (0.6%), optic disc drusen in 4 eyes (2 patients) (0.6%), pseudotumor cerebri in 2 eyes (1 patient) (0.3%), and cerebral palsy in 2 eyes (1 patient) (0.3%).

Conclusion: Decrease in RNFL thickness on OCT images alone may be misleading in glaucoma examination. In cases where optic disc cupping is not evident, diagnosis should not be based on OCT RNFL examinations alone, and the patient's medical history, detailed ophthalmic examination, OCT optic disc parameters, HRT, and visual field tests should all be carefully evaluated together.

Keywords: Anterior ischemic optic neuropathy, glaucoma, optic coherence tomography, retinal nerve fiber layer

Introduction

Optical coherence tomography (OCT) was first used in the 1990s for glaucoma and retinal diseases.[1,2,3,4] Today, it is increasingly used in nearly all sub-specialties of ophthalmology.

Glaucomatous optic neuropathy is characterized by thinning of the peripapillary retinal nerve fiber layer (RNFL) and optic disc cupping as a result of axonal and secondary retinal ganglion cell loss. RNFL defects on OCT are one of the earliest signs of glaucoma.[5,6,7,8,9] In ophthalmology practice, clinicians sometimes have difficulty with the differential diagnosis of RNFL defects resembling glaucoma, but it may be possible to distinguish these cases from glaucomatous eyes with a careful fundus examination and Heidelberg retinal tomography (HRT) II imaging.[10]

RNFL thinning is not specific to glaucomatous optic neuropathy and may also be seen in various nonglaucomatous optic neuropathies and central nervous system diseases.[11,12,13,14] In such clinical cases, RNFL thinning accompanied by optic disc cupping may be considered a finding in favor of glaucoma.[6,7,8,9,10]

In this study, we reviewed the examination findings and etiologies of patients who were referred to our glaucoma

Address for Correspondence: Sirel Gür Güngör MD, Başkent University Faculty of Medicine Department of Ophthalmolgy, Ankara, Turkey
Phone: +90 312 212 68 68 E-mail: sirelgur@yahoo.com **ORCID-ID:** orcid.org/0000-0001-6178-8362
Received: 19.09.2016 **Accepted:** 03.02.2017

outpatient clinic with possible glaucomatous RNFL damage but were found to have nonglaucomatous RNFL defects upon detailed ophthalmologic examination, OCT, and HRT II evaluation.

Materials and Methods

The names of 357 patients referred to our clinic for suspected or prediagnosed glaucoma based on RNFL defect identified during ophthalmologic examination and OCT between 2011 and 2015 were noted. The study was approved by Başkent University Institutional Review Board (project no: KA17-240) and supported by Başkent University Research Fund. Data regarding detailed ophthalmologic and systemic history, best corrected visual acuity, intraocular pressure measurement by applanation tonometry, central corneal thickness, and slit-lamp anterior segment and dilated fundus examinations were recorded. The patients had also undergone fundus photography and 24-2 visual field, OCT, and HRT II imaging. Patients with ophthalmologic diseases other than neuroophthalmologic conditions that may affect visual field, OCT and HRT II, those with spherical refraction greater than ±5 diopter (D) or astigmatism greater than ±3 D, those who had previous ocular surgery other than cataract surgery, those whose HRT II images were of poor quality, and those who had less than 5/10 signal strength on OCT were excluded from the study.

Non-arteritic ischemic optic neuropathy (NAION) diagnosis was based on a history of acute, painless incomplete vision loss combined with optic disc edema, and superficial hemorrhage at the margins of the optic disc in the adjacent retinal area.[15,16,17] The patients were asked in detail about signs and symptoms suggestive of arteritic anterior ischemic optic neuropathy as described by Beck et al.[18] These include systemic symptoms of giant cell arteritis, sudden decrease in visual acuity to hand movement or lower, chalky white edema of the optic disc, occlusion of one or more posterior ciliary arteries in fundus fluorescein angiography, and high erythrocyte sedimentation rate (55 mm/hour).

Visual field was assessed via 24-2 full-threshold test using Humphrey automatic perimetry (Humphrey Instruments, Inc., Dublin, California, USA). The test was repeated for patients with over 33% false positivity and false negativity and over 20% fixation loss. Cirrus HD spectral domain OCT (Carl Zeiss Meditec, Dublin, CA, USA) was used to evaluate the optic disc head and RNFL. For HRT II (HRT II, Heidelberg Engineering, Dossenheim, Germany) measurements, three topographical images were obtained from each patient and automatically rendered into a single averaged topographical image for analysis. An experienced technician identified the optic disc margins on the averaged topographical image using a color photograph of the optic disc.

Glaucoma diagnosis was based on a lack of optic disc pallor in patients having visual field defect consistent with typical glaucomatous optic disc appearance. Daytime measurements were repeated for patients whose intraocular pressure measurements were below 21 mmHg. Typical glaucomatous optic disc appearance involves vertical cup-to-disc (C/D) ratio greater than 0.6, localized thinning of the neural rim, splinter hemorrhages, and/or visible nerve fiber layer defect.

Patients were noted as having nonglaucomatous RNFL damage when RNFL defect was detected on OCT but the optic disc appeared nonglaucomatous in both dilated fundus examination and optic nerve topographic imaging by OCT and HRT (C/D ratio <0.6, optic disc parameters within normal limits). These patients' ophthalmologic data and results of neurologic consultation were analyzed retrospectively.

Results

Of the 357 patients referred to our clinic for RNFL thinning, 216 (60.5%) were diagnosed with open-angle glaucoma, 33 (9.2%) with low-pressure glaucoma, and 39 (10.9%) with pre-perimetric glaucoma. In 14 patients (3.9%), ophthalmologic examination was normal and no RNFL damage was detected in OCT examination. In 39 patients (10.9%), ophthalmologic and optic disc examinations were completely normal. OCT and HRT disc parameters were appropriate for the patients' ages. No etiological factors were found to explain RNFL defect on OCT. These patients were followed for approximately 25.2±12.31 months (12-47 months) and exhibited no progression. The RNFL damage seen in these patients was considered artifact or anatomic variation.

Twenty-two eyes of 16 patients (4.5%) were included in our analysis. Optic disc examination of these eyes revealed no glaucomatous cupping. Both OCT and HRT II disc topographic analyses were consistent with the optic disc examinations, and the C/D ratios were normal. The mean age of these patients was 53.8±11.5 years (43-70 years). Nine were male, 7 were female. The average corrected visual acuity of the patients was 0.8±0.4 (0.05-1.0). All of the patients had intraocular pressure values below 21 mmHg. The average intraocular pressure was 16.2±12.3 mmHg (8-19 mmHg) and the average central corneal thickness was 546.32±24.46 µm (536-587 µm). Eighteen eyes of 14 patients exhibited RNFL damage with optic disc pallor. The disc parameters determined by OCT and HRT are presented in Tables 1 and 2.

OCT revealed superior, temporal, and inferior RNFL damage in 8 eyes; superior, nasal, and inferior RNFL damage in 4 eyes; superior and temporal RNFL damage in 4 eyes; and 360º RNFL damage in 6 eyes. Table 3 shows the distribution of RNFL defects based on disease.

Nine eyes had generalized depression of the visual field, 2 had superotemporal quadrantanopsia, 1 had superior and inferior arcuate defect, 1 had depression in the nasal quadrant, and 5 had inferior hemifield defect. There was no visual field loss in 4 eyes. Patients with no visual field loss had RNFL

defects associated with optic disc drusen. Evaluation of visual field parameters revealed a median deviation of -11.7±10.8 (-31.12-0.62) and pattern standard deviation of 6.5±4.2 (1.6-13.05).

Upon detailed review of these patients' medical history and systemic and neurological examination, 11 eyes (10 patients) (2.8%) were diagnosed with previous ischemic optic neuropathy (Figure 1), 3 eyes (2 patients) (0.6%) with optic neuritis associated with multiple sclerosis (MS) (Figure 2), 4 eyes (2 patients) (0.6%) with optic disc drusen, 2 eyes (1 patient) (0.3%) with pseudotumor cerebri (PTC), and 2 eyes (1 patient) (0.3%) with cerebral palsy. The distribution of etiological factors according to the RNFL defects is shown in Table 4. Ischemic optic neuropathy, MS, PTC, and cerebral palsy are presented collectively as neuroophthalmologic diseases.

Of the patients diagnosed with NAION (10 patients, 11 eyes), 3 were followed in our clinic in the acute period, but the remaining 7 were diagnosed after reviewing the symptoms with the patient and requesting a detailed examination report from the hospital where the patient was treated. For all patients, at least 6 months had passed since the acute optic disc edema period and the optic disc margins could be clearly distinguished during the study.

Discussion

RNFL thinning is seen on OCT in both glaucoma and nonglaucomatous optic neuropathies and central nervous system diseases.[12,19,20] These diseases include ischemic optic neuropathy, optic neuritis, hereditary optic neuropathy, traumatic optic neuropathy, MS, and degenerative diseases such as Alzheimer's and Parkinson's disease.[11,12,13,14,19,20,21,22]

In our study, NAION was the most common diagnosis in patients with RNFL thinning who presented with suspected glaucoma. NAION is believed to be caused by acute perfusion deficiency around the optic nerve head. Although the actual etiology has not yet been clarified, a possible reason is reduced circulation to the posterior ciliary arteries.[23,24] NAION patients have small disc area, no or minimal physiological cupping, and characteristic disc structures such as "crowded disc", in which there is an excessive number of central retinal vein branches within the disc.[25] Horowitz et al.[13] compared RNFL thickness measured by OCT (at least 6 months after loss of vision) of 18 AION eyes with hemifield defect with the RNFL thickness of 29 glaucomatous eyes with hemifield defect, and found that the RNFL in the area corresponding to the visual field defect was similar between the two groups. However, the authors reported that the glaucomatous eyes exhibited more extensive RNFL thinning in quadrants which were unrelated to the visual field loss. They attributed this difference to the etiological differences underlying the RNFL thinning in glaucoma and NAION.

The acute phase of NAION does not mimic glaucoma symptoms. The optic nerve edema occurring in acute NAION is associated with increased RNFL thickness; Contreras et al.[26] showed that RNFL thickness in eyes with acute NAION was 96.4% greater than in the patients' fellow eyes. At 6-month follow-up, the RNFL of these patients was thinnest in the superior quadrant, followed by inferior, temporal, and nasal quadrants. This pattern explains why the inferior visual field is most affected in eyes with AION.[27]

Yang et al.[28] used Fourier domain OCT to compare optic nerve head and RNFL thickness in individuals with glaucoma, with NAION, and in healthy individuals. In their study,

Table 1. Optic disc parameters on optical coherence tomography in patients with nonglaucomatous retinal nerve fiber layer damage

	Mean	Standard deviation	Minimum	Maximum
Average RNFL thickness (µm)	79.7	20.3	52	117
Rim area (mm^2)	1.5	0.4	1.1	2.1
Disc area (mm^2)	1.8	0.2	1.5	2.1
Average C/D	0.4	0.2	0.1	0.6
Vertical C/D	0.4	0.2	0.1	0.6
Cup volume (mm^3)	0.1	0.1	0	0.2

C/D: Cup-to-disc ratio, RNFL: Retinal nerve fiber layer

Table 2. Optic disc parameters on Heidelberg retinal tomography in patients with nonglaucomatous retinal nerve fiber layer damage

	Mean	Standard deviation	Minimum	Maximum
Average RNFL thickness (µm)	0.2	0.1	0.1	0.3
Rim area (mm^2)	1.6	0.3	1.1	1.9
Disc area (mm^2)	1.9	0.4	1.2	2.2
Linear C/D	0.3	0.2	0.1	0.5
Rim volume	0.4	0.2	0.1	0.6

C/D: Cup-to-disc ratio, RNFL: Retinal nerve fiber layer

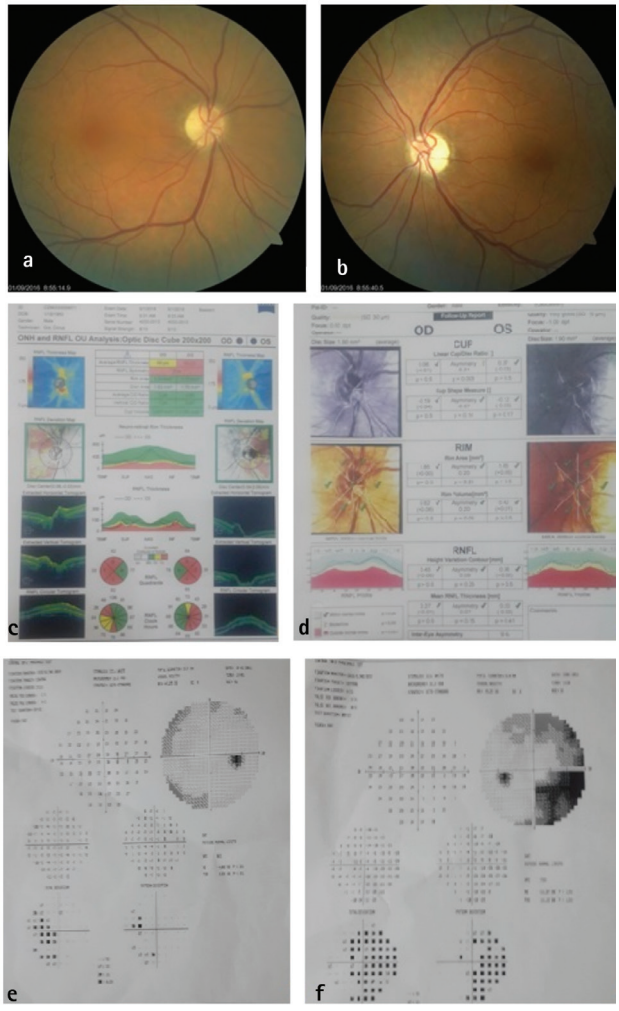

Figure 1. A 65-year-old male patient with bilateral non-arteritic ischemic optic neuropathy: a, b) There is no cupping in either eye and optic disc pallor is evident in the left eye; c) Optical coherence tomography shows retinal nerve fiber layer (RNFL) defects in both eyes; d) Heidelberg retinal tomography images are within normal limits; e, f) A visual field defect is detected in the region corresonding to RNFL thinning

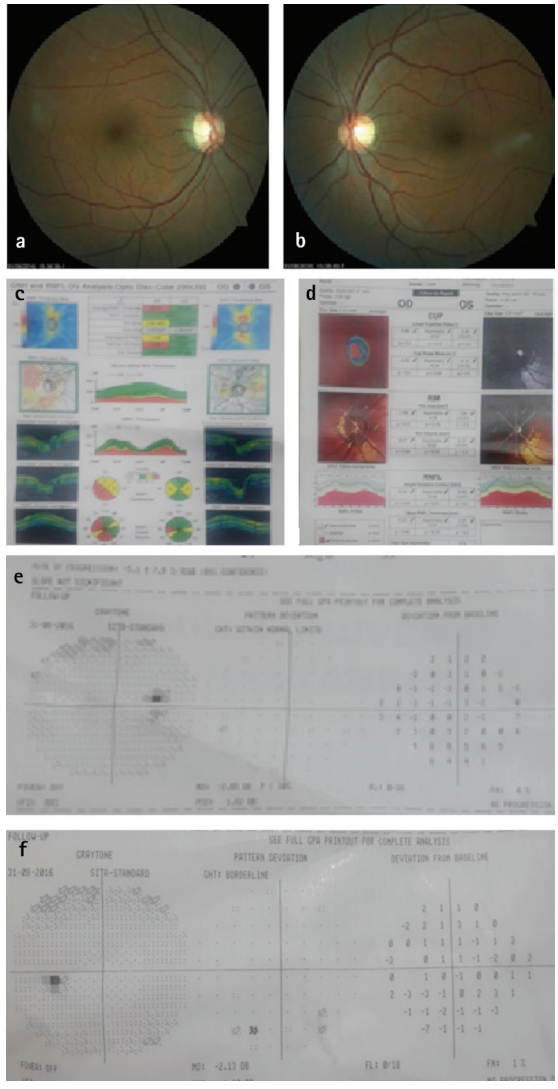

Figure 2. A patient with history of multiple sclerosis-associated retrobulbar optic neuritis. Optic disc examination, visual field test, and Heidelberg retinal tomography are within normal limits, while optical coherence tomography reveals retinal nerve fiber layer defect in the right eye

glaucomatous eyes exhibited larger cup area and volume, higher C/D ratio, and smaller rim area and disc volume. NAION eyes had the smallest cup area and volume, while their rim area and volume and disc volume were comparable to those of the control group. While RNFL thickness is most commonly seen in the superotemporal and inferotemporal zones in glaucomatous eyes, it is mostly seen in the superonasal region in eyes with NAION. In our study, eyes with NAION exhibited RNFL thinning in the superonasal and inferior zones in 2 eyes, whereas the superotemporal RNFL was affected in 1 eye, the superotemporal and inferior RNFL in 6 eyes, and 360° RNFL in 2 eyes.

MS patients may have subclinical RNFL thinning, even if they have no history of optic neuritis.[29,30,31] The etiology of RNFL damage in 3 eyes of 2 patients included in this research was attributed to MS and previous optic neuritis history. Bock et al.[30] compared RNFL thickness measurements in OCT of patients with and without optic neuritis history and patients with glaucomatous optic neuropathy. They found that although the average and quadrant RNFL thicknesses in all three groups were less than those of the control group, there were no differences in RNFL thickness between the three groups. Temporal peripapillary area was found to be thinner in patients with a history of optic neuritis. The patients included in our study also exhibited similar thinning in the temporal RNFL. In a study conducted by Yılmazbaş et al.[32], the RNFL thickness of affected eyes in patients with MS-associated unilateral optic neuritis was lower when compared to their healthy fellow eyes and to the control group. Daldal et al.[33] compared the RNFL thickness of patients with MS-related

Table 3. Distribution of retinal nerve fiber layer damage according to disease

RNFL location	NAION, 11 eyes (10 patients)	Optic neuritis, 3 eyes (2 patients)	PTS, 2 eyes (1 patient)	Cerebral palsy, 2 eyes (1 patient)	Optic disc drusen, 4 eyes (2 patients)
Superior/temporal/inferior	6	2	-	-	-
Superior/nasal/inferior	2	-	-	-	2
Superior/temporal	1	1	-	-	2
360°	2	-	2	2	-

RNFL: Retinal nerve fiber layer, NAION: Nonarteritic ischemic optic neuropathy, PTC: Pseudotumor cerebri

Table 4. Prevalence of retinal nerve fiber layer defects according to etiology

	Primary open-angle glaucoma	Low-pressure glaucoma	Pre-perimetric glaucoma	Normal (no RNFL defect)	Artifact/anatomic variation RNFL defect	Neuroophthalmologic disease	Optic disc drusen
Patient number (n)	216	33	39	14	39	14	2
Percentage (%)	60.5	9.2	10.9	3.9	10.9	3.9	0.6

RNFL: Retinal nerve fiber layer

optic neuritis history and patients with no optic neuritis history to a healthy control group, and found a greater reduction in RNFL thickness in the eyes with history of optic neuritis. In their study, RNFL thinning occurred most commonly in the temporal zone, as in our research.

In our study, we identified optic disc drusen in 4 eyes of 2 patients during glaucoma examination performed due to RNFL loss. Optic disc drusen may damage nerve axons, consequently leading to RNFL defects. These defects may affect the visual field and raise suspicion of glaucoma.[34] In addition, drusen may apply local pressure to the venous and arterial vessels, resulting in thinning of the RNFL. There have been few studies on the differential diagnosis between glaucoma and RNFL defects caused by drusen. Roh et al.[35] demonstrated that patients with optic disc drusen have thinner RNFL in the superior and inferior quadrants compared to a healthy control group. Of the 4 eyes with optic disc drusen that were included in our study, 2 had superior, nasal, and inferior RNFL thinning and 2 had superior and temporal RNFL thinning. None of the patients with optic disc drusen included in our study had visual field defect due to RNFL thinning. In patients with optic disc drusen who develop glaucoma, it may be difficult to identify the exact cause of RNFL damage and prescribe treatment. In such cases, it is useful to monitor RNFL damage with progression analysis methods. However, it should be kept in mind that RNFL damage may continue in both conditions.

PTC was identified in the detailed examination of a patient with RNFL defect that was included in our study. The patient had been prescribed oral acetazolamide treatment but did not regularly attend follow-up appointments. Chronic papilledema is a major cause of progressive and permanent vision loss in PTC patients.[36,37,38] RNFL thickness increases during the papilledema period and OCT may be used to monitor optic disc edema. There are studies in the literature reporting improvements in RNFL thickness and visual field parameters after PTC treatment.[39,40] Other studies have also suggested that OCT can be used to monitor the results of medical and surgical treatment of PTC.[41,42] However, in the presence of papilledema it is not possible to quantify retinal nerve loss using OCT because RNFL thickness increases in optic disc edema, thus preventing the detection of axonal loss.[43] When patients develop optic atrophy in the chronic period, RNFL thinning is already an expected outcome.[44]

In the present study, one patient was diagnosed with cerebral palsy. This patient's optic disc did not appear glaucomatous and there was optic atrophy. Cerebral palsy may be accompanied by unilateral or bilateral optic atrophy. The most common cause of optic atrophy in cerebral palsy is direct trauma to the orbit during birth or, less frequently, trauma to the base of the skull.[45,46,47]

Conclusion

RNFL thinning may occur in neuroophthalmologic diseases and optic disc anomalies. In the differential diagnosis of glaucomatous and nonglaucomatous optic neuropathies, OCT evaluation should include not only RNFL measurements but also disc topography parameters. A careful ophthalmologic examination and HRT optic disc topography, if available, can also facilitate differential diagnosis.

Ethics

Ethics Committee Approval: KA17/240 Başkent University.

Informed Consent: Retrospective study.
Peer-review: Externally peer-reviewed.

Authorship Contributions

Surgical and Medical Practices: Sirel Gür Güngör, Ahmet Akman, Concept: Ahmet Akman, Design: Ahmet Akman, Data Collection or Processing: Sirel Gür Güngör, Analysis or Interpretation: Sirel Güngör, Literature Search: Sirel Gür Güngör, Writing: Sirel Gür Güngör, Ahmet Akman.

Conflict of Interest: No conflict of interest was declared by the authors.

Financial Disclosure: The authors declared that this study received no financial support

References

1. Schuman JS, Hee MR, Arya AV, Pedut-Kloizman T, Puliafito CA, Fujimoto JG, Swanson EA. Optical coherence tomography: a new tool for glaucoma diagnosis. Curr Opin Ophthalmol. 1995;6:89-95.
2. Puliafito CA, Hee MR, Lin CP, Reichel E, Schuman JS, Duker JS, Izatt JA, Swanson EA, Fujimoto JG. Imaging of macular diseases with optical coherence tomography. Ophthalmology. 1995;102:217-229.
3. Hee MR, Puliafito CA, Wong C, Duker JS, Reichel E, Schuman JS, Swanson EA, Fujimoto JG. Optical coherence tomography of macular holes. Ophthalmology. 1995;102:748-756.
4. Hee MR, Puliafito CA, Duker JS, Reichel E, Coker JG, Wilkins JR, Schuman JS, Swanson EA, Fujimoto JG. Topography of diabetic macular edema with optical coherence tomography. Ophthalmology. 1998;105:360-370.
5. Kwon YH, Fingert JH, Kuehn MH, Alward WL. Primary open-angle glaucoma. N Engl J Med. 2009;360:1113-1124.
6. Magacho L, Marcondes AM, Costa VP. Correlation between optic disc topography and retinal nerve fibre layer measurements in glaucoma. Acta Ophthalmol Scand. 2005;83:322-327.
7. Shimazawa M, Tomita G, Taniguchi T, Sasaoka M, Hara H, Kitazawa Y, Araie M. Morphometric evaluation of changes with time in optic disc structure and thickness of retinal nerve fibre layer in chronic ocular hypertensive monkeys. Exp Eye Res. 2006;82:427-440.
8. Toprak AB, Yilmaz OF. Relation of optic disc topography and age to thickness of retinal nerve fibre layer as measured using scanning laser polarimetry, in normal subjects. Br J Ophthalmol. 2000;84:473-478.
9. Yucel YH, Gupta N, Kalichman MW, Mizisin AP, Hare W, de Souza Lima M, Zangwill L, Weinreb RN. Relationship of optic disc topography to optic nerve fiber number in glaucoma. Arch Ophthalmol. 1998;116:493-497.
10. Bayer A, Erdurman C, Uysal Y, Bakır B, Kılıç S, Bayraktar MZ. Glokomlu olgularla normal olguları ayırt etmede konfokal tarayıcı laser tomografi. MN Oftalmoloji. 2003;10:241-244.
11. Paquet C, Boissonnot M, Roger F, Dighiero P, Gil R, Hugon J. Abnormal retinal thickness in patients with mild cognitive impairment and Alzheimer's disease. Neurosci Lett. 2007;420:97-99.
12. Inzelberg R, Ramirez JA, Nisipeanu P, Ophir A. Retinal nerve fiber layer thinning in Parkinson disease. Vision Res. 2004;44:2793-2797.
13. Horowitz J, Fishelzon-Arev T, Rath EZ, Segev E, Geyer O. Comparison of optic nerve head topography findings in eyes with nonarteritic anterior ischemic optic neuropathy and eyes with glaucoma. Graefes Arch Clin Exp Ophthalmol. 2010;248:845-851.
14. Pueyo V, Ara JR, Almarcegui C, Martin J, Güerri N, García E, Pablo LE, Honrubia FM, Fernandez FJ. Sub-clinical atrophy of the retinal nerve fibre layer in multiple sclerosis. Acta Ophthalmol. 2010;88:748-752.
15. Saito H, Tomidokoro A, Sugimoto E, Aihara M, Tomita G, Fujie K, Wakakura M, Araie M. Optic disc topography and peripapillary retinal nerve fiber layer thickness in nonarteritic ischemic optic neuropathy and open-angle glaucoma. Ophthalmology. 2006;113:1340-1344.
16. Chan CK, Cheng AC, Leung CK, Cheung CY, Yung AY, Gong B, Lam DS. Quantitative assessment of optic nerve head morphology and retinal nerve fibre layer in non-arteritic anterior ischaemic optic neuropathy with optical coherence tomography and confocal scanning laser ophthalmoloscopy. Br J Ophthalmol. 2009;93:731-735.
17. Bellusci C, Savini G, Carbonelli M, Carelli V, Sadun AA, Barboni P. Retinal nerve fiber layer thickness in nonarteritic anterior ischemic optic neuropathy: OCT characterization of the acute and resolving phases. Graefes Arch Clin Exp Ophthalmol. 2008;246:641-647.
18. Beck RW, Servais GE, Hayreh SS. Anterior ischemic optic neuropathy. IX. Cup-to-disc ratio and its role in pathogenesis. Ophthalmology. 1987;94:1503-1508.
19. Pasol J. Neuro-ophthalmic disease and optical coherence tomography: glaucoma look-alikes. Curr Opin Ophthalmol. 2011;22:124-132.
20. Moschos MM, Tagaris G, Markopoulos I, Margetis I, Tsapakis S, Kanakis M, Koutsandrea C. Morphologic changes and functional retinal impairment in patients with Parkinson disease without visual loss. Eur J Ophthalmol. 2011;21:24-29.
21. Kim TW, Hwang JM. Stratus OCT in dominant optic atrophy: features differentiating it from glaucoma. J Glaucoma. 2007;16:655-658.
22. Cunha LP, Costa-Cunha LV, Malta RF, Monteiro ML. Comparison between retinal nerve fiber layer and macular thickness measured with OCT detecting progressive axonal loss following traumatic optic neuropathy. Arq Bras Oftalmol. 2009;72:622-625.
23. Hayreh SS. Anterior ischaemic optic neuropathy. II. Fundus on ophthalmoscopy and fluorescein angiography. Br J Ophthalmol. 1974;58:964-980.
24. Tesser RA, Niendorf ER, Levin LA. The morphology of an infarct in nonarteritic anterior ischemic optic neuropathy. Ophthalmology. 2003;110:2031-2035.
25. Burde RM. Optic disk risk factors for nonarteritic anterior ischemic optic neuropathy. Am J Ophthalmol. 1993;116:759-764.
26. Contreras I, Noval S, Rebolleda G, Munoz-Negrete FJ. Follow-up of nonarteritic anterior ischemic optic neuropathy with optical coherence tomography. Ophthalmology. 2007;114:2338-2344.
27. Hayreh SS, Zimmerman B. Visual field abnormalities in nonarteritic anterior ischemic optic neuropathy: their pattern and prevalence at initial examination. Arch Ophthalmol. 2005;123:1554-1562.
28. Yang Y, Zhang H, Yan Y, Gui Y, Zhu T. Comparison of optic nerve morphology in eyes with glaucoma and eyes with non-arteritic anterior ischemic optic neuropathy by Fourier domain optical coherence tomography. Exp Ther Med. 2013;6:268-274.
29. Optic Neuritis Study Group. Multiple sclerosis risk after optic neuritis: final optic neuritis treatment trial follow-up. Arch Neurol. 2008;65:727-732.
30. Bock M, Brandt AU, Dörr J, Kraft H, Weinges-Evers N, Gaede G, Pfueller CF, Herges K, Radbruch H, Ohlraun S, Bellmann-Strobl J, Kuchenbecker J, Zipp F, Paul F. Patterns of retinal nerve fiber layer loss in multiple sclerosis patients with or without optic neuritis and glaucoma patients. Clin Neurol Neurosurg. 2010;112:647-652.
31. Petzold A, de Boer JF, Schippling S, Vermersch P, Kardon R, Green A, Calabresi PA, Polman C. Optical coherence tomography in multiple sclerosis: a systematic review and meta-analysis. Lancet Neurol. 2010;9:921-932.
32. Yılmazbaş P, Erdemoğlu AK, Onaran Z, Güllü R, Bak G. Tek taraflı optik nevrit geçiren multipl sklerozisli hastalarda diğer gözde retina sinir lifi kalınlığı. Türkiye Klinikleri J Ophthalmol. 2010;19:103-106.
33. Daldal H, Tök ÖY, Şengeze N, Koyuncuoğlu HR, Tök L, Özkaya D, Bardak YK. Multipl sklerozda retina sinir lifi tabakası kalınlığı. Turk J Ophthalmol. 2011;41:1-5.
34. Wilkins JM, Pomeranz HD. Visual manifestations of visible and buried optic disc drusen. J Neuroophthalmol. 2004;24:125-129.
35. Roh S, Noecker RJ, Schuman JS, Hedges TR 3 rd, Weiter JJ, Mattox C. Effect of optic nerve head drusen on nerve fiber layer thickness. Ophthalmology. 1998;105:878-885.

36. Corbett JJ, Savino PJ, Thompson HS, Kansu T, Schatz NJ, Orr LS, Hopson D. Visual loss in pseudotumor cerebri. Follow-up of 57 patients from five to 41 years and a profile of 14 patients with permanent severe visual loss. Arch Neurol. 1982;39:461-474.
37. Wall M, George D. Idiopathic intracranial hypertension. A prospective study of 50 patients. Brain. 1991;114:155-180.
38. Hedges TR 3rd, Legge RH, Peli E, Yardley CJ. Retinal nerve fiber layer changes and visual field loss in idiopathic intracranial hypertension. Ophthalmology. 1995;102:1242-1247.
39. Skau M, Sander B, Milea D, Jensen R. Disease activity in idiopathic intracranial hypertension: a 3-month follow-up study. J Neurol. 2011; 258:277-283.
40. Yri HM, Wegener M, Sander B, Jensen R. Idiopathic intracranial hypertension is not benign: a long-term outcome study. J Neurol. 2012;255:886-894.
41. Skau M, Milea D, Sander B, Wegener M, Jensen R. OCT for optic disc evaluation in idiopathic intracranial hypertension. Graefes Arch Clin Exp Ophthalmol. 2011;249:723-730.
42. Scott CJ, Kardon RH, Lee AG, Frisen L, Wall M. Diagnosis and grading of papilledema in patients with raised intracranial pressure using optical coherence tomography vs clinical expert assessment using a clinical staging scale. Arch Ophthalmol. 2010;128:705-711.
43. Monteiro ML, Afonso CL. Macular thickness measurements with frequency domain-OCT for quantification of axonal loss in chronic papilledema from pseudotumor cerebri syndrome. Eye (Lond). 2014;28:390-398.
44. Starks V, Gilliland G, Vrcek I, Gilliland C. Effect of optic nerve sheath fenestration for idiopathic intracranial hypertension on retinal nerve fiber layer thickness. Orbit. 2016;35:87-90.
45. Vannas M. Zur Schervenatrophie nach Geburtsverletzung. Acta Ophthalmol. 1933;11:514-525.
46. Scheiman MM. Optometric findings in children with cerebral palsy. Am J Optom Physiol Opt. 1984;61:321-323.
47. Jakobson L, Hellstrom A, Flodmark O. Large cups in normal-sized optic discs: a variant of optic nerve hypoplasia in children with periventricular leukomalacia. Arch Ophthalmol. 1997;115:1263-1269.

DOI: 10.4274/tjo.28863
Turk J Ophthalmol 2017;47:274-278

Original Article

Outcomes of Intravitreal Dexamethasone Implant in the Treatment of Recalcitrant Diabetic Macular Edema

Dorukcan Akıncıoğlu, Murat Küçükevcilioğlu, Ali Hakan Durukan, Seçkin Aykaş, Önder Ayyıldız, Fazıl Cüneyt Erdurman

Gülhane Training and Research Hospital, Ophthalmology Clinic, Ankara, Turkey

Abstract

Objectives: To investigate the efficacy and safety of intravitreal dexamethasone (OZURDEX®) implantation in patients with recalcitrant diabetic macular edema.

Materials and Methods: This is a retrospective non-randomized study of patients who underwent intravitreal dexamethasone implantation for recalcitrant diabetic macular edema. Main outcome measures included changes in best corrected visual acuity (BCVA), central macular thickness (CMT), and incidence of ocular side effects.

Results: Fifty-seven eyes of thirty-eight patients (20 females, 18 males; mean age 65±7 years) were included in the study. The mean hemoglobin A1c level was 7.9±1.7%. Before entering the study, patients had undergone 5.71±3.40 anti-vascular endothelial growth factor (anti-VEGF) and 3.44±2.46 intravitreal triamcinolone acetonide injections. The mean duration of diabetes and diabetic macular edema was 17.2±6.4 years and 60.2±17.6 months, respectively. At baseline, mean CMT was 506.76±166.74 µm, and the mean BCVA was 0.68±0.38 LogMAR. Mean CMT significantly decreased to 341.36±146.26 µm ($p<0.001$), 324.41±114.58 µm ($p<0.001$), and 384.82±151 µm ($p<0.001$) at 1, 3, and 4 months of follow-up and increased again to 462.29±152.87 µm at 5 months. Sixteen eyes (28%) received second injections after mean of 7.4±2.3 months and mean CMT was again significantly decreased at 7, 8, and 9 months. Significant improvement in mean BCVA (0.54±0.41 LogMAR; $p<0.001$) occurred only at 1 month after implantation. However, subgroup analysis revealed significant BCVA improvement in the pseudophakic group at 1, 3, and 4 months. Among phakic patients, 50% showed cataract progression and 28% had elevated intraocular pressure increase which was managed medically.

Conclusion: Intravitreal dexamethasone implantation was effective for the first 4 months in eyes with recalcitrant diabetic macular edema. However, it is hard to displace anti-VEGF agents as first-line therapy due to steroid-related complications.

Keywords: Dexamethasone, recalcitrant, diabetic, implant

Introduction

Diabetic macular edema (DME) causes reduced central vision due to swelling or thickening of the retinal tissue in the foveal region.[1] Vision loss is seen in up to 33% of eyes with DME if untreated,[2] and 6.8% of people with diabetes demonstrate DME.[3] Lack of improvement solely with strict glycemic control gave rise to serial clinical trials, and laser photocoagulation is considered to be the gold standard based on the Early Treatment Diabetic Retinopathy Study (ETDRS).[4] Although this study showed that focal laser treatment reduced the risk of visual loss in patients with DME by 50%, visual field defects and subjective visual complaints were considered a serious problem because focal laser treatment was based on disrupting leaking vessels to reduce retinal thickness. Another study revealed increased cytokine levels in the posterior segment causing disruption of blood-retina barrier and leading to edema.[5] Therefore, targeted therapy was regarded as the new choice. Several studies supported ranibizumab as a favorable alternative to laser therapy. RESTORE provided long-term safety and efficacy data for

Address for Correspondence: Dorukcan Akıncıoğlu MD, Gülhane Training and Research Hospital, Ophthalmology Clinic, Ankara, Turkey
Phone: +90 533 458 94 55 E-mail: dr.dorukcan@yahoo.com **ORCID-ID**: orcid.org/0000-0001-6409-9802
Received: 27.07.2016 **Accepted:** 20.01.2017

ranibizumab (Lucentis™, Genentech, San Francisco, CA, USA),[6] RISE and RIDE reported favorable results in subjects with clinically significant macular edema,[7] and the Diabetic Retinopathy Clinical Research Network study offered long-term outcomes of laser treatment for DME in combination with anti-vascular endothelial growth factor (VEGF) agents.[8] Moreover, the BOLT study showed significant visual gain with bevacizumab (Avastin®, Genentech, San Francisco, CA, USA) in comparison to laser therapy alone.[9] The VEGF-Trap molecule was later designed to decrease VEGF levels more effectively. Two randomized clinical trials (VIVID and VISTA) comparing aflibercept (EYLEA®; Regeneron pharmaceuticals, Inc., Tarrytown, NY, USA) with laser therapy demonstrated its superior efficacy and safety compared to laser therapy.[10] Nevertheless, ranibizumab is not effective in up to 23% of patients, who are referred to as non-responders.[11]

As DME is a consequence of vascular leakage or proliferation triggered by inflammation, anti-VEGF coverage alone may not be sufficient. Increased concentrations of other pro-inflammatory molecules also mediate its pathophysiology; therefore, corticosteroids, which downregulate many inflammatory molecules including VEGF, are used to restore the blood-retina barrier. A comparative study revealed that ranibizumab with prompt or delayed laser photocoagulation is superior to intravitreal triamcinolone acetonide (IVTA) with laser, especially in phakic eyes, due to the well-known adverse effects of TA.[12] Moreover, the combination of IVTA and anti-VEGF injections is not superior to anti-VEGF monotherapy.[13] A highly potent corticosteroid, dexamethasone, failed to resolve DME in a pilot series of single intravitreal injection.[14] This failure was attributed to the short half-life of intravitreal injections, leading to the development of an implant to provide sustained release.[15] The MEAD study, which pooled the data of 2 randomized, multicenter, masked, sham-controlled, phase 3 clinical trials to evaluate the dexamethasone biodegradable implant (OZURDEX®, Allergan, Irvine, CA, USA), demonstrated at least 15-letter improvement in best corrected visual acuity (BCVA) from baseline in 22.2% patients receiving the 0.7 mg implant.[16] In the currrent study, we aimed to evaluate the effects of a single or two consecutive intravitreal dexamethasone (IV-DEX) implants in eyes with recalcitrant DME.

Materials and Methods

We retrospectively reviewed the records of 48 patients who underwent IV-DEX injection due to recalcitrant DME between January 2014 and June 2015 at Gülhane Training and Research Hospital, Ophthalmology Clinic. The protocol was in accordance with the principles of the Declaration of Helsinki and ethics committee approval was obtained. Of the 48 patients, 10 were excluded due to missing data or follow-up, which yielded 38 patients for the analysis. Patients in the study group had diabetes mellitus for a mean of 17.2±6.4 years, and the mean follow-up for DME was 60.2±17.6 months. Patients with recalcitrant DME who met the following criteria were included: age older than 18 years, at least 1 eye with an initial acuity of 0.3 logarithm of the minimum angle of resolution (LogMAR) or worse due to DME, central foveal thickness (CFT) ≥300 µm on spectral domain OCT, and a minimum follow-up of 6 months post-injections. Recalcitrant DME was defined as persistent macular edema with CFT ≥300 µm, lasting 3 months after at least 3 intravitreal anti-VEGF and 3 IVTA injections with 2 sessions of focal grid laser photocoagulation. Exclusion criteria were intraocular surgery within the last 3 months, vitreoretinal interface pathology in the study eye that could prevent improvement, and any other ocular comorbidity contributing to significantly decreased vision. After a detailed explanation of possible risks and benefits of this drug of choice, informed consent was obtained from all patients. Clinical data regarding type and duration of diabetes mellitus, previous treatments, and HbA1c level were recorded. All patients underwent complete ophthalmologic examination including BCVA using standardized ETDRS charts, tonometry, and anterior segment and fundus examination followed by CFT measurements using Heidelberg SPECTRALIS OCT imaging (Heidelberg Engineering, Heidelberg, Germany).

All patients received IV-DEX in the study eye in the operating room under topical anesthesia, and topical moxifloxacin (VIGAMOX®) eyedrop was prescribed four times daily for seven days after injection. The patients were examined on postoperative day 7 for any sign of infection. After injection, the main outcomes including BCVA, CFT, and intraocular pressure (IOP) were assessed at month 1, 3, and every month thereafter. Primary outcome measures were the changes in BCVA and CFT from baseline.

Foveal thickness changes were analyzed using paired t-test, and Wilcoxon test was used to compare preoperative and postoperative LogMAR visual acuity outcomes.

Results

We analyzed 57 eyes of 38 patients, and baseline characteristics are given in Table 1. All patients had type 2 diabetes, and the mean HbA1c was 7.9±1.7%. Previous intravitreal treatments and laser therapies are given in Table 2. At baseline, the mean CFT was 506.76±166.7 µm, and decreased to 341.36±146.2 µm at 1 month ($p<0.0001$, paired t-test). Statistically significant decrease was maintained during the following 4 months. The mean decreases in CFT at 5 and 6 months were not significant in comparison to baseline measurements, though they were still below the baseline values. Figure 1 shows the change in CFT. Inter-visit comparisons revealed significant reductions in CFT up to 3 months. Though there was no significant difference between

visits at 3 and 4 months (-83.61 µm, p=0.17), measurements at 4 months were still significantly lower when compared to baseline (p<0.0001, paired t-test). Sixteen eyes (28%) underwent second IV-DEX injections with a mean interval of 7.4±2.3 months and CFT decrease was significant at 7, 8, and 9 months. Delay in the second injection was a result of state health policy, which does not approve consecutive injections before 6 months. Twenty-one (36%) eyes remained stable and were followed without injections, while 20 eyes (36%) switched to other agents due to ocular complications, mostly raised IOP.

At baseline, the mean BCVA was 0.68±0.38 LogMAR (range 0.10-1.80), and improved significantly only at 1 month (0.54±0.41 LogMAR) (p<0.0001, Wilcoxon). Figure 2 shows the mean BCVA values during follow-up. On the other hand, subgroup analysis revealed interesting results. When we analyzed phakic and pseudophakic patients separately, the difference in BCVA was significant in the pseudophakic group throughout the 4-month follow-up, whereas there was no significant change in the phakic group.

The cataract progression rate was 50% in phakic eyes, and the mean time for cataract surgery was 5.4±1.1 months from IV-DEX injection. IOP elevation greater than or equal to 10 mmHg from baseline at any visit was seen in 28% of patients, and all patients were managed with medical therapy.

Discussion

In this study, we aimed to analyze IV-DEX injection as a choice of treatment for recalcitrant DME that is refractory to laser photocoagulation and intravitreal injections of both anti-VEGF and IVTA. There is no consensus or international definition for recalcitrant DME in the English or Turkish literature. Some clinicians consider DME as refractory when there is no improvement following intravitreal injections and some clinicians consider DME as refractory when nonresponsive to maximally applied laser photocoagulation and intravitreal injections of anti-VEGF/TA.[17,18,19] In the current study, anatomical and functional improvement was significant and maintained for 4 months after injection. Our results are consistent with Zucchiatti et al.[20] showing improvement in BCVA and CFT as early as the first days after injection and maintained until the fourth month. On the other hand, our results regarding duration of effect are not consistent with the MEAD study, which defined the minimum interval as 6 months.

At 1 month, the mean CFT improved significantly and remained stable throughout the 4-month follow-up. CFT improvement was also significant at 7, 8, and 9 months because second IV-DEX injections were given at a mean of 7.4±2.3 months. As the healthcare regulations of our country prevented us from doing second injections earlier, it is difficult to draw a conclusion about the efficacy of second injections

Table 1. Baseline characteristics of the study population

Sex Male Female	 18 (47%) 20 (53%)
Mean hemoglobin A1c	7.9±1.7%
Diabetic retinopathy Nonproliferative Proliferative	 57% 43%
Lens status Phakic Pseudophakic	 43% 57%

Table 2. Previous treatments for diabetic macular edema

Intravitreal injections (mean ± standard deviation) Anti-VEGF Triamcinolone acetonide	 5.71±3.40 3.44±2.46
Laser photocoagulation None Panretinal Grid Panretinal + grid	 30.7% 13.2% 37.7% 18.4%
VEGF: Vascular endothelial growth factor	

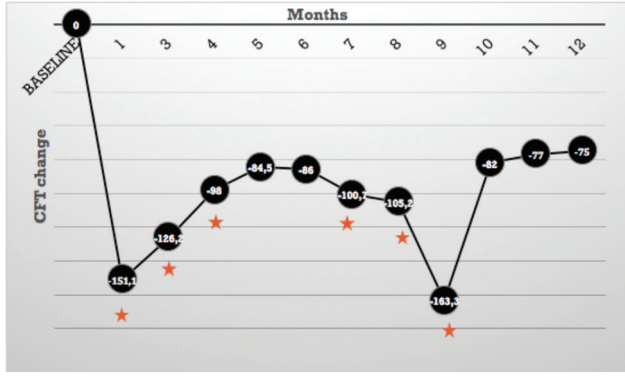

Figure 1. Mean change in central foveal thickness from baseline at each follow-up assessment
*Statistically significant, CFT: Central foveal thickness

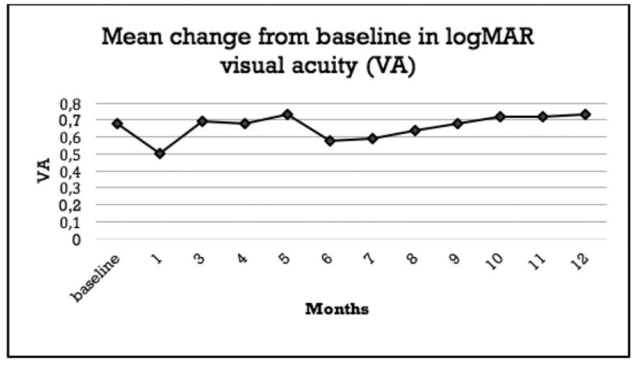

Figure 2. Mean best corrected visual acuity changes from baseline to 12 months
VA: Visual acuity

because there is no consistency in the timing of second IV-DEX injections. Moreover, 23% of the study eyes had higher CFT measurements than baseline at 5 months (rebound effect). In this particular group, common characteristics were similar with the rest of the study group and health status was stable. Moreover, their reductions in CFT following injection were similar to the rest of the study group. Therefore, we were unable to identify the exact reason for this rebound effect. Our results regarding CFT are consistent with previous studies demonstrating that statistically significant efficacy continues for 4 months and tends to decrease thereafter.[21,22]

In our series, BCVA improvement was significant only at 1 month after injection, but subgroup analysis revealed significant improvement lasting 4 months in pseudophakic eyes. Nonsignificant BCVA improvement in general may be due to cataract progression, which was noted as early as the 3-month follow-up.

As all of our patients were previously treated, tissue integrity was already compromised. It is known that the shorter the duration of DME, the lower the chance of irreversible damage to the retinal structures.[23] In addition, Guigou et al.[24] suggest previous treatments as a negative factor due to irreversible damage to the retinal structure in macular edema. Contrary to clinical trials, there were no treatment-naive eyes in the current study, with the study eyes having a mean of 5.71±3.40 intravitreal anti-VEGF and 3.44±2.46 IVTA injections, and a laser treatment rate of 69.3% before IV-DEX injection. This might explain why we did not achieve significant improvements in BCVA.

Conclusion

Our experience regarding IV-DEX implants in recalcitrant DME cases revealed a good efficiency. Nevertheless, it seems unlikely to displace anti-VEGF agents as first-line therapy due to steroid-related complications.

Ethics

Ethics Committee Approval: GATA - 09.02.2016/83/313.

Informed Consent: Retrospective analysis of clinical data.

Peer-review: Externally peer-reviewed.

Authorship Contributions

Surgical and Medical Practices: Murat Küçükevcilioğlu, Ali Hakan Durukan, Seçkin Aykaş, Concept: Ali Hakan Durukan, Fazıl Cüneyt Erdurman, Design: Önder Ayyıldız, Data Collection or Processing: Dorukcan Akıncıoğlu, Analysis or Interpretation: Dorukcan Akıncıoğlu, Murat Küçükevcilioğlu, Literature Search: Dorukcan Akıncıoğlu, Writing: Dorukcan Akıncıoğlu.

Conflict of Interest: No conflict of interest was declared by the authors.

Financial Disclosure: The authors declared that this study received no financial support.

References

1. Pelzek C, Lim JI. Diabetic macular edema: review and update. Ophthalmol Clin North Am. 2002;15:555-563.
2. Early Treatment Diabetic Retinopathy Study Research Group: Photocoagulation for diabetic macular edema : ETDRS report No 4. Int Ophthalmic Clin. 1987;27:265-72.
3. Yau JW, Rogers SL, Kawasaki R, Lamoureux EL, Kowalski JW, Bek T, Chen SJ, Dekker JM, Fletcher A, Grauslund J, Haffner S, Hamman RF, Ikram MK, Kayama T, Klein BE, Klein R, Krishnaiah S, Mayurasakorn K, O'Hare JP, Orchard TJ, Porta M, Rema M, Roy MS, Sharma T, Shaw J, Taylor H, Tielsch JM, Varma R, Wang JJ, Wang N, West S, Xu L, Yasuda M, Zhang X, Mitchell P, Wong TY; Meta-Analysis for Eye Disease (META-EYE) Study Group. Global prevalence and major risk factors of diabetic retinopathy. Diabetes Care. 2012;35:556-564.
4. No authors listed. Photocoagulation for diabetic macular edema: Early Treatment Diabetic Retinopathy Study report nummer 1. Early Treatment Diabetic Retinopathy Study Research Group. Arch Ophthalmic. 1985;103:1796-1806.
5. Funatsu H, Yamashita H, Noma H, Mimura T, Yamashita T, Hori S. Increased levels of vascular endothelial growth factor and interleukin-6 in the aqueous humor of diabetics with macular edema. Am J Ophthalmol. 2002;133:70-77.
6. Schmidt-Erfurth U, Lang GE, Holz FG, Schlingemann RO, Lanzetta P, Massin P, Gerstner O, Bouazza AS, Shen H, Osborne A, Mitchell P; RESTORE Extension Study Group. Three-year outcomes of individualized ranibizumab treatment in patients with diabetic macular edema: the RESTORE extension study. Ophthalmology. 2014;121:1045-1053.
7. Nguyen QD, Brown DM, Marcus DM, Boyer DS, Patel S, Feiner L, Gibson A, Sy J, Rundle AC, Hopkins JJ, Rubio RG, Ehrlich JS; RISE and RIDE Research Group. Ranibizumab for diabetic macular edema: results from 2 phase III randomized trials: RISE and RIDE. Ophthalmology. 2012;119:789-801.
8. Elman MJ, Ayala A, Bressler NM, Browning D, Flaxel CJ, Glassman AR, Jampol LM, Stone TW; Diabetic Retinopathy Clinical Research Network. Intravitreal ranibizumab for diabetic macular edema with prompt versus deferred laser treatment: 5-year randomized trial results. Ophthalmology. 2015;122:375-381.
9. Rajendram R, Fraser-Bell S, Kaines A, Michaelides M, Hamilton RD, Esposti SD, Peto T, Egan C, Bunce C, Leslie RD, Hykin PG. A 2-year prospective randomized controlled trial of intravitreal bevacizumab or laser therapy (BOLT) in the management of diabetic macular edema: 24-month data: report 3. Arch Ophthalmol. 2012;130:972-979.
10. Brown DM, Schmidt-Erfurth U, Do DV, Holz FG, Boyer DS, Midena E, Heier JS, Terasaki H, Kaiser PK, Marcus DM, Nguyen QD, Jaffe GJ, Slakter JS, Simader C, Soo Y, Schmelter T, Yancopoulos GD, Stahl N, Vitti R, Berliner AJ, Zeitz O, Metzig C, Korobelnik JF. Intravitreal Aflibercept for Diabetic Macular Edema: 100-Week Results From the VISTA and VIVID Studies. Ophthalmology. 2015;122:2044-2052.
11. Bressler SB, Qin H, Beck RW, Chalam KV, Kim JE, Melia M, Wells JA 3rd; Diabetic Retinopathy Clinical Research Network. Factors associated with changes in visual acuity and central subfield thickness at 1 year after treatment for diabetic macular edema with ranibizumab. Arch Ophthalmol. 2012;130:1153-1161.
12. Elman MJ, Bressler NM, Qin H, Beck RW, Ferris FL 3rd, Friedman SM, Glassman AR, Scott IU, Stockdale CR, Sun JK; Diabetic Retinopathy Clinical Research Network. Expanded 2-year follow-up of ranibizumab plus prompt or deferred laser or triamcinolone plus prompt laser for diabetic macular edema. Ophthalmology. 2011;118:609-614.
13. Soheilian M, Ramezani A, Obudi A, Bijanzadeh B, Salehipour M, Yaseri M, Ahmadieh H, Dehghan MH, Azarmina M, Moradian S, Peyman GA. Randomized trial of intravitreal bevacizumab alone or combined with triamcinolone versus macular photocoagulation in diabetic macular edema. Ophthalmology. 2009;116:1142-1150.

14. Chan CK, Mohamed S, Lee VY, Lai TY, Shanmugam MP, Lam DS. Intravitreal dexamethasone for diabetic macular edema: a pilot study. Ophthalmic Surg Lasers Imaging. 2010;40:26-30.
15. Haller JA, Dugel P, Weinberg DV, Chou C, Whitcup SM. Evaluation of safety and performance of an applicator for a novel intravitreal dexamethasone drug delivery system for the treatment of macular edema. Retina. 2009;29:46-51.
16. Boyer DS, Yoon YH, Belfort R Jr, Bandello F, Maturi RK, Augustin AJ, Li XY, Cui H, Hashad Y, Whitcup SM; Ozurdex MEAD Study Group. Three-year, randomized, sham-controlled trial of dexamethasone intravitreal implant in patients with diabetic macular edema. Ophthalmology. 2014;121:1904-1914.
17. Zhioua I, Semoun O, Lalloum F, Souied EH. Intravitreal dexamethasone implant in patients with ranibizumab persistent diabetic macular edema. Retina. 2015;35:1429-1435.
18. Totan Y, Güler E, Gürağaç FB. Dexamethasone Intravitreal Implant for Chronic Diabetic Macular Edema Resistant to Intravitreal Bevacizumab Treatment. Curr Eye Res. 2016;41:107-113.
19. Dutra Medeiros M, Postorino M, Navarro R, Garcia-Arumi J, Mateo C, Corcostegui B. Dexamethasone intravitreal implant for treatment of patients with persistent diabetic macular edema. Ophthalmologica. 2014;231:141-146.
20. Zucchiatti I, Lattanzio R, Querques G, Querques L, Del Turco C, Cascavilla ML, Bandello F. Intravitreal dexamethasone implant in patients with persistent diabetic macular edema. Ophthalmologica. 2012;228:117-122.
21. Kuppermann BD, Blumenkranz MS, Haller JA, Williams GA, Weinberg DV, Chou C, Whitcup SM; Dexamethasone DDS Phase II Study Group. Randomized controlled study of an intravitreous dexamethasone drug delivery system in patients with persistent macular edema. Arch Ophthalmol. 2007;125:309-317.
22. Haller JA, Kuppermann BD, Blumenkranz MS, Williams GA, Weinberg DV, Chou C, Whitcup SM; Dexamethasone DDS Phase II Study Group: Randomized controlled trial of an intravitreous dexamethasone drug delivery system in patients with diabetic macular edema. Arch Ophthalmol. 2010;128:289-296.
23. Pelosini L, Hull CC, Boyce JF, McHugh D, Stanford MR, Marshall J. Optical coherence tomography may be used to predict visual acuity in patients with macular edema. Invest Ophthalmol Vis Sci. 2011;52:2741-2748.
24. Guigou S, Hajjar C, Parrat E, Merite PY, Pommier S, Matonti F, Prost-Magnin O, Meyer F. Multicenter Ozurdex® assessment for diabetic macular edema: MOZART study. J Fr Ophtalmol. 2014;37:480-485.

DOI: 10.4274/tjo.68335
Turk J Ophthalmol 2017;47:279-284

Original Article

Optic Coherence Angiography Findings in Type-2 Macular Telangiectasia

Hilal Nalcı, Figen Şermet, Sibel Demirel, Emin Özmert
Ankara University Faculty of Medicine, Department of Ophthalmology, Ankara, Turkey

Abstract

Objectives: To evaluate the vascular changes of idiopathic macular telangiectasia type 2 (MacTel 2) patients with optical coherence tomography angiography (OCTA) and correlate these changes with the findings of spectral domain optical coherence tomography (SD-OCT).

Materials and Methods: Simultaneous SD-OCT and OCTA images of 10 eyes of 6 patients who were diagnosed as MacTel 2 in Ankara University Faculty of Medicine, Department of Ophthalmology were obtained and graded according to the OCTA grading system for MacTel 2.

Results: Ten eyes of 6 patients were included. Four (66%) patients were female and 2 (34%) were male. The disease was grade 0 in 2 eyes, grade 1 in 2 eyes, grade 2 in 3 eyes, grade 3 in 1 eye, grade 4 in 1 eye, and grade 5 in 1 eye. The most common findings in grade 1, 2, and 3 non-proliferative disease were thinning of the outer retinal layers, presence of intraretinal hyporeflective layers and inner limiting membrane draping. In cases with subretinal choroidal neovascularisation (CNV) in OCTA, CNV or CNV scar was present in the B-scan SD-OCT images. In a case in which OCT was within normal limits, vascular changes consistent with grade 1 disease were observed in OCTA. On the contrary, 2 patients with significant foveal atrophy and macular hole in B-scan showed changes of early disease in OCTA. In some of the eyes, OCTA revealed an intact superficial vascular layer despite visible changes in the deep layer and the presence of neovascularisation.

Conclusion: OCTA yields findings which are important for understanding the pathogenesis of the disease and providing better follow-up. Contrary to fundus fluorescein angiography, changes in the deep arterial plexus in the early disease and CNV can be clearly observed with OCTA. To achieve the best results in clinical practice, en face flow maps should be evaluated together with B-scan SD-OCT images.

Keywords: Macular telangiectasia type-2, optic coherence tomography angiography, spectral domain optic coherence tomography

Introduction

Idiopathic macular telangiectasia type 2 (MacTel 2 or perifoveal telangiectasia) is an acquired vascular disease of the macula primarily involving neural and glial cell degeneration and loss. This condition, named by Yannuzzi et al.,[1] refers to idiopathic juxtaretinal telangiectasia (IJRT) type 2A according to the classification system introduced by Gass and Blodi[2] in 1993. It is the most common type of IJRT, and includes cases that are usually bilateral, occult, and nonexudative. The disease typically presents in the fifth and sixth decades and affects men and women equally, although various studies have reported contradictory findings on the latter point.[3,4,5]

Clinically, it is characterized by loss of transparency in the foveal region, intraretinal crystalline deposit accumulation, hyperplastic retinal pigment epithelium migration, macular pigment loss, and progressive abnormalities in the juxtafoveolar retinal vessels. These include right-angle veins, subretinal and outer retinal neovascularization, and vascular invasion of the foveal avascular zone.[6] Optical coherence tomography (OCT) allows better understanding of retinal pathologies. Characteristic findings of the disease include

Address for Correspondence: Hilal Nalcı MD, Ankara University Faculty of Medicine, Department of Ophthalmology, Ankara, Turkey
Phone: +90 506 254 49 41 E-mail: hilalnalci@hotmail.com **ORCID-ID:** orcid.org/0000-0003-4463-1413
Received: 29.09.2016 **Accepted:** 18.11.2016

macular thinning, hyporeflective cavitations in the inner and outer retinal layers, development of full-thickness macular hole in the absence of vitreoretinal traction, and atrophic changes in the outer retinal layer.[7,8]

From its initial description to the present day, there has been no consensus regarding the mechanism of perifoveal telangiectasia. However, it is currently believed that the degeneration of Müller cells, which serve protective and supportive functions, is the primary pathology, and the damage to the retinal layers, atrophy, and vascular changes develop secondarily.[3]

Optical coherence tomography angiography (OCTA) is an imaging method that visualizes the movements of blood cells using motion contrast, thus providing information about blood flow. Thusly, imaging of the retinal vascular layers is possible without the need for intravenous contrast injection. As opposed to fundus fluorescein angiography (FFA), in which layers other than the superficial vascular plexus appear only as background hyperfluorescence, OCTA enables separate imaging of the superficial and deep vascular layers and the choroidal vessels.[9]

In this study, we aimed to use OCTA to evaluate vascular anomalies in patients with MacTel 2 and elucidate the relationship between these and retinal anomalies detected on OCT.

Materials and Methods

Optovue spectral domain OCT (SD-OCT) and OCTA images were recorded simultaneously from 6 patients diagnosed with MacTel 2 in the Ophthalmology Department of the Ankara University Faculty of Medicine. Patients were considered to have MacTel 2 in the presence of findings such as reduced autofluorescence in the central macula on fundus autofluorescence; loss of retinal transparency, intraretinal pigment, presence of right-angle venules, and telangiectatic vessel appearance on fundus examination; and OCT showing interior limiting membrane drape, retinal pigment epithelium migration creating intraretinal hyperreflectivity, atrophy of the outer retinal layers, and presence of intraretinal hyporeflective cavitation. OCTA en face flow maps were created using RTVue XR Avanti version 2015.1.1.98 and Split Spectrum Amplitude Decorrelation Angiography images were obtained. Images that could not be evaluated due to low resolution were excluded. Each eye was graded based on the MacTel OCTA grading system according to Chen et al.[10] (Table 1).

Results

Ten eyes of 6 patients were included in the study. Four (66%) of the patients were female, 2 (34%) were male. Their mean age was 67.6 years. The OCT and OCTA findings of the patients are shown in Table 2. Disease severity was grade 0 in 2 eyes, grade 1 in 2 eyes, grade 2 in 3 eyes, grade 3 in 1 eye, grade 4 in 1 eye, and grade 5 in 1 eye. Neovascularization was not observed in any of the grade 1, 2, or 3 eyes. In these cases, the most common findings on OCT images were thinning and atrophy in the outer retina and inner/outer segment layers, intraretinal hyporeflective cavitations, and ILM drape (Figures

Table 1. Staging of idiopathic macular telangiectasia type 2 patients based on optical coherence tomography angiography imaging

Grade	Findings
1	Normal superficial capillary network
	Telangiectatic changes in the deep capillary network, predominantly temporal of the fovea
2	Mild/moderate telangiectatic changes in the superficial capillary network
	Marked telangiectatic changes in the deep capillary network temporal of the fovea
	Reduced vascular density with capillary closure in the superficial and deep capillary networks
	Irregular capillary size and shape in the perifoveal region of the superficial and deep capillary networks
	Dilated arterioles and right angle venules
3	FAZ irregularity
	Reduced vascular density with increased capillary closure in the superficial and deep capillary networks
	Vascular invasion reaching the RPE layer
	Vascular invasion of the FAZ
	Pigment accumulation causing optical shadowing
	One or more sets of feeding and draining vessels in the superficial and deep layers
4	Abnormal FAZ shape with abnormal shape and dragging of vessels in the perifoveal region
	Visible blood flow through the SRNV formed in the outer retina, RPE, and choroid
5	Marked thinning and reduced vascular density in the outer retina
	Larger vascular diameter but reduced vascular density in the SRNV
	Blood flow visible in the disciform/fibrovascular layer and may advance to the deep choroid

FAZ: Foveal avascular zone, RPE: Retina pigment epithelium, SRNV: Subretinal neovascularization

1 and 2). In patients with subretinal neovascularization apparent on OCTA, B-scan images from the same cross-section revealed classic CNV or CNV scar (Figure 3). In one patient, OCT images were considered normal, whereas vascular changes consistent with grade 1 disease were observed on OCTA (Figure 4). In contrast, 2 patients who showed pronounced foveal atrophy and macular hole on B-scan imaging had only early-stage changes in OCTA (Figures 5 and 6). Another striking finding was that in some of the patients, the superficial layer was intact despite pronounced changes and neovascularization in the deep layer (Figures 7 and 8).

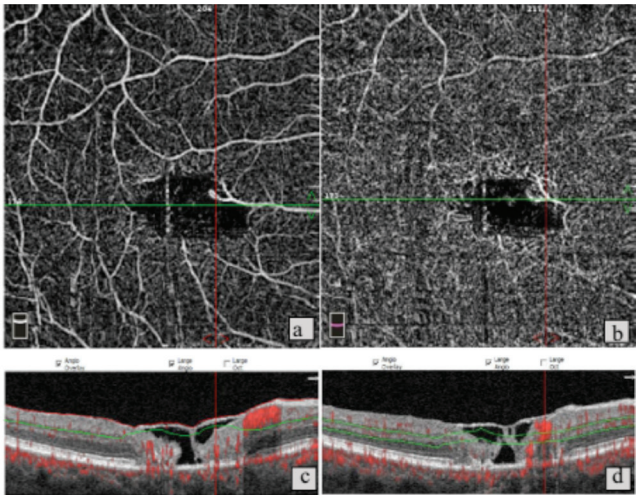

Figure 1. Patient 6, right eye. a) Foveal avascular zone (FAZ) irregularity and reduced vascular density in the superficial vascular network; b) Optical coherence tomography angiography in the same eye shows stage 3 disease with irregularity and vascular invasion of the FAZ; c,d) B-scan imaging shows foveal atrophy accompanied by outer retinal atrophy, inner segment/outer segment band defect, and stage 2 macular hole without internal limiting membrane drape or traction

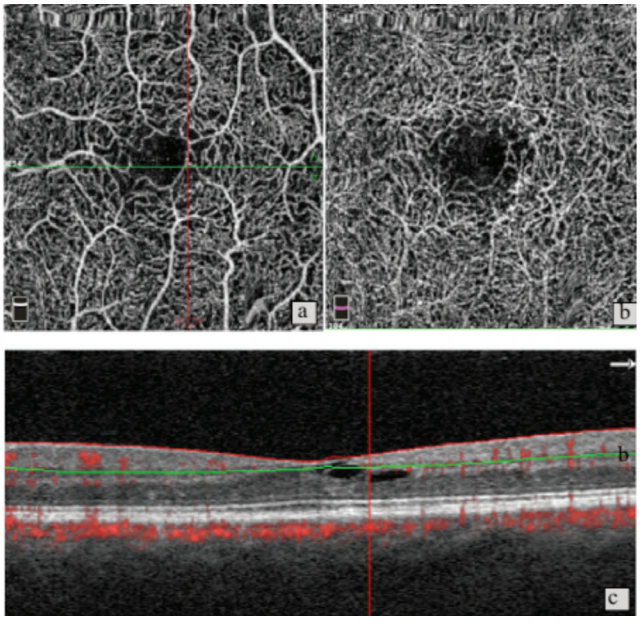

Figure 2. Patient 1, left eye, stage 2. a) Optical coherence tomography angiography shows minimal increase in space between vessels in the superficial vascular network; b) in the same eye, increased space between vessels and telangiectatic changes in the deep vascular network; c) B-scan imaging shows intraretinal hyperreflective cavitations

Discussion

OCTA provides valuable information regarding disease severity and neovascularization activity in patients with parafoveal telangiectasia. In a study using OCTA, Spaide et al.[9] demonstrated that FFA primarily shows the superficial vascular network of the retina and is inadequate for visualizing the deep capillary layer and the choroid. Consistent with other

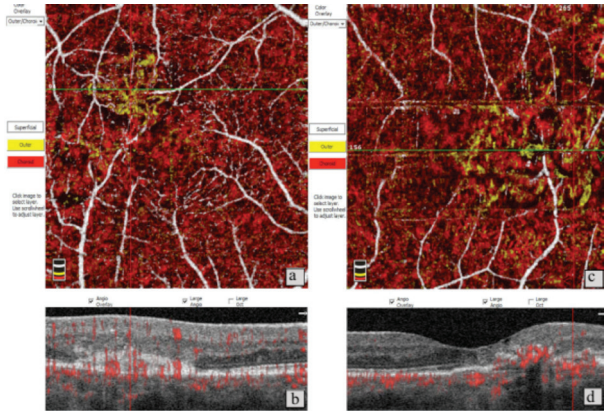

Figure 3. a) Patient 4, right eye, stage 4. Optical coherence tomography angiography shows neovascularization in the deep capillary network; b) B-scan optical coherence tomography in the same eye reveals classic choroidal neovascularization; c) Same patient's left eye, stage 5. d) OCT shows pronounced atrophy of the outer retinal layers and a large, scarred fibrovascular membrane

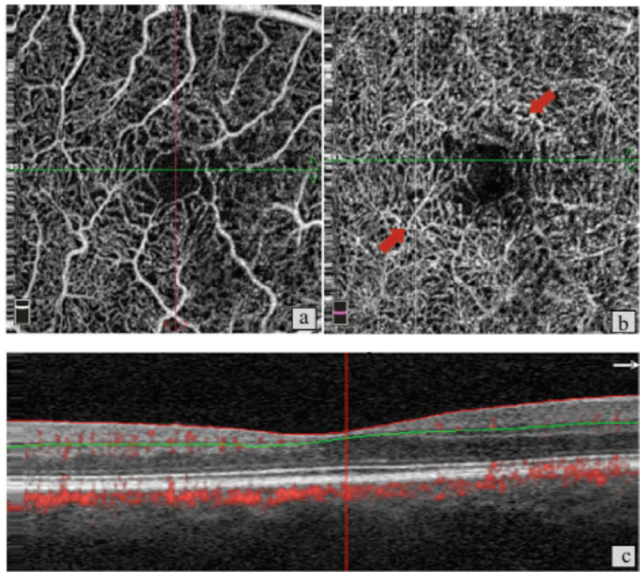

Figure 4. Patient 1, right eye. a) Superficial capillary plexus appears normal on optical coherence tomography angiography imaging; b) Widened vessels and telangiectases are apparent in the deep vascular network; c) B-scan optical coherence tomography imaging is within normal limits

Table 2. Spectral domain optical coherence tomography and optical coherence tomography angiography findings of the patients

Patient	Laterality	OCT	Grade	OCTA
Patient 1	Right	Normal	1	Minimal increase in the space between vessels and telangiectatic changes in the superficial and deep vascular networks
Patient 1	Left	Intraretinal hyporeflective cavitation ILM drape	2	Reduced vascular density and telangiectatic changes in the superficial and deep vascular networks
Patient 2	Left	Stage 2 full-thickness macular hole Intraretinal cysts	1	Telangiectatic vessels in the deep vascular network
Patient 3	Right	Atrophy in the outer retinal layers IS/OS band defect Intraretinal hyporeflective cavitation ILM drape	0	Normal
Patient 3	Left	Normal	0	Normal
Patient 4	Right	Atrophy in the outer retinal layers IS/OS band defect Pigment epithelium migration Hyperreflective points in the outer retinal layers CNV	4	Increased space between the vessels in the superficial and deep vascular networks Neovascularization in the outer retinal layer
Patient 4	Left	Atrophy in the outer retinal layers IS/OS band defect Hyperreflective area consistent with CNV scar in the outer retina Intraretinal cavitation ILM drape	5	Neovascularization in the outer retina
Patient 5	Right	Intraretinal cysts Atrophy in the outer retinal layers IS/OS band defect Hyperreflective spots in the outer retinal layers	2	Pronounced telangiectatic vessels and reduced vascular density in the superficial and deep vascular networks Right angle venules FAZ irregularity
Patient 6	Right	Atrophy in the outer retinal layers IS/OS band defect Partial thickness macular hole ILM drape	3	FAZ irregularity Vascular invasion of the FAZ Vascular invasion reaching the RPE layer
Patient 6	Left	Atrophy in the outer retinal layers IS/OS band defect Intraretinal hyporeflective cavitation Stage 2 macular hole	2	FAZ irregularity Right angle venules Pronounced telangiectatic vessels and reduced vascular density in the superficial and deep vascular networks

FAZ: Foveal avascular zone, ILM: Internal limiting membrane, IS/OS: Inner segment/outer segment, CNV: Choroidal neovascularization, RPE: Retinal pigment epithelium, OCT: Optical coherence tomography, OCTA: Optical coherence tomography angiography

OCTA studies, in our series we observed that the superficial vascular network of some MacTel 2 patients was remarkably well preserved, even in advanced disease, while pronounced changes were evident in the deep capillary network. In addition, abnormalities may occur in the deep vascular network even in early disease stages where OCT is within normal limits, and FFA alone is not sufficient to evaluate these patients. It has also been shown that FFA findings which may be evaluated as perifoveal vascular leakage and lead to unnecessary injections in clinical practice are due to telangiectatic vessels in the deep vascular layer.[11] OCTA clearly demonstrates that leakage simulating choroidal neovascularization on FFA is not a result of the formation of new vessels. Other advantages over FFA are that it is easy to perform, can be repeated frequently, and is non-invasive.

In the current series, OCTA evaluation of patients with advanced atrophic changes in the foveal region and macular hole revealed minimal changes consistent with grade 0 or 1 disease in the foveal vascular network. These findings support the theory that retinal structural changes seen in MacTel 2 are not secondary to vascular anomalies, but are a primary condition.[12,13] Müller cells are known to play important roles in the maintenance of foveal structural integrity, neuronal support, and continuity of the blood-retina barrier.[14,15] It is believed that macular hole and intraretinal cavitation arise due to neural atrophy and disruption of the foveal structure resulting from the destruction of Müller cells.[13] These findings appear independent of vascular changes and show the clinical importance of en face circulation maps in combination with B-scan OCT.

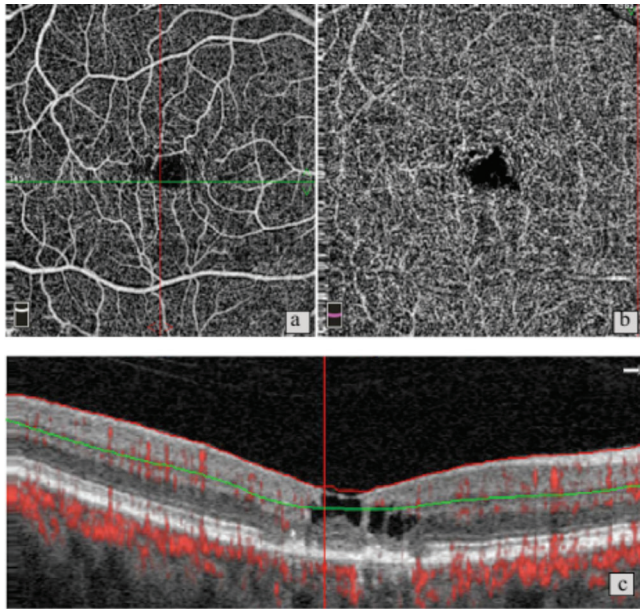

Figure 5. Patient 3, right eye. a) Capillary plexus appears within normal limits on optical coherence tomography angiography imaging; b) No findings other than minimal vessel thickening in the deep layer; c) B-scan OCT imaging shows pronounced internal limiting membrane drape, cavitation, and atrophy in the outer segments

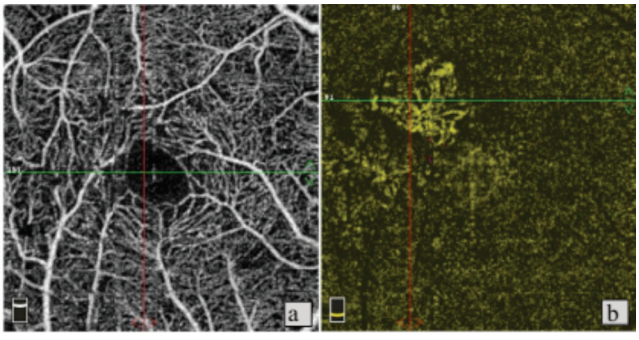

Figure 7. Patient 4, right eye. a) No pronounced changes in the superficial vascular layer; b) Neovascularization in the normally avascular outer retinal area

On the other hand, a patient with grade 2 disease in the left eye exhibited no pronounced abnormality in the right eye on OCT, while OCTA revealed reduced vascular density and telangiectatic vessels in the deep vascular plexus. On careful examination of SD-OCT images of this eye, it was noted that the foveal pit was asymmetric. Similarly, Charbel Issa et al.[16] studied patients with marked MacTel 2 in one eye and apparently healthy fellow eyes and detected foveal pit asymmetry and temporal foveal thinning which were associated with very early disease.

Another finding we observed in our cases is that the formation of new vessels was not limited to the choroid, but could also occur between the outer retinal layer and the choroidal vascular network, which is usually avascular. This finding is also similar to those observed by Spaide et al.[17,18]

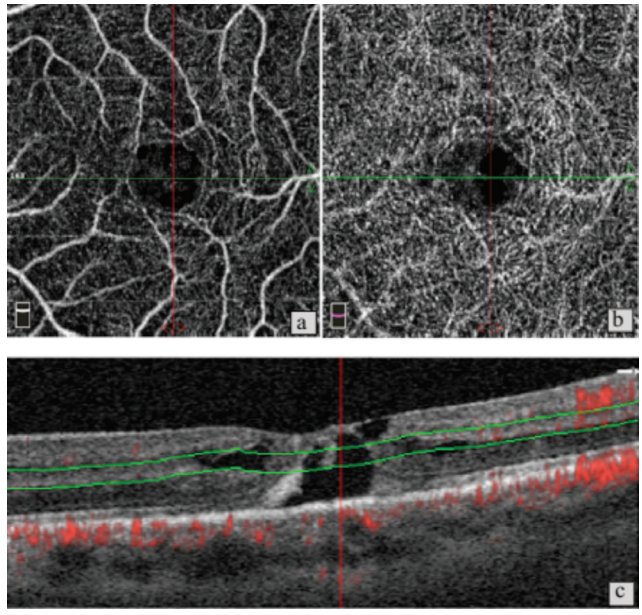

Figure 6. Patient 2, right eye, stage 1. a) Optical coherence tomography angiography reveals no pronounced changes in the superficial capillary network; b) Mild telangiectatic changes in the deep capillary plexus; c) B-scan imaging shows marked intraretinal cavitation and stage 1 macular hole

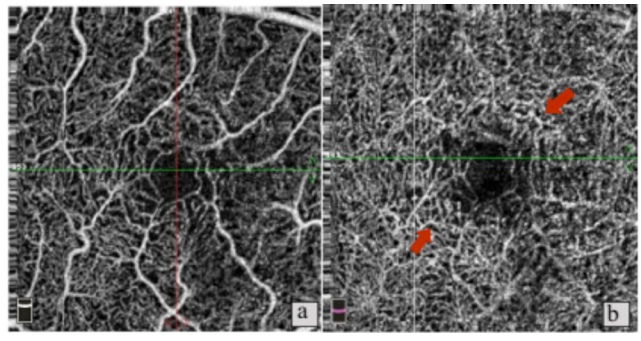

Figure 8. Patient 1, right eye. A) Superficial capillary layer appears normal; B) Thickening and telangiectases in the vessels of the deep capillary network

In their OCTA studies of MacTel 2, they emphasized the antiangiogenic properties of Müller cells, stating that hypoxia due to deep vascular network dysfunction and suppression of antiangiogenic factors due to Müller cell degeneration may lead to intraretinal neovascularization. Several previous studies have indicated that neovascularization in MacTel 2 originates more from retinal vascular structures rather than the choroid.[19,20] In their study using OCTA, Zhang et al.[21] showed that these subretinal neovascular complexes may not be only retinal, but may also be connected to the choroidal vasculature.

The fact that the severity of intraretinal and vascular changes are mutually independent supports the view that the primary pathology of MacTel 2 is not vascular. Moreover, it has been shown that Müller cell loss may be another factor that leads to telangiectasia.[22] Spaide et al.[17,18] also emphasized the

importance of Müller cells in intraretinal vascular circulation and retinal support. Thus, it seems that Müller cell loss is responsible not only for intraretinal neural cell death and morphologic changes, but also vascular telangiectasia, leakage, and neovascularization.

Conclusion

The results of this pilot study demonstrate that OCTA, which has recently been introduced into clinical use, offers insight into the pathogenesis of MacTel 2 and is useful as an auxiliary method to OCT in patient follow-up, but does not directly correlate with OCT findings in terms of the extent of anatomic abnormalities.

Ethics

Ethics Committee Approval: Ankara University Faculty of Medicine Clinical Research Ethics Committee (13-827-17).

Informed Consent: The study is retrospective in nature.

Peer-review: Externally peer-reviewed.

Authorship Contributions

Surgical and Medical Practices: Sibel Demirel, Figen Şermet, Emin Özmert, Concept: Sibel Demirel, Figen Şermet, Emin Özmert, Hilal Nalcı, Design: Sibel Demirel, Figen Şermet, Emin Özmert, Hilal Nalcı, Data Collection or Processing: Hilal Nalcı, Sibel Demirel, Analysis or Interpretation: Hilal Nalcı, Sibel Demirel, Literature Search: Hilal Nalcı, Writing: Hilal Nalcı, Sibel Demirel, Figen Şermet, Emin Özmert.

Conflict of Interest: No conflict of interest was declared by the authors.

Financial Disclosure: The authors declared that this study received no financial support

References

1. Yannuzzi LA, Bardal AM, Freund KB, Chen KJ, Eandi CM, Blodi B. Idiopathic macular telangiectasia. Arch Ophthalmol. 2006;124:450-460.
2. Gass JD, Blodi BA. Idiopathic juxtafoveolar retinal telangiectasis. Update of classiŞcation and follow-up study. Ophthalmology. 1993;100:1536-1546.
3. Wu L, Evans T, Arevalo JF. Idiopathic macular telangiectasia type 2 (idiopathic juxtafoveolar retinal telangiectasis type 2A, Mac Tel 2). Surv Ophthalmol. 2013;58:536-559.
4. Lee SW, Kim SM, Kim YT, Kang SW. Clinical features of idiopathic juxtafoveal telangiectasis in Koreans. Korean J Ophthalmol. 2011;25:225-230.
5. Aung KZ, Wickremasinghe SS, Makeyeva G, Robman L, Guymer RH. The prevalence estimates of macular telangiectasia type 2: the Melbourne Collaborative Cohort Study. Retina. 2010;30:473-478.
6. Gass JD, Oyakawa RT. Idiopathic juxtafoveolar retinal telangiectasis. Arch Ophthalmol. 1982;100:769-780.
7. Karth PA, Raja SC, Brown DM, Kim JE. Outcomes of macular hole surgeries for macular telangiectasia type 2. Retina. 2014;34:907-915.
8. Cohen SM, Cohen ML, El-Jabali F, Pautler SE. Optical coherence tomography Şndings in nonproliferative group 2a idiopathic juxtafoveal retinal telangiectasis. Retina. 2007;27:59-66.
9. Spaide RF, Klancnik JM Jr, Cooney MJ. Retinal vascular layers imaged by fluorescein angiography and optical coherence tomography angiography. JAMA Ophthalmol. 2015;133:45-50.
10. Chen CJ, Olson M, Chen R OCT Aangiography Examination of Type 2 Idiopathic Type 2 Telangiectasia. In: Lumbroso B, Huang D, Jia Y, Chen CJ, Rispoli M, Romano A, Waheed NK, eds. Clinical OCT Angiography Atlas (1st ed). New Delphi; Jaypee Brothers Medical Publishers Ltd; 2015:100-110.
11. Thorell MR, Zhang Q, Huang Y, An L, Durbin MK, Laron M, Sharma U, Stetson PF, Gregori G, Wang RK, Rosenfeld PJ. Swept source OCT angiography of macular telangiectasia type 2. Ophthalmic Surg Lasers Imaging Retina. 2014;45:369-380.
12. Gupta V, Gupta A, Dogra MR, Agarwal A. Optical coherence tomography in group 2A idiopathic juxtafoveolar telangiectasis. Ophthalmic Surg Lasers Imaging. 2005;36:482-486.
13. Surguch V, Gamulescu MA, Gabel VP. Optical coherence tomography findings in idiopathic juxtafoveal retinal telangiectasis. Graefes Arch Clin Exp Ophthalmol. 2007;245:783-788.
14. Bringmann A, Iandiev I, Pannicke T, Wurm A, Hollborn M, Wiedemann P, Osborne NN, Reichenbach A. Cellular signaling and factors involved in Müller cell gliosis:neuroprotective and detrimental effects. Prog Retin Eye Res. 2009;28:423-451.
15. Unterlauft JD, Eichler W, Kuhne K, Yang XM, Yafai Y, Wiedemann P, Reichenbach A, Claudepierre T. Pigment epithelium-derived factor released by Müller glial cells exerts neuroprotective effects on retinal ganglion cells. Neurochem Res 2012;37:1524-1533.
16. Charbel Issa P, Heeren TF, Kupitz EH, Holz FG, Berendschot TT. Very Early Disease Manifestations Of Macular Telangiectasia Type 2. Retina. 2016;36:524-534.
17. Spaide RF, Klancnik JM Jr, Cooney MJ, Yannuzzi LA, Balaratnasingam C, Dansingani KK, Suzuki M. Volume Rendering Optical Coherence Tomography Angiography of Macular Telangiectasia Type 2. Ophthalmology. 2015;122:2261-2269.
18. Spaide RF, Klancnik JM Jr, Cooney MJ. Retinal vascular layers in macular telangiectasia type 2 imaged by optical coherence tomographic angiography. JAMA Ophthalmol. 2015;133:66-73.
19. Davidorf FH, Pressman MD, Chambers RB. Juxtafoveal telangiectasis-a name change? Retina. 2004;24:474-478.
20. Soheilian M, Tavallali A, Peyman GA. IdentiŞcation of intraretinal neovascularization by high-speed indocyanine green angiography in idiopathic perifoveal telangiectasia. Ophthalmic Surg Lasers Imaging. 2007;38:167-169.
21. Zhang Q, Wang Rk, Chen Cl, Legarreta Ad, Durbin MK, An L, Sharma U, Stetson PF, Legarreta JE, Roisman L, Gregori G, Rosenfeld PJ. Swept Source Optıcal Coherence Tomography Angiography Of Neovascular Macular Telangiectasia Type 2. Retina. 2015;35:2285-2299.
22. Shen W, Fruttiger M, Zhu L, Chung SH, Barnett NL, Kirk JK, Lee S, Coorey NJ, Killingsworth M, Sherman LS, Gillies MC. Conditional Müllercell ablation causes independent neuronal and vascular pathologies in an oveltransgenic model. J Neurosci. 2012;32:15715-15727.

DOI: 10.4274/tjo.72593
Turk J Ophthalmol 2017;47:285-291

Review

Limbal Stem Cell Deficiency and Treatment with Stem Cell Transplantation

Özlem Barut Selver*, Ayşe Yağcı*, Sait Eğrilmez*, Mehmet Gürdal**, Melis Palamar*, Türker Çavuşoğlu***, Utku Ateş****, Ali Veral*****, Çağrı Güven******, Jose Mario Wolosin*******

*Ege University Faculty of Medicine, Department of Ophthalmology, İzmir, Turkey
**Ege University Faculty of Medicine, Department of Medical Biochemistry, İzmir, Turkey
***Ege University Faculty of Medicine, Department of Histology and Embriology, İzmir, Turkey
****İstanbul Bilim University Faculty of Medicine, Department of Histology and Embryology, İstanbul, Turkey
*****Ege University Faculty of Medicine, Department of Pathology, İzmir, Turkey
******Ege University Faculty of Medicine, Department of Gynecology and Obstetrics, İzmir, Turkey
*******Icahn Faculty of Medicine at Mount Sinai, Department of Ophthalmology and Black Family Stem Cell Institute, New York, USA

Abstract

The cornea is the outermost tissue of the eye and it must be transparent for the maintenance of good visual function. The superficial epithelium of the cornea, which is renewed continuously by corneal stem cells, plays a critical role in the permanence of this transparency. These stem cells are localized at the cornea-conjunctival transition zone, referred to as the limbus. When this zone is affected/destroyed, limbal stem cell deficiency ensues. Loss of limbal stem cell function allows colonization of the corneal surface by conjunctival epithelium. Over 6 million people worldwide are affected by corneal blindness, and limbal stem cell deficiency is one of the main causes. Fortunately, it is becoming possible to recover vision by autologous transplantation of limbal cells obtained from the contralateral eye in unilateral cases. Due to the potential risks to the donor eye, only a small amount of tissue can be obtained, in which only 1-2% of the limbal epithelial cells are actually limbal stem cells. Vigorous attempts are being made to expand limbal stem cells in culture to preserve or even enrich the stem cell population. *Ex vivo* expanded limbal stem cell treatment in limbal stem cell deficiency was first reported in 1997. In the 20 years since, various protocols have been developed for the cultivation of limbal epithelial cells. It is still not clear which method promotes effective stem cell viability and this remains a subject of ongoing research. The most preferred technique for limbal cell culture is the explant culture model. In this approach, a small donor eye limbal biopsy is placed as an explant onto a biocompatible substrate (preferably human amniotic membrane) for expansion. The outgrowth (cultivated limbal epithelial cells) is then surgically transferred to the recipient eye.

Due to changing regulations concerning cell-based therapy, the implementation of cultivated limbal epithelial transplantation in accordance with Good Laboratory Practice using xenobiotic-free systems is becoming widely accepted both in Turkey and worldwide.

Keywords: Limbal stem cell deficiency, cultured cells, stem cell transplantation

Address for Correspondence: Özlem Barut Selver MD, Ege University Faculty of Medicine, Department of Ophthalmology, İzmir, Turkey
Phone: +90 505 648 72 68 E-mail: ozlem.barut@deu.edu.tr **ORCID-ID:** orcid.org/0000-0003-3333-3349
Received: 28.11.2016 **Accepted:** 06.02.2017

Introduction

Limbal Stem Cell Deficiency

Limbal stem cell deficiency (LSCD) is a complex pathology with a multifactorial etiology, in which the cornea partially or completely loses its regenerative ability.[1] Stem cell loss resulting from severe damage to the limbal zone leads to permanent corneal epithelial defects and vision loss due to conjunctivalization (Figure 1).[2]

Etiology

The circumstances that lead to LSCD are divided into two main groups, primary causes and secondary causes (Table 1).

Figure 1. Photograph of a patient with limbal stem cell deficiency caused by chemical injury (acetone) showing conjunctivalization and marked vascularization advancing toward the central cornea

Table 1. Classification of the causes of limbal stem cell deficiency

Primary LSCD	Secondary LSCD
Aniridia	**Traumatic**
Congenital erythrokeratoderma	Chemical burns
Xeroderma pigmentosum	Thermal burns
Peters' anomaly	**Acquired**
Brown syndrome	Cicatricial ocular surface diseases
Keratitis-ichthyosis-deafness syndrome	Vernal keratoconjunctivitis
	Ultraviolet exposure
	Ionizing radiation
	Surgeries in the limbic region
	Contact lens use
	Preservative toxicity
	Aging
	Iatrogenic
	Cryotherapy
	Chemotherapeutic agents
	Infection
	Viral
	Bacterial
	Parasitic
	Oncologic
	Ocular surface tumors

Clinically, secondary causes are encountered more frequently than primary causes, in which genetic factors play a role in the etiology (e.g. aniridia, Figure 2).[3,4]

Signs and Symptoms

LSCD has nonspecific symptoms including reduced visual acuity, photophobia, epiphora, blepharospasm, redness associated with chronic inflammation, and recurring attacks of pain due to epitheliopathy.[4,5]

On slit-lamp examination, the corneal epithelium presents a dull and irregular reflex. Depending on the severity of LSCD, thick fibrovascular pannus formation, chronic keratitis, scarring, and calcification may occur. The cornea often exhibits abnormal fluorescein staining due to increased permeability resulting from corneal conjunctivalization.[4]

Diagnosis

It is important to establish a definitive diagnosis in LSCD. Failure to do so may result in the patient undergoing cornea transplantation, which has poor outcomes in this disease.[6]

Despite the many findings of LSCD, only conjunctivalization and goblet cell migration onto the corneal surface are important for diagnosis. Clinical signs of conjunctivalization are deterioration of the limbal palisades of Vogt or delayed fluorescein staining of the cornea. A primary diagnosis of conjunctivalization may be established by demonstrating the presence of goblet cells in the cornea using impression cytology (Figure 3).[1]

Treatment Methods

There are several approaches to the treatment of LSCD. Among them are autologous and allograft limbal graft transplantations as well as cultivated limbal epithelial transplantation (CLET), which is becoming increasingly important.[6]

Autologous limbal grafts may be used in unilateral LSCD, with success rates of over 80% reported in the literature.[7,8] Although not yet proven conclusively, the risk of LSCD development in the donor bed limits the ability to obtain sufficient donor tissue in autologous limbal grafts.[9]

Allograft is a treatment option in bilateral LSCD, but its success is limited due to the risk of immune reaction and allograft rejection.[5,6] The expectations of long-term success with keratolimbal allografts are low, as success rates reported in the literature are around 50%.[10,11]

Although various surgical treatments are available, there is still no known reliable and effective treatment method for cases of severe LSCD, especially bilateral cases.[6] For these reasons, the development of new treatment strategies such as limbal cell culture has become an inescapable necessity.[12,13,14,15,16,17]

The relatively new cell therapy methods recently introduced to clinical practice are still not fully understood with regard to their biological backgrounds. In particular, the characteristics of limbal stem cells and their microenvironments are among

Table 2. Features of the cell culture methods utilized in published prospective studies of the long-term outcomes of cultured limbal epithelial transplant

Author	Year	Biopsy origin	Number of patients	Culture type	Culture medium	Culture substrate	Follow-up period (months)	Success rate
Pauklin et al.[44]	2010	30 Autologous 14 Allogenic	44	Explant	Autologous serum	HAM	28.5	84.1%
Schwab et al.[53]	2000	10 Autologous 4	14	Suspension	Bovine serum	HAM	13	71.4%
Tsai et al.[17]	2000	6 Autologous	6	Explant	Bovine serum	HAM	15	100%
Prabhasawat et al.[54]	2012	12 Autologous 7 Allogenic	19	Explant	Serum-free	HAM	26.1	73.7%
Shortt et al.[42]	2008	7 Autologous 3 Allogenic	10	Suspension	Bovine serum	HAM	9.3	60%
Kolli et al.[55]	2010	8 Allogenic	8	Explant	Autologous serum	HAM	19	100%
Zakaria et al.[56]	2014	15 Autologous 3 Allogenic	18	Explant	Commercial human serum	HAM	22	66.7%

HAM: Human amniotic membrane

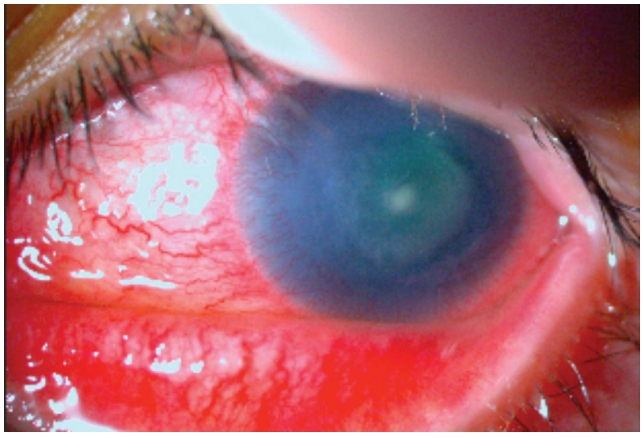

Figure 2. A patient with aniridia exhibits signs of limbal stem cell deficiency

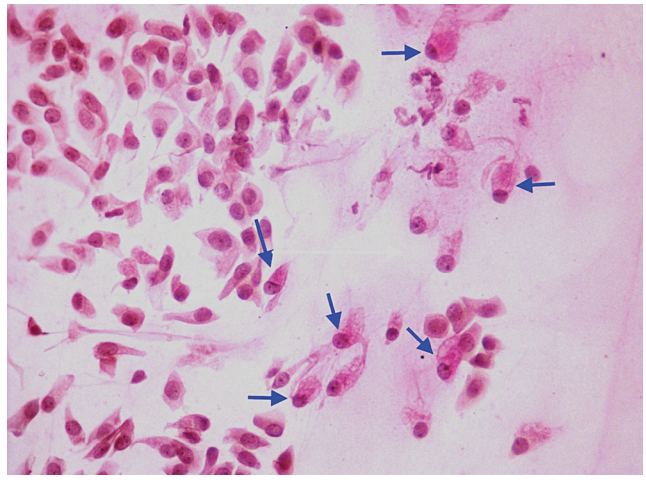

Figure 3. Impression cytology showing goblet cells (arrow) and squamous cells (PASx100)

the main research topics in current limbal stem cell culture studies.[18] Both established and developing techniques based on the transplantation of cultivated limbal stem or precursor cells have been shown to be useful for the treatment of serious ocular surface diseases, with success rates of approximately 73% for allogenic and 77% for autologous methods.[19] However, the question of which technique is the most suitable remains to be answered.[12,16,20]

In 1997, Pellegrini et al.[13] first reported that limbal stem cells can be cultivated on a "feeder layer" in the journal *Lancet*. Later, researchers used autologous limbal epithelial cells cultivated on human amniotic membrane (HAM) for cornea reconstruction.[17] However, these methods were not sufficient for the formation of fully stratified and well-differentiated epithelial layers. As the markers specific to limbal stem cells could not yet be fully determined, it is not possible to adequately isolate them using physical techniques. Therefore, most studies have focused on characterization of the stem cell microenvironment which governs the genes that control limbal epithelial cell differentiation, and determining the signals required for the differentiation of the temporarily proliferating cells in limbal basal epithelium.[21,22,23,24]

CLET, which is becoming increasingly common, is the most advanced treatment method based on existing techniques. Better identification of stem cell properties and microenvironments and the discovery and development of new stem cell sources will allow us to develop ideal treatments and achieve better clinical results in the future.[3,25,26]

Cultivated Limbal Epithelial Cells

Tissue sources for cultivation: The basic tissue sources for limbal epithelial cells are autologous limbal biopsy tissues,

usually obtained from the patient's healthy fellow eye in unilateral cases, and allogenic limbal biopsy tissues obtained from a living relative or from a cadaver in bilateral cases.[27,28,29]

Culture method: A limbal biopsy approximately 1x2 mm in size is obtained from the donor eye and transferred to the laboratory for culturing. There are two main culture methods: cell suspension culture and explant culture.[30]

a. Suspension culture: The biopsy sample taken from the limbal area is dissociated into individual cells using enzymes such as dispase, trypsin, and collagenase. These individual cells are grown in culture medium.[31,32]

b. Explant culture: The explant tissue is placed on a substrate, allowing the proliferation and growth of cells onto the substrate surface (Figure 4).[33]

Several culture components are used in both of these cultivation methods to promote in vitro growth.

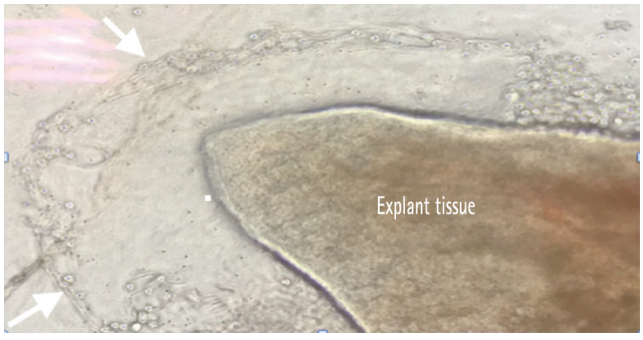

Figure 4. Inverted light microscopy (Olympus; CKX41) image showing explant biopsy tissue and cells (white arrows) proliferating from the edges of the tissue onto the human amniotic membrane

Culture Components

a. 3T3 cells: 3T3 cells are mouse fibroblasts which are commonly used to enable the formation of epithelial layer in the culture. However, the use of these cells theoretically carries risks such as animal cell transplantation, infection, rejection, and microchimerism. Therefore, it is not typically preferred for clinical applications.[34]

b. HAM: HAM is a non-immunogenic biomembrane that has been applied clinically for many years to facilitate wound healing.[35] Most researchers prefer to use deepithelialized HAM because morphological studies have shown that it better supports limbal epithelium growth.[14] Although it is currently the most commonly used substrate in the clinical application of CLET, HAM has certain disadvantages including biological instability, lack of standardized preparation protocols, and a theoretical risk of infection.[19,36,37]

c. Fibrin gel: Fibrin gel is a bioabsorbant membrane composed of fibrinogen. Like HAM, a theoretical risk of infection cannot be ruled out because the fibrogen is human-derived.[38,39,40]

Culture Medium: During the limbal epithelium cell culture process, the culture medium is enriched with serum in order to facilitate proliferation and growth of the epithelium. Although bovine serum has traditionally been used for this purpose,[13,41,42] recent legal regulations and the subsequent focus on xenobiotic-free culture systems have led to the increasing use of autologous serum.[43,44]

Culture Duration: The time required for culturing is about 2 weeks, but this period may be extended when

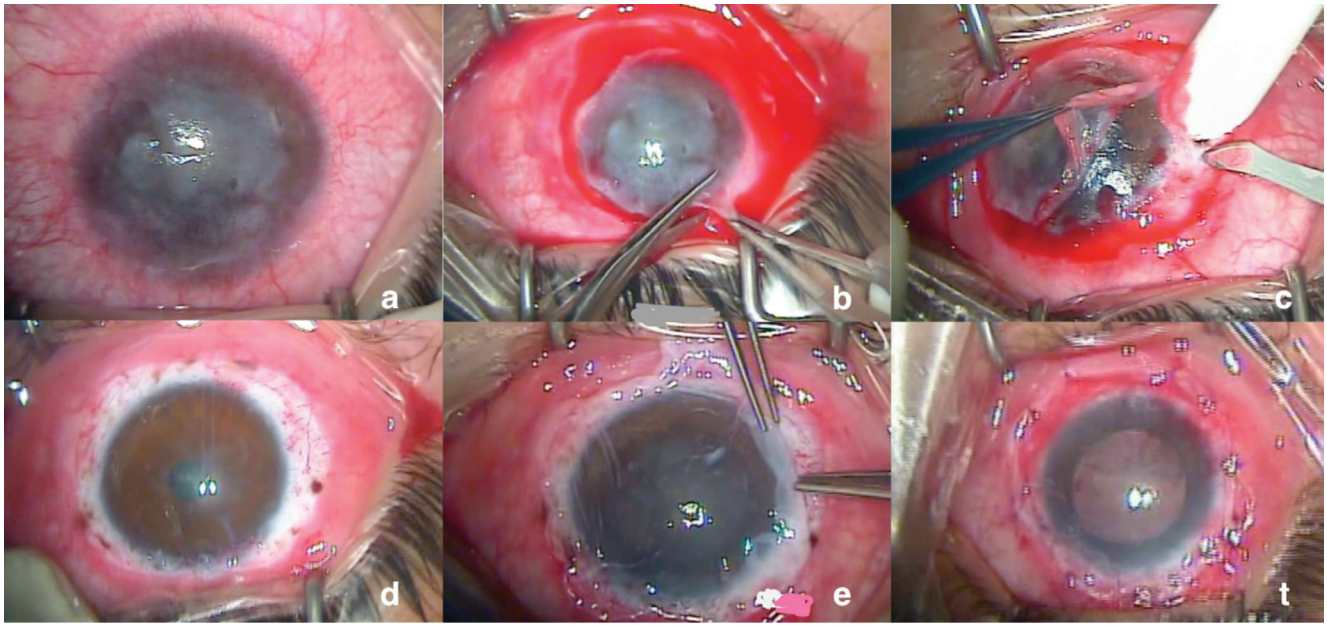

Figure 5. Stages of cultivated limbal epithelial transplantation

using the air-lifting technique, in which the culture is exposed to the air-liquid interface in order create a multilayer epithelium.[19,39,40,44,45,46]

Cultivated Limbal Epithelial Transplantation

a. Preparation of the ocular surface: Prior to CLET, the eye with LSCD (Figure 5a) undergoes peritomy (Figure 5b), the fibrovascular pannus tissue is cleared from the ocular surface (Figure 5c), and superficial keratectomy is performed when necessary. After achieving hemostasis via cauterization, the ocular surface is ready for CLET (Figure 5d).

b. CLET: The cultivated limbal epithelium is transferred from the laboratory to the operating room and transplanted to the prepared ocular surface with the epithelial side up. It is usually fixed to the cornea or the episclera using 10-0 nylon sutures (Figure 5e).

c. Application of a protective membrane/contact lens: Following transplantation, usually a protective HAM or sometimes a bandage lens is placed to prevent the transplanted cells from being adversely effected by eyelid movements. If HAM is used, it is fixed to the conjunctiva using 8-0 vicryl sutures (Figure 5f).[19,28,47]

The methods employed in published prospective studies evaluating the long-term outcomes of CLET in LSCD are summarized in Table 2.

New Regulations

The use of cell therapies is becoming increasingly common worldwide, thus necessitating the development of new standards and protocols.[48] The need for xenobiotic-free methods in CLET emerged due to the risks associated with the use of animal-derived components, including the transmission of a number of diseases (e.g. prion disease), the development of tumorigenic effects, and immune reactions.[25,34,49,50] Furthermore, in order to protect public health when transplanting processed medical products into humans, these techniques must be performed under good laboratory practices, a requirement which has been passed into law in many European countries.[39,43,51]

In Turkey, the Regulation on Human Tissue and Cells and the Quality and Reliability of Related Health Centers issued by the Ministry of Health of the Republic of Turkey was published in the official journal dated October 27, 2010.[52]

Conclusion

The dynamic equilibria that ensure the continuity of epithelialization are important in the processes of ocular surface healing and homeostatic regulation. LSCD, which arises as a result of the disturbance of these dynamic balances, is a painful and tiring condition which impairs vision and reduces quality of life. Multidisciplinary basic and clinical studies are ongoing to develop more effective treatments for LSCD. Surgical success is expected to increase with the development of targeted and effective methods that suppress inflammation by restoring ocular surface homeostasis, enhancing regeneration, and inhibiting neovascularization. Advances in the identification and implementation of ideal scaffolds for stem cell proliferation and in our understanding of the limbal microenvironment will lead to increases in the quantity and quality of the stem cell populations used in CLET, which will in turn result in improved healing and graft success. For ocular surface restoration, especially in bilateral cases lacking an autologous cell source, further development of tissue engineering techniques and the ability to transform non-limbal stem cell sources (e.g. induced pluripotent stem cells) into limbal stem cells by modifying their models of biological behavior may open new horizons in the treatment of this complex pathology.

Ethics

Peer-review: Externally and internally peer-reviewed.

Authorship Contributions

Concept: Özlem Barut Selver, Ayşe Yağcı, Sait Eğrilmez, Design: Özlem Barut Selver, Mehmet Gürdal, Utku Ateş, Sait Eğrilmez, Data Collection or Processing: Özlem Barut Selver, Ayşe Yağcı, Analysis or Interpretation: Özlem Barut Selver, Ayşe Yağcı, Sait Eğrilmez, Jose Mario Wolosin, Literature Search: Özlem Barut Selver, Mehmet Gürdal, Ayşe Yağcı, Melis Palamar, Writing: Özlem Barut Selver, Ayşe Yağcı Sait Eğrilmez, Mehmet Gürdal, Melis Palamar, Türker Çavuşoğlu, Utku Ateş, Ali Veral, Çağrı Güven, Jose Mario Wolosin.

Conflict of Interest: No conflict of interest was declared by the authors.

Financial Disclosure: The authors declared that this study received no financial support.

References

1. Liang L, Sheha H, Li J, Tseng SC. Limbal stem cell transplantation: new progresses and challenges. Eye (Lond). 2009;23:1946-1953.
2. Shapiro MS, Friend J, Thoft RA. Corneal re-epithelialization from the conjunctiva. Invest Ophthalmol Vis Sci. 1981;21:135-142.
3. Khan-Farooqi H, Chodosh J. Autologous Limbal Stem Cell Transplantation: The Progression of Diagnosis and Treatment. Semin Ophthalmol. 2016;31:91-98.
4. Dua HS. Stem cells of the ocular surface: scientific principles and clinical applications. Br J Ophthalmol. 1995;79:968-969.
5. Espana EM, Grueterich M, Romano AC, Touhami A, Tseng SC. Idiopathic limbal stem cell deficiency. Ophthalmology. 2002;109:2004-2010.
6. Daniels JT, Dart JK, Tuft SJ, Khaw PT. Corneal stem cells in review. Wound Repair Regen. 2001;9:483-494.
7. Cauchi PA, Ang GS, Azuara-Blanco A, Burr JM. A Systematic Literature Review of Surgical Interventions for Limbal Stem Cell Deficiency in Humans. Am J Ophthalmol. Am J Ophthalmol. 2008;146:251-259.
8. Kenyon KR, Tseng SC. Limbal autograft transplantation for ocular surface disorders. Ophthalmology. 1989;96:709-722.

9. Jenkins C, Tuft S, Liu C, Buckley R. Limbal transplantation in the management of chronic contact-lens-associated epitheliopathy. Eye (Lond). 1993;7:629-633.
10. Lim P, Fuchsluger TA, Jurkunas UV. Limbal stem cell deficiency and corneal neovascularization. Semin Ophthalmol. 2009;24:139-148.
11. Solomon A, Ellies P, Anderson DF, Touhami A, Grueterich M, Espana EM, Ti SE, Goto E, Feuer WJ, Tseng SC. Long-term outcome of keratolimbal allograft with or without penetrating keratoplasty for total limbal stem cell deficiency. Ophthalmology. 2002;109:1159-1166.
12. Koizumi N, Inatomi T, Suzuki T, Sotozono C, Kinoshita S. Cultivated Corneal Epithelial Transplantation for Ocular Surface Reconstrauction in Acute of Stevebs Johnson Syndrome. Arc Ophthalmol. 2001;119:298-300.
13. Pellegrini G, Traverso CE, Franzi AT, Zingirian M, Cancedda R, De Luca M. Long-term restoration of damaged corneal surfaces with autologous cultivated corneal epithelium. Lancet. 1997;349:990-993.
14. Koizumi N, Fullwood NJ, Bairaktaris G, Inatomi T, Kinoshita S, Quantock AJ. Cultivation of corneal epithelial cells on intact and denuded human amniotic membrane. Investig Ophthalmol Vis Sci. 2000;41:2506-2513.
15. Grueterich M, Espana EM, Tseng SC. Ex vivo expansion of limbal epithelial stem cells: amniotic membrane serving as a stem cell niche. Surv Ophthalmol. 2003;48:631-646.
16. Nakamura T, Koizumi N, Tsuzuki M, Inoki K, Sano Y, Sotozono C, Kinoshita S. Successful regrafting of cultivated corneal epithelium using amniotic membrane as a carrier in severe ocular surface disease. Cornea. 2003;22:70-71.
17. Tsai RJ, Li LM, Chen JK. Reconstruction of damaged corneas by transplantation of autologous limbal epithelial cells. N Engl J Med. 2000;343:86-93.
18. Schlötzer-Schrehardt U, Dietrich T, Saito K, Sorokin L, Sasaki T, Paulsson M, Kruse FE. Characterization of extracellular matrix components in the limbal epithelial stem cell compartment. Exp Eye Res. 2007;85:845-860.
19. Baylis O, Figueiredo F, Henein C, Lako M, Ahmad S. 13 years of cultured limbal epithelial cell therapy: a review of the outcomes. J Cell Biochem. 2011;112:993-1002.
20. Zhao Y, Ma L. Systematic review and meta-analysis on transplantation of ex vivo cultivated limbal epithelial stem cell on amniotic membrane in limbal stem cell deficiency. Cornea. 2015;34:592-600.
21. Wolosin JM, Schütte M, Zieske JD, Budak MT. Changes in connexin43 in early ocular surface development. Curr Eye Res. 2002;24:430-438.
22. Li DQ, Chen Z, Song XJ, de Paiva CS, Kim Hs, Pflugfelder SC. Partial enrichment of a population of human limbal epithelial cells with putative stem cell properties based on collagen type IV adhesiveness. Exp Eye Res. 2005;80:581-590.
23. Papini S, Rosellini A, Nardi M, Giannarini C, Revoltella RP. Selective growth and expansion of human corneal epithelial basal stem cells in a three-dimensional-organ culture. Differentiation. 2005;73:61-68.
24. Selver OB, Durak I, Gürdal M, Baysal K, Ates H, Ozbek Z, Wang Z, Wu A, Wolosin JM. Corneal recovery in a rabbit limbal stem cell deficiency model by autologous grafts of tertiary outgrowths from cultivated limbal biopsy explants. Mol Vis. 2016;22:138-149.
25. Nakamura T, Kinoshita S. New hopes and strategies for the treatment of severe ocular surface disease. Curr Opin Ophthalmol. 2011;22:274-278.
26. Holland EJ. Management of Limbal Stem Cell Deficiency : A Historical Perspective , Past , Present , and Future. Cornea. 2015;34:9-15.
27. Daya SM, Chan CC, Holland EJ; Members of The Cornea Society Ocular Surface Procedures Nomenclature Committee. Cornea Society Nomenclature for Ocular Surface Rehabilitative Procedures. Cornea. 2011;30:1115-1119.
28. Burman S, Sangwan V. Cultivated limbal stem cell transplantation for ocular surface reconstruction. Clin Ophthalmol. 2008;2:489-502.
29. Durak İ, Selver ÖB, Erdal E, Kunter İ, Söylemezoğlu ZÖ, Wolosin JM. Limbal Kök Hücre Yetmezliğinde Kültüre Edilmiş Limbal Epitel Hücreleri ile Oküler Yüzey Rekonstrüksiyonunun Bir Yıllık Sonuçları. Turk J Ophthalmol. 2012;42:172-176.
30. Meyer-Blazejewska EA, Kruse FE, Bitterer K, Meyer C, Hofmann-Rummelt C, Wünsch PH, Schlötzer-Schrehardt U. Preservation of the limbal stem cell phenotype by appropriate culture techniques. Invest Ophthalmol Vis Sci. 2010;51:765-774.
31. Koizumi N, Cooper LJ, Fullwood NJ, Nakamura T, Inoki K, Tsuzuki M, Kinoshita S. An evaluation of cultivated corneal limbal epithelial cells, using cell-suspension culture. Invest Ophthalmol Vis Sci. 2002;43:2114-2121.
32. Zhang X, Sun H, Tang X, Ji J, Li X, Sun J, Ma Z, Yuan J, Han ZC. Comparison of cell-suspension and explant culture of rabbit limbal epithelial cells. Exp Eye Res. 2005;80:227-233.
33. Selver OB, Barash A, Ahmed M, Wolosin JM. ABCG2-dependent dye exclusion activity and clonal potential in epithelial cells continuously growing for 1 month from limbal explants. Invest Ophthalmol Vis Sci. 2011;52:4330-4337.
34. Schwab IR, Johnson NT, Harkin DG. Inherent risks associated with manufacture of bioengineered ocular surface tissue. Arch Ophthalmol. 2006;124:1734-1740.
35. Dua HS, Gomes JA, King AJ, Maharajan VS. The amniotic membrane in ophthalmology. Surv Ophthalmol. 2004;49:51-77.
36. Levis H, Daniels JT. New technologies in limbal epithelial stem cell transplantation. Curr Opin Biotechnol. 2009;20:593-597.
37. Shortt AJ, Secker GA, Lomas RJ, Wilshaw SP, Kearney JN, Tuft SJ, Daniels JT. The effect of amniotic membrane preparation method on its ability to serve as a substrate for the ex-vivo expansion of limbal epithelial cells. Biomaterials. 2009;30:1056-1065.
38. Li Y, Meng H, Liu Y, Lee BP. Fibrin gel as an injectable biodegradable scaffold and cell carrier for tissue engineering. Sci World J. 2015;2015:685-690.
39. Rama P, Matuska S, Paganoni G, Spinelli A, De Luca M, Pellegrini G. Limbal stem-cell therapy and long-term corneal regeneration. N Engl J Med. 2010;363:147-155.
40. Rama P, Bonini S, Lambiase A, Golisano O, Paterna P, De Luca M, Pellegrini G. Autologous fibrin-cultured limbal stem cells permanently restore the corneal surface of patients with total limbal stem cell deficiency. Transplantation. 2001;72:1478-1485.
41. Sangwan VS, Matalia HP, Vemuganti GK, Fatima A, Ifthekar G, Singh S, Nutheti R, Rao GN. Clinical outcome of autologous cultivated limbal epithelium transplantation. Indian J Ophthalmol. 2006;54:29-34.
42. Shortt AJ, Secker GA, Rajan MS, Meligonis G, Dart JK, Tuft SJ, Daniels JT. Ex Vivo Expansion and Transplantation of Limbal Epithelial Stem Cells. Ophthalmology. 2008;115:1989-1997.
43. Kolli S, Ahmad S, Lako M, Figueiredo F. Successful clinical implementation of corneal epithelial stem cell therapy for treatment of unilateral limbal stem cell deficiency. Stem Cells. 2010;28:597-610.
44. Pauklin M, Fuchsluger TA, Westekemper H, Steuhl KP, Meller D. Midterm results of cultivated autologous and allogeneic limbal epithelial transplantation in limbal stem cell deficiency. Dev Ophthalmol. 2010;45:57-70.
45. Nakamura T, Inatomi T, Sotozono C, Ang LP, Koizumi N, Yokoi N, Kinoshita S. Transplantation of Autologous Serum-Derived Cultivated Corneal Epithelial Equivalents for the Treatment of Severe Ocular Surface Disease. Ophthalmology. 2006;113:1765-1772.
46. Colabelli Gisoldi RA, Pocobelli A, Villani CM, Amato D, Pellegrini G. Evaluation of molecular markers in corneal regeneration by means of autologous cultures of limbal cells and keratoplasty. Cornea. 2010;29:715-722.
47. Kolli S, Ahmad S, Lako M, Figueiredo F. Successful clinical implementation of corneal epithelial stem cell therapy for treatment of unilateral limbal stem cell deficiency. Stem Cells. 2010;28:597-610.

48. Menzel-Severing J, Kruse FE, Schlötzer-Schrehardt U. Stem cell-based therapy for corneal epithelial reconstruction: present and future. Can J Ophthalmol. 2013;48:13-21.
49. Basu S, Fernandez MM, Das S, Gaddipati S, Vemuganti GK, Sangwan VS. Clinical outcomes of xeno-free allogeneic cultivated limbal epithelial transplantation for bilateral limbal stem cell deficiency. Br J Ophthalmol. 2012;96:1504-1509.
50. Zamudio A, Wang Z, Chung SH, Wolosin JM. Inhibition of TGFβ cell signaling for limbal explant culture in serumless, defined xeno-free conditions. Exp Eye Res. 2016;145:48-57.
51. Ramírez BE, Sánchez A, Herreras JM, Fernández I, García-Sancho J, Nieto-Miguel T, Calonge M. Stem Cell Therapy for Corneal Epithelium Regeneration following Good Manufacturing and Clinical Procedures. Biomed Res Int. 2015;2015:408-495.
52. T.C. Sağlık Bakanlığı. İnsan Doku Ve Hücreleri İle Bunlarla İlgili Merkezlerin Kalite ve Güvenliği Hakkında Yönetmelik. Resmî Gazete. 2010:27742.
53. Schwab IR, Reyes M, Isseroff RR. Successful transplantation of bioengineered tissue replacements in patients with ocular surface disease. Cornea. 2000;19:421-426.
54. Prabhasawat P, Ekpo P, Uiprasertkul M, Chotikavanich S, Tesavibul N. Efficacy of cultivated corneal epithelial stem cells for ocular surface reconstruction. Clin Ophthalmol. 2012;6:1483-1492.
55. Kolli S, Ahmad S, Lako M, Figueiredo F. Successful clinical implementation of corneal epithelial stem cell therapy for treatment of unilateral limbal stem cell deficiency. Stem Cells. 2010;28:597-610.
56. Zakaria N, Possemiers T, Dhubhghaill SN, Leysen I, Rozema J, Koppen C, Timmermans JP, Berneman Z, Tassignon MJ. Results of a phase I/II clinical trial: standardized, non-xenogenic, cultivated limbal stem cell transplantation. J Transl Med. 2014;12:58.

DOI: 10.4274/tjo.69922
Turk J Ophthalmol 2017;47:292-295

Case Report

Diagnosis of Nephropathic Cystinosis in a Child During Routine Eye Exam

Mahmut Ecel*, Ayça Sarı**, Ali Delibaş***
*Private Tarsus Medical Park Hospital, Ophthalmology Clinic, Mersin, Turkey
**Mersin University Faculty of Medicine, Department of Ophthalmology, Mersin, Turkey
***Mersin University Faculty of Medicine, Department of Pediatric Nephrology, Mersin, Turkey

Abstract
We present a 7-year-old patient who was diagnosed with asymptomatic nephropathic cystinosis following the detection of the pathognomonic corneal white crystalline opacities during a routine eye examination.
Keywords: Cystinosis, cornea, nephropathy

Introduction

Cystinosis is a rare metabolic disease with autosomal recessive inheritance,[1] characterized by the accumulation of cystine crystals in various tissues including the kidneys, bone marrow, pancreas, thyroid, muscle, brain, and eyes.[2,3] Cystinosis can clinically manifest as a nephropathic or non-nephropathic form. The nephropathic form is further divided into two subtypes: infantile cystinosis and juvenile cystinosis.[4] The non-nephropathic form is also known as ocular cystinosis. In ocular cystinosis, pathognomonic yellow-white crystalline deposits are observed in the cornea, but the kidneys are not affected.[4]

Case Report

A 7-year-old female patient with no complaints presented to our clinic for routine eye examination. Her uncorrected vision was perfect in both eyes. On anterior segment examination, yellowish-white crystallized opacities were observed throughout the corneal stroma bilaterally (Figure 1A, 1B). Anterior segment examination was otherwise unremarkable and fundus examination was normal in both eyes. The patient was referred to the university hospital with a prediagnosis of cystinosis. In the biochemical analyses done at the hospital, urinalysis revealed hemoglobin 1+ and protein 2+; 24-hr urine analysis results were phosphorus: 14.4 mg/dL (phosphaturia), creatinine: 16.6 mg/dL (reduced clearance), phosphorus: 3.73 mg/dL (hypophosphatemia); and blood biochemistry test showed normal albumin, calcium, and sodium levels. The patient was diagnosed with nephropathic cystinosis based on these findings and the presence of ocular crystalline deposits. Following cysteamine treatment, clearance and phosphorus levels returned to normal in the follow-up 24-hr urinalysis. Treatment with topical 0.05% cysteamine drops 5 times daily was initiated for the corneal opacities. At 1-year follow-up, the patient had perfect vision in both eyes. Although the topical cysteamine therapy had not reduced the opacities in the cornea caused by cystine crystals, no ocular or systemic complications were observed.

Discussion

Cystinosis is a lysosomal storage disease with an autosomal recessive inheritance pattern. Impairment of the transporter system responsible for transporting cystine out of lysosomes results in the accumulation of cystine crystals in tissues such as the kidneys, eyes, bone marrow, liver, spleen, pancreas, thyroid,

Address for Correspondence: Mahmut Ecel MD, Private Tarsus Medical Park Hospital, Ophthalmology Clinic, Mersin, Turkey
Phone: +90 324 614 77 00 E-mail: ecelmaho@yahoo.com **ORCID-ID**: orcid.org/0000-0001-8370-991X
Received: 09.07.2016 **Accepted:** 16.12.2016

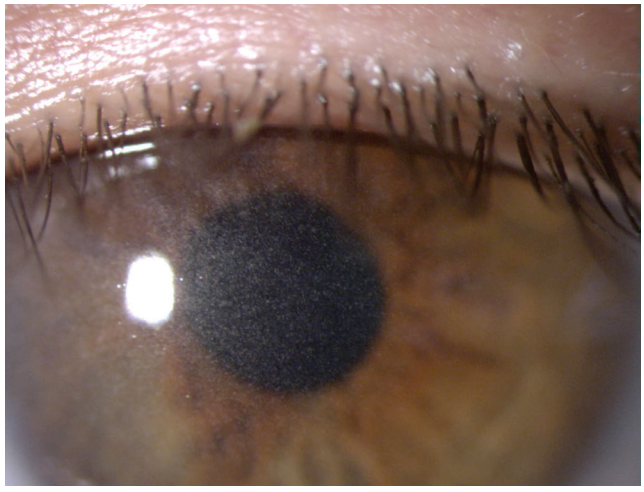

Figure 1A. Yellowish-white accumulated crystals observed throughout the entire corneal stroma of the right eye

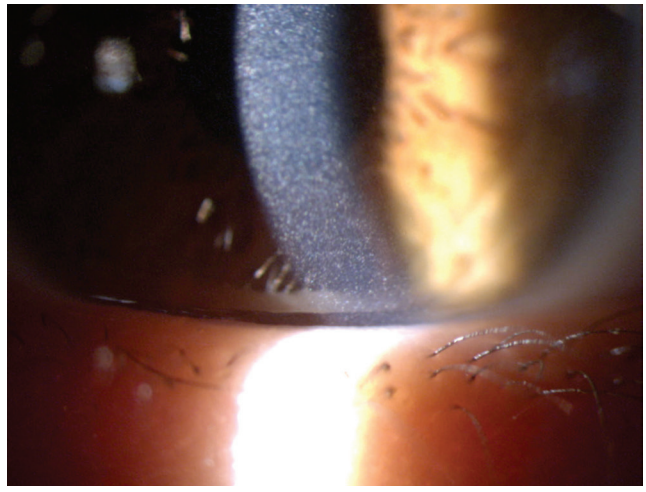

Figure 1B. The appearance of cystine crystals in the left eye at a magnification of x16

skeletal muscles, thyroid, and brain.[4] Electron microscopic and ultrastructural examinations of the crystals have shown that they formed of intralysosomal L-cysteine.[5] Most of the cases in the literature are of infantile type, which is the clinically most severe form.[6]

Ocular cystinosis is diagnosed when the pathognomonic refractive cystine crystal accumulations are observed throughout the conjunctiva and entire cornea (central and peripheral) on anterior segment examination.[6] These deposits can be located in the corneal epithelium, stroma, and endothelium, and their distribution may be associated with disease course and duration.[7] The corneal crystals begin to accumulate in infancy, being found in almost all cases of nephropathic cystinosis at 16 months.[7] They first accumulate in the peripheral cornea and progress toward the center with age.[8] While these crystalline deposits often do not cause visual impairment, in rare cases they may form band keratopathy, thus affecting the central cornea and reducing visual acuity.[9] Superficial punctate and filamentary keratopathy are frequently observed in adults, whereas band keratopathy, peripheral corneal neovascularization, and posterior synechiae associated with increased iris thickness are seen in the elderly.[10] Rare long-term complications of infantile and juvenile cystinosis include patchy pigmentary retinopathy, pigmentary changes in the macula, and involvement of the iris, ciliary body, choroid, and optic nerve due to the cystine accumulations.[10] The most common symptoms in older patients is photophobia and associated blepharospasm.[11] In addition, color vision, peripheral vision, and night vision may be reduced due to anterior and posterior segment complications.[11] Depigmentation of the peripheral retina with pigment epithelium mottling is the most common posterior segment complication.[12] In about 10-15% of patients, retinopathy leads to blindness.[13]

Ocular cystinosis is considered one of the corneal crystalline keratopathies. The term crystalline keratopathy describes a group of diseases in which crystal deposits form on the anterior surface of the corneal epithelium or stroma due to a variety of reasons such as infection, corneal dystrophies, or systemic causes. The etiology of crystalline keratopathy may be ocular, systemic, or medication-induced. Infectious causes include *de novo*, recent refractive or corneal surgeries, and interventions such as keratoplasty. Corneal dystrophies that cause crystalline keratopathy include Schnyder crystalline cornea dystrophy and Bietti crystalline corneoretinal dystrophy. Schnyder dystrophy is a slowly progressive corneal dystrophy with autosomal dominant inheritance.[14] Clinical manifestations include opacification of the central or midperipheral cornea, dense arcus senilis, reduced corneal sensitivity, and recurrent corneal erosion.[15] Bietti corneal dystrophy shows an autosomal recessive inheritance pattern and is characterized by progressive night blindness and narrowing of the visual field. Clinical manifestations include sparkling, yellowish retinal crystals resembling chalk powder, choroidal atrophy and sclerosis, and yellow-white crystals in the superficial stroma and subepithelial layer of the peripheral cornea. Monoclonal gammopathy and multiple myeloma lymphoproliferative disorders may also cause crystalline keratopathy.[16] Corneal accumulations may also form in the epithelium or stroma. Diagnosis is made by conjunctival biopsy, or blood or bone marrow smear. Drug-induced crystalline keratopathy may also occur with the use of fluoroquinolone (ciprofloxacin) drops. The effects usually resolve spontaneously when the topical fluoroquinolone is discontinued.

Infantile nephropathic cystinosis accounts for 95% of cystinosis cases and is the most severe form of the disease. The renal phenotype consists of Fanconi syndrome, in which progressive glomerular dysfunction and loss eventually lead to end-stage renal failure.[17] It initially manifests as asymptomatic aminoaciduria. Proximal tubular dysfunction which develops between 6-12 months of age leads to the loss of amino

acids, sodium, potassium, bicarbonate, magnesium, carnitine, calcium, phosphate, glucose, and low-to-middle molecular weight proteins in the urine, resulting in the development of Fanconi syndrome.[18] Infants may present with lack of appetite, polyuria, polydipsia, severe dehydration and electrolyte imbalance, vomiting, constipation, and sometimes vitamin D-resistant rickets. Biochemical tests may reveal hypokalemia, metabolic acidosis, hypophosphatemia, hypocalcemia, low carnitine level, and hyponatremia. If left untreated, end-stage renal failure develops by the end of the first decade.[19]

Five percent of cystinosis patients are diagnosed with the juvenile form. It appears in late childhood or early adolescence.[20] This form is less severe than nephropathic cystinosis, with milder disease course and symptoms. Children with juvenile cystinosis do not exhibit significant retardation of growth or development.

In 50-70% of patients, fibrosis resulting from accumulation of cystine crystals in thyroid follicular cells causes primary hypothyroidism in the second decade of life.[21] Patients exhibit subclinical hypothyroidism characterized by normal T3-T4 levels and elevated TSH.

Endocrine and exocrine pancreatic insufficiency often occurs in patients with cystinosis after renal transplantation.[22] Around the age of 18, 50% of infantile cystinosis patients develop gradual reduction of insulin secretion and C-peptide production, resulting in glucose intolerance and diabetes.

Primary hypogonadism occurs in 70% of male cystinosis patients.[23] Azoospermia may cause infertility. Female patients are usually asymptomatic.

Central nervous system involvement may cause hypotonia, tremors, delayed speech, gross and fine motor impairment, idiopathic intracranial hypertension, neurocognitive dysfunction, behavioral disorders, and encephalopathy.[23] Cerebral cortical atrophy, hydrocephalus, demyelination, and vacuolar necrotic brain changes may develop at later ages.

The cysteamine used in the treatment of cystinosis acts by disrupting the disulfide bonds of the cystine molecule, allowing the resulting intermediary metabolites to be eliminated from the body without accumulating. Topical cysteamine therapy administered in ocular cystinosis aims to reduce the cystine crystals that have accumulated in the cornea and to prevent complications they may cause. It has been shown that treating patients for 6 months with topical 0.05% cysteamine drops administered 5 times daily resulted in reduction of corneal cystine crystals, improvement in visual acuity, and decreased photophobia and blepharospasm. However, there was no decrease in corneal crystals after topical cysteamine use in our patient.

Cystinosis is a metabolic disease that causes the accumulation of cystine crystals throughout the body and most commonly affects the eyes and kidneys. Ophthalmologists play an important mediator role in diagnosing asymptomatic cystinosis patients by anterior segment examination, especially during routine eye examination. Patients diagnosed with cystinosis should be referred to pediatric nephrology for systemic involvement and possible complications. Early initiation of cysteamine therapy is beneficial for preventing the development of late-stage renal failure.

Ethics

Informed Consent: It was taken.

Peer-review: Externally and internally peer-reviewed.

Authorship Contributions

Surgical and Medical Practices: Mahmut Ecel, Ayça Sarı, Ali Delibaş, Concept: Mahmut Ecel, Ayça Sarı, Design: Mahmut Ecel, Ayça Sarı, Data Collection or Processing: Mahmut Ecel, Analysis or Interpretation: Mahmut Ecel, Literature Search: Mahmut Ecel, Ayça Sarı, Writing: Mahmut Ecel.

Conflict of Interest: No conflict of interest was declared by the authors.

Financial Disclosure: The authors declared that this study received no financial support.

References

1. Demir M, İskeleli G, Arslan O. İnfantil sistinozis olgusu. Turk J Ophthalmol. 1997;27:80-82.
2. Kalatzis V, Cherqui S, Antignac C, Gasnier B. Cystinosin, the protein defective in cystinosis, is a H(+) driven lysosomal cystine transporter. EMBO J. 2001;20:5940-5949.
3. Town M, Jean G, Cherqui S, Attard M, Forestier L, Whitmore SA, Callen DF, Gribouval O, Broyer M, Bates GP, van't Hoff W, Antignac C. A novel gene encoding an integral membrane protein is mutatedin nephropathic cystinosis. Nat Genet. 1998;18:319-324.
4. Gahl WA, Thoene JG, Schneider JA. Cystinosis. N Engl J Med. 2002;347:111-121.
5. Yağmur M, Polat S, Ersöz C, Ersöz TR, Kaya M. Adolesan sistinozis olgu sunumu ve ultrastrüktürel çalışma. Turk J Ophthalmol. 1994;24;476-477.
6. Tsilou E, Zhou M, Gahl W, Sieving PC, Chan CC. Ophthalmic manifestations and histopathology of infantile nephropathic cystinosis: report of a case and review of the literature. Surg Ophthalmol. 2007;52:97-105.
7. Scorsese J, Faggioni R. Ocular manifestations of cystinosis. Ophthalmologica. 1969;159:24-30.
8. Gahl WA, Kuehl EM, Iwata F, Lindblad A, Kaiser-Kupfer MI. Corneal crystals in nephropathic cystinosis: natural history and treatment with cysteamine eyedrops. Mol Genet Metab. 2000;71:100-120.
9. Kaiser-Kupfer MI, Caruso RC, Minkler DS, Gahl WA. Long-term ocular manifestations in nephropathic cystinosis. Arch Ophthalmol. 1986;104:706-711.
10. Schneider JA, Katz B, Melles RB. Update on nephropathic cystinosis. Pediatr Nephrol. 1990;4:645-653.
11. Elder MJ, Astin CL. Recurrent corneal erosion in cystinosis. J Pediatr Ophthalmol Strabismus. 1994;31:270-271.
12. Tsilou ET, Rubin BI, Reed G, Caruso RS, Iwata F, Balog J, Gahl WA, Kaiser-Kupfer MI. Nephropathic cystinosis: posterior segment manifestations and effects of cysteamine therapy. Ophtalmology. 2006;113:1002-1009.
13. Gahl WA, Kuehl EM, Iwata F, Lindblad A, Kaiser-Kupfer MI. Corneal crystals in nephropathic cystinosis: natural history and treatment with cysteamine eye drops. Mol Genet Metab. 2000;71:100-120.

14. Weiss JS. Schnyder's dystrophy of the cornea. A Swede-Finn connection. Cornea. 1992;11:93-101
15. Gaynor PM, Zhang WY, Weiss JS, Skarlatos SI, Rodrigues MM, Kruth HS. Accumulation of HDL apolipoproteins accompanies abnormal cholesterol accumulation in Schnyder's corneal dystrophy. Arterioscler Thromb Vasc Biol. 1996;16:992-999.
16. Garibaldi DC, Gottsch J, de la Cruz Z, Haas M, Green WR. Immunotactoid keratopathy: A clinicopathologic case report and a review of reports of corneal involvement in systemic paraproteinemias. Surv Ophthalmol. 2005;50:61-80.
17. Nesterova G, Gahl WA. Cystinosis: the evolution of a treatable disease. Pediatr Nephrol. 2013;28:51-59.
18. Roth KS, Foreman JW, Segal S. The Fanconi syndrome and mechanisms of tubular transport dysfunction. Kidney Int. 1981;20:705-716.
19. Brodin Sartorius A, Tete MJ, Niaudet P, Antignac C, Guest G, Ottolenghi C, Charbit M, Moyse D, Legendre C, Lesavre P, Cochat P, Servais A. Cysteamine therapy delays the progression of nephropathic cystinosis in late adolescents and adults. Kidney Int. 2012;81:179-189.
20. Servais A, Morinière V, Grünfeld JP, Noël LH, Goujon JM, Chadefaux-Vekemans B, Antignac C. Late-onset nephropathic cystinosis: clinical presentation, outcome, and genotyping. Clin J Am Soc Nephrol. 2008;3:27-35.
21. Gahl WA, Reed GF, Thoene JG, Schulman JD, Rizzo WB, Jonas AJ, Denman DW, Schlesselman JJ, Corden BJ, Schneider JA. Cysteamine therapy for children with nephropathic cystinosis. N Engl J Med. 1987;316:971-977.
22. Broyer M, Tete MJ, Guest G, Bertheleme JP, Labrousse F, Poisson M. Clinical polymorphism of cystinosis encephalopathy. Results of treatment with cysteamine. J Inherit Metab Dis. 1996;19:65-75.
23. Gahl WA, Schneider JA, Thoene JG, Chesney R. The course of nephropathic cystinosis after age 10 years. J Pediatr. 1986;109:605-608.

DOI: 10.4274/tjo.67503
Turk J Ophthalmol 2017;47:296-297

Case Report

Preventable Diving-related Ocular Barotrauma: A Case Report

Serkan Ergözen
ASAL Hyperbaric Oxygen Treatment Center, Undersea and Hyperbaric Medicine Clinic, Ankara, Turkey

Abstract

The mystical beauty of the subaquatic world is undoubtedly attractive, and many techniques and forms of equipment have been developed in the last few decades to allow us to explore the underwater world. A swimmer or diver needs swimming goggles or a diving mask to have clear vision because of the refraction problem between the eye and the water interface. Although these items are effective for clear vision, they can result in "ocular or facial barotrauma of descent" during diving. It is possible to prevent these types of barotrauma with correct techniques and precautions, thus enabling the continuation of recreational diving without recurrence. In this paper, we report a case of subconjunctival hemorrhage caused by breath-hold diving and discuss the causes of ocular barotrauma of descent and preventive measures.

Keywords: Ocular barotrauma, diving, subconjunctival haemorrhage, prevention

Introduction

During the last century, advances in diving techniques and equipment have made breath-hold and equipped dives more common among people who want to explore the underwater environment.

Swimmers and divers need swimming goggles or a diving mask to resolve the problem of refraction between the eye and water interface. Using these, they can see clearly when they look into water and although very useful for visual acuity under water, problems can result because of increasing pressure over the mask or goggles while diving. If the wrong equipment is used or the right technique is not implemented, the diver might experience "ocular or facial barotrauma of descent". This case report aims to help ophthalmologists recognize subconjunctival hemorrhage due to diving activities, understand the reasons for this trauma, and present precautions to avert repeated traumas.

Case Report

A 28-year-old male presented at the outpatient clinic with the complaint of bleeding in his left eye. He reported that he had made repeated breath-hold dives to a depth of approximately 10 to 12 meters. He could equalize his ears by swallowing without any difficulties. After diving, his wife noticed rubescence in his left eye. He consulted a local ophthalmologist and was diagnosed with subconjunctival hemorrhage. No treatment was applied and he was recommended to refrain from diving again as he had a history of repeated instances of subconjunctival hemorrhage. The hemorrhage was attributed to sensitivity of the conjunctiva to something while diving. The patient did not dive again during his holiday.

After his vacation, the patient presented at our outpatient clinic to learn if this condition was related to any diving disorder. He was anxious about the recommendation to not dive again. The eye was in better condition than on the first

Address for Correspondence: Serkan Ergözen MD, ASAL Hyperbaric Oxygen Treatment Center, Undersea and Hyperbaric Medicine Clinic, Ankara, Turkey
Phone: +90 312 231 35 57 E-mail: srknergozen@gmail.com **ORCID-ID:** orcid.org/0000-0003-1171-3703
Received: 11.07.2016 **Accepted:** 18.11.2016

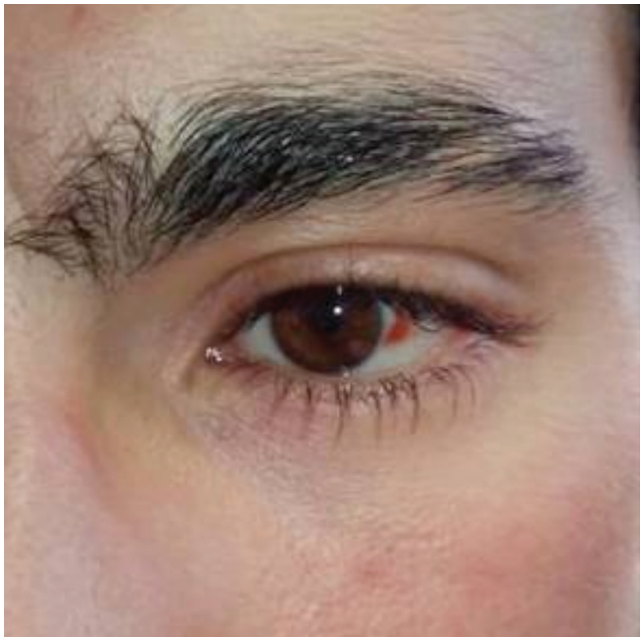

Figure 1. Subconjunctival hemorrhage in the patient's left eye at presentation

day because subconjunctival hemorrhage heals spontaneously and quickly (Figure 1). When questioned, the patient reported no underlying disease which could explain the situation but it was learned that he had been wearing swimming goggles when diving and had a history of repeated subconjunctival hemorrhage. The patient was informed about barotrauma when diving and it was recommended that he use a diving mask instead of goggles and practice correct technique for mask equalization.

Discussion

Breath-hold diving activities (such as snorkeling and spearfishing) are becoming more popular because of the attractive environment of subaquatic world. According to Boyle's Law, one of the physical laws of gases, there is an inverse proportion between the volume and pressure of a gas when a constant temperature is maintained.[1] During a dive, pressure increases outside the goggles or mask but the pressure inside remains at atmospheric value, resulting in negative pressure. This negative pressure pulls the eyes and periorbital soft tissues into the goggles and can sometimes create tissue damage. When the pressure gradient is higher due to deeper dives, the likelihood of eye and periorbital soft tissue damage also increases. Tissue damage is mostly minor, such as subconjunctival hemorrhage, but in severe cases it might be more significant, such as subperiosteal hemorrhage which requires surgical intervention.[2,3,4] Subconjunctival hemorrhage caused by diving does not require treatment and heals spontaneously, although recurrent hemorrhages resulting from recreational diving might be distressing for the patient.

This kind of ocular and periorbital soft tissue damage is well known by diving medicine physicians and can be prevented by using a diving mask instead of goggles while diving. The correct technique is to equalize the inside pressure of the mask to the outside water pressure by exhaling from the nose into the mask while descending, thereby neutralizing the vacuum effect. When ascending, the expanding volume of air will escape from the mask passively, causing no harm.[5]

Subconjunctival hemorrhage caused by diving with swimming goggles is a preventable condition. It is important that patients are questioned about goggle use if they present with subconjunctival hemorrhage after diving. When the use of goggles is determined as the cause of bleeding, the recommendation should be made to use a diving mask and equalize the pressure inside the mask to the outside water pressure by exhaling from the nose into the mask while descending.

Ethics

Informed Consent: It was taken.

Peer-review: Externally peer-reviewed.

Financial Disclosure: The author declared that this study received no financial support.

References

1. Kindwall EP. The Physics of Diving and Hyperbaric Pressures. In: Kindwall EP, Whelan HT, eds. Hyperbaric Medicine Practice (3rd ed). USA; Best Publishing Company; 2008:23-38.
2. Rosenberry C, Angelidis M, Devita D. Orbital subperiosteal hematoma from scuba diving. Wilderness Environ Med. 2010;21:250-252.
3. Woo D, Rogers S, Leong J, Clement CI, Kourt G. Non-traumatic subperiosteal orbital haemorrhage secondary to barotrauma. Orbit. 2012;31:347-349.
4. Dolar A, Ardagil BA, Yaylalı SA, Erbil HH. Tüplü Dalış İle İlişkili Oküler Patolojiler, Bir Subkonjonktival Kanama Olgusu - Olgu Sunumu. Turk J Ophthalmol. 2008;38:446-448.
5. Edmonds C, McKenzie B, Thomas R, Pennefather J. Other Barotraumas. In: Edmonds C, McKenzie B, Thomas R, Pennefather J, eds. Diving Medicine for SCUBA Divers (5th ed); Australia; Carl Edmonds; 2013:130-134.

DOI: 10.4274/tjo.56873
Turk J Ophthalmol 2017;47:298-301

Case Report

Posterior Polar Central Choroidal Dystrophy: A Case Report

Funda Dikkaya, Mustafa Özsütçü, Merve Özbek, Sevil Karaman Erdur, Fevzi Şentürk
İstanbul Medipol University Faculty of Medicine, Department of Ophthalmology, İstanbul, Turkey

Abstract

A 52-year-old male presented with a 25-year history of decreasing vision. Best corrected visual acuity was 0.3 in his right and 0.2 in his left eye. Fundoscopic examination showed bilateral symmetric atrophy of the retinal pigment epithelium and choriocapillaris in the posterior polar areas between vascular arcades and surrounding the optic disc. On fluorescein angiography, the large choroidal vessels beneath these affected regions were easily seen. Fundus autofluorescence imaging showed clearly defined hypoautofluorescent areas that corresponded to the aforementioned lesions. Atrophy of the choriocapillaris and outer retinal layer were detected in optical coherence tomography. Photopic and scotopic responses were subnormal in flash electroretinogram (ERG), and responses were also minimal in pattern ERG and multifocal ERG. The patient was diagnosed with posterior polar central choroidal dystrophy. We aimed to present the results of fluorescein angiography, fundus autofluorescence imaging, optical coherence tomography, and electrophysiological tests in this rare case of posterior polar central choroidal dystrophy.

Keywords: Posterior polar central choroidal dystrophy, fluorescein angiography, fundus autofluorescence imaging, optical coherence tomography

Introduction

Posterior polar central choroidal dystrophy is a form of choroidal dystrophy characterized by loss of retinal pigment epithelium (RPE) and choriocapillaris. Involvement occurs in the posterior fundus within the vascular arcades and sometimes surrounding the optic nerve. This term was first used by Yannuzzi[1] and since then there have been no further reports of this rare condition. In this case report, we present the results of fluorescein angiography, fundus autofluorescence (FAF) imaging, optical coherence tomography (OCT) and electrophysiological testing in this rare disease.

Case Report

A 52-year-old male patient had a 25-year history of decreasing vision in both eyes. He denied any family history of similar ocular disorders. Best corrected visual acuity was 0.3 in his right and 0.2 in his left eye with Snellen testing. His refraction was -3.00 180°-0.75 in the right eye and -3.50 160°-0.50 in the left eye. Slit-lamp examination was normal in both eyes and intraocular pressure was 15 mmHg in the right eye, 16 mmHg in the left eye. Fundoscopic examination showed bilateral symmetrical RPE and choriocapillaris atrophy in the posterior polar areas between the vascular arcades and around the optic nerve. No flecks or drusen were observed (Figure 1A, B). On fluorescein angiography, large choroidal vessels were easily observed beneath these affected regions due to loss of the pigment epithelium and choriocapillaris (Figure 1C, D). FAF imaging showed clearly defined hypoautofluorescent areas that corresponded to the aforementioned lesions (Figure 2). Atrophy of the choriocapillaris and outer retinal layer were detected in OCT (Figure 3). Central macular thickness was

Address for Correspondence: Funda Dikkaya MD, İstanbul Medipol University Faculty of Medicine, Department of Ophthalmology, İstanbul, Turkey
Phone: +90 505 364 30 86 E-mail: fundadikkaya@hotmail.com **ORCID-ID:** orcid.org/0000-0003-2312-2521
Received: 19.08.2016 **Accepted:** 12.12.2016

about 58 µm and central choroidal thickness was about 118 µm for both eyes. Electroretinogram (ERG) and visual evoked potential (VEP) revealed that the patient's b-wave amplitude on dark-adapted 0.01 ERG (rod response) was below the normal limit in both eyes. On dark-adapted 3.0 ERG, both a- and b-wave implicit times were prolonged in both eyes, and a-wave and b-wave amplitudes were reduced in both eyes. Light-adapted 3.0 ERG (cone response) revealed reduced a- and b-wave amplitudes. Pattern ERG responses were minimal. On light-adapted 30 Hz flicker ERG 30 Hz amplitudes were attenuated in both eyes. (16.2 µV, 13.5 µV) (normal range: 57-223 µV) (Figure 4, Table 1). There was a reduction in amplitude of all waveforms on the multifocal ERG (Figure 5). Pattern VEP responses were minimal and flash VEP was within normal limits (Figure 6).

Discussion

Primary choroidal dystrophies which affect the central macula are referred to as central areolar choroidal dystrophy, posterior polar central choroidal dystrophy, posterior polar annular dystrophy, posterior polar hemispheric dystrophy, and central and peripheral annular choroidal dystrophy.[1] All forms of these choroidal dystrophies feature varying patterns of atrophy involving both the RPE and choriocapillaris. In posterior polar central choroidal dystrophy, the atrophic abnormality involves the posterior fundus within the vascular arcades and sometimes the area surrounding the optic nerve.[1]

OCT, which provides detailed analysis of retinal architecture, revealed atrophy of the choriocapillaris and outer retinal layers, and FAF images helped to localize the boundaries of the atrophic area.

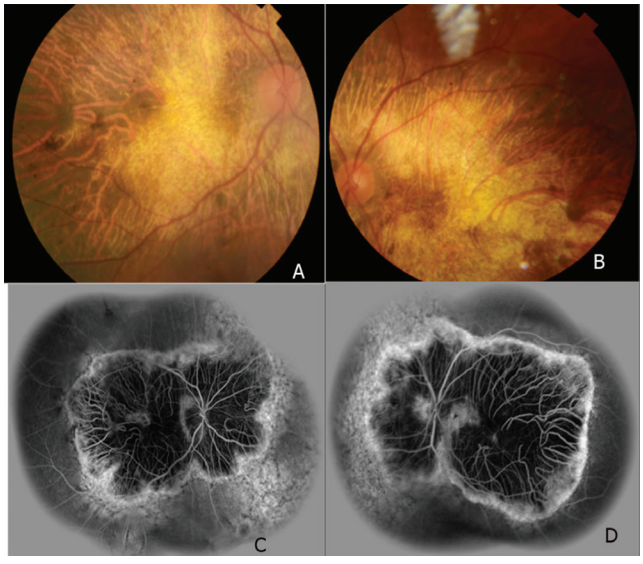

Figure 1. Right (A) and left (B) fundus images showing retinal pigment epithelium and choriocapillaris atrophy in the posterior polar areas between vascular arcades and around the optic nerve. Right (C) and left (D) fluorescein angiography demonstrating loss of choriocapillaris and retina pigment epithelium

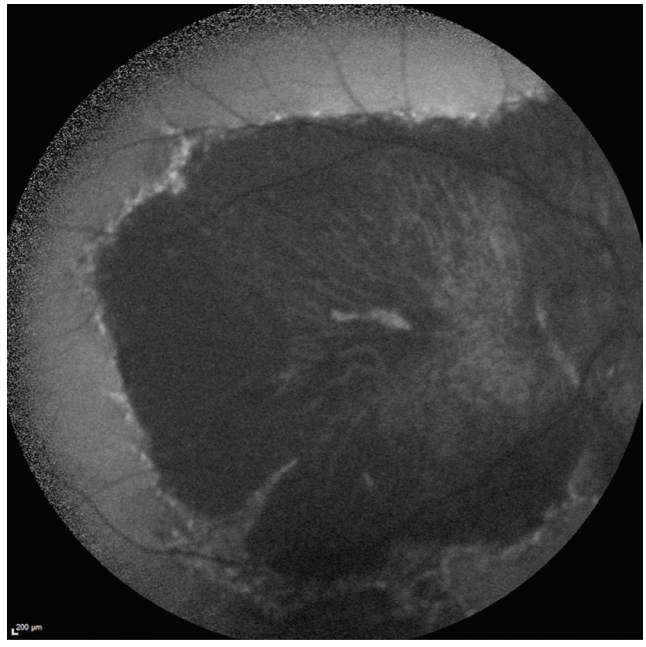

Figure 2. Fundus autofluorescence imaging of the right eye showing hypoautofluorescent areas corresponding to the atrophic area

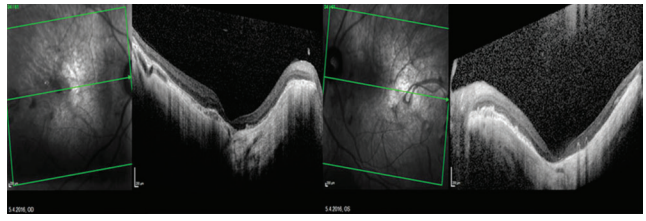

Figure 3. Optical coherence tomography images showing atrophy of the choriocapillaris and outer retinal layer

Table 1. Results of full-field electroretinogram

Test	a-wave amplitude (µV)	b-wave amplitude (µV)	a-wave implicit time (ms)	b-wave implicit time (ms)
Dark-adapted 0.01 ERG	R:35.0 L:50.8 (n=95.0-305)		R:35.0 L:50.8 (n=95.0-305)	R:94.2 L:98.0 (n=67-91)
Dark-adapted 3.0 ERG	R:52.1 L:61.5 (n=155-356)	R:95.1 L:113 (n=290-654)	R:24.1 L:25 (n=14-22)	R:49.9 L:53.4 (n=33-46)
Light-adapted 3.0 ERG	R:5.66 L:8.69 (n=26.0-62.0)	R:71.7 L:51.7 (n=103-250)	R:11.7 L:12.3 (n=13-16)	R:38.2 L:39.6 (n=29-33)
R: Right eye, L: Left eye , n: Normal range				

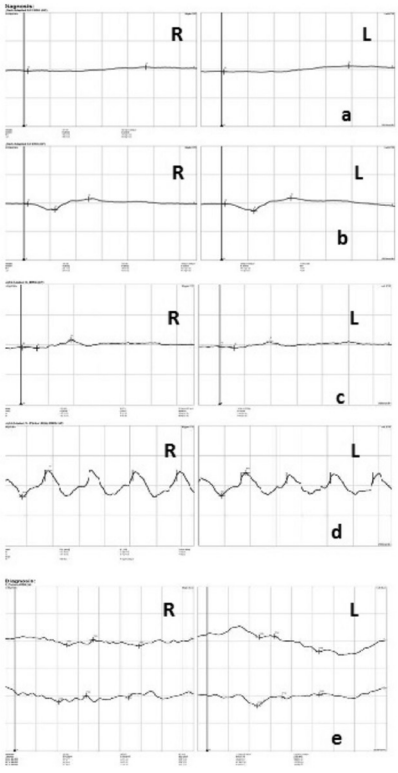

Figure 4. Full-field electroretinogram of right (R) and left (L) eyes. a) Dark adapted 0.01 ERG, b) Dark adapted 3.0 ERG, c) Light adapted 3.0 ERG, d) Light adapted 3.0 flicker 30 Hz ERG, e) Pattern ERG

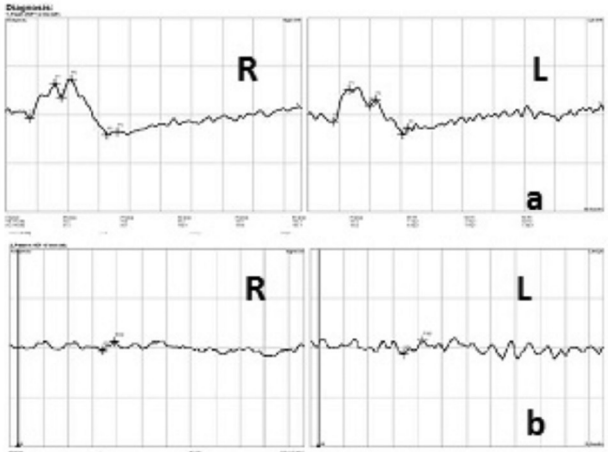

Figure 6. Visual evoked potential results of right (R) and left (L) eyes. a) Flash VEP, b) Pattern VEP

The differential diagnosis of this condition included central areolar choroidal dystrophy, geographic atrophy, and pathologic myopia. We excluded pathologic myopia because the patient had refractive error less than -6.0 D. In central areolar choroidal dystrophy, atrophy of the RPE and choriocapillaris occurs in the foveal region and does not spread through the vascular arcade. The results of an electrophysiological study in a patient

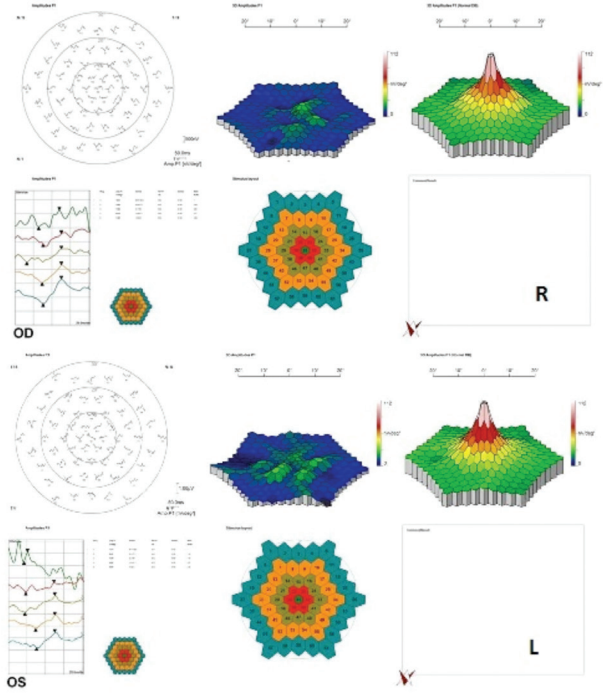

Figure 5. Multifocal electroretinogram of right (R) and left (L) eyes

with central areolar choroidal dystrophy have been reported in the literature. Ponjavic et al.[2] reported the result of full-field electroretinography in this disorder. They showed that the cone b-wave amplitude in ERG is decreased and the cone b-wave implicit time is prolonged. This result shows that although it is a choroidal disease, it also affects most or all of the retinal cones. Lotery et al.[3] reported that pattern VEP and pattern ERG are the most sensitive electrophysiological tests which show abnormality in clinically normal but genetically affected central areolar choroidal dystrophy patients. Eventually in later disease stages, atrophy results in abnormal cone and rod responses on full-field ERG due to widespread photoreceptor dysfunction.

In another case report, full-field and multifocal ERG results of a patient with central areolar choroidal dystrophy showed normal photopic and scotopic responses in the full-field ERG and severely depressed retinal function of the perifoveal macula corresponding to the atrophic area in the multifocal ERG.[4]

Posterior polar central choroidal dystrophy affects a larger area than central areolar choroidal dystrophy and in our case the patient was in the advanced stage. Therefore, the patient demonstrated abnormal photopic and scotopic responses in full-field ERG as well as pattern VEP and pattern ERG. At the same time, all waves showed reduced amplitude in multifocal ERG.

Another disease in the differential diagnosis may be geographic atrophy, which is a devastating complication of age-related macular degeneration. Geographic atrophy of the

RPE may be classified as drusen-related or neovascularization-related.[5] Because there were no drusen or fibrovascular tissue in either eye and the findings were symmetrical, this diagnosis was excluded.

Based on all of these findings, we diagnosed the patient with posterior polar central choroidal dystrophy. We share the results of fluorescein angiography, FAF imaging, OCT, and electrophysiological tests in our case in order to remind clinicians of this rare disease.

Ethics

Informed Consent: It was taken.

Peer-review: Externally peer-reviewed.

Authorship Contributions

Surgical and Medical Practices: Funda Dikkaya, Mustafa Özsütçü, Fevzi Şentürk, Concept: Funda Dikkaya, Mustafa Özsütçü, Sevil Karaman Erdur, Fevzi Şentürk, Design: Funda Dikkaya, Mustafa Özsütçü, Sevil Karaman Erdur, Fevzi Şentürk, Data Collection or Processing: Funda Dikkaya, Merve Özbek, Sevil Karaman Erdur, Analysis or Interpretation: Funda Dikkaya, Mustafa Özsütçü, Fevzi Şentürk, Literature Search: Funda Dikkaya, Merve Özbek, Sevil Karaman Erdur, Writing: Funda Dikkaya, Sevil Karaman Erdur, Fevzi Şentürk.

Conflict of Interest: No conflict of interest was declared by the authors.

Financial Disclosure: The authors declared that this study received no financial support.

References

1. Yannuzzi LA. Posterior polar central choroidal dystrophy. In: Yannuzzi LA, ed. The Retina Atlas. Saunders; 2010:85.
2. Ponjavic V, Andreasson S, Ehinger B. Full-field electroretinograms in patients with central areolar choroidal dystrophy. Acta Ophthalmol (Copenh). 1994;72:537-544.
3. Lotery AJ, Silvestri G, Collins AD. Electrophysiology findings in a large family with central areolar choroidal dystrophy. Doc Ophthalmol. 1998-1999;97:103-119.
4. Hartley KL, Blodi BA, VerHoeve JN. Use of the multifocal electroretinogram in the evaluation of a patient with central areolar choroidal dystrophy. Am J Ophthalmol. 2002;133:852-854.
5. Dannis RP, Lavine JA, Domalpally A. Geographic atrophy in patients with advanced dry age-related macular degeneration: current challenges and future prospects. Clin Ophthalmol. 2015;9:2159-2174.

DOI: 10.4274/tjo.09068
Turk J Ophthalmol 2017;47:302-305

Case Report

Assessment of Spectral-Domain Optical Coherence Tomography Findings in Three Cases of X-Linked Juvenile Retinoschisis in the Same Family

Sibel Doğuizi, Mehmet Ali Şekeroğlu, Salih Çolak, Mustafa Alpaslan Anayol, Pelin Yılmazbaş
Ulucanlar Eye Training and Research Hospital, Ophthalmology Clinic, Ankara, Turkey

Abstract

X-linked juvenile retinoschisis (XLRS) is an X-linked hereditary retinal dystrophy characterized by splitting of the neurosensory retina. On fundus examination, the macula often has a spoke wheel appearance with foveal cystic lesions, and separation of the retinal layers is typical on spectral-domain optical coherence tomography (SD-OCT). Patients with XLRS can exhibit different clinical courses, stages, and SD-OCT findings, even among members of the same family. SD-OCT is an important imaging method that allows us to achieve more detailed information about XLRS. In this study, we report three patients in the same family who have different clinical features and SD-OCT findings.

Keywords: Hereditary retinal dystrophy, spectral-domain optical coherence tomography, X-linked juvenile retinoschisis

Introduction

X-linked juvenile retinoschisis (XLRS) is a hereditary retinal dystrophy with a prevalence ranging between 1:5,000 and 1:25,000. It is the most common form of macular degeneration among male children and adolescents, and females are carriers due to its X-linked recessive inheritance pattern.[1] The first symptoms typically appear in school-age children 5-10 years old, and visual acuity during this period is usually between 20/200 and 20/50.[1,2] Fundus examination often reveals a bicycle spoke wheel appearance indicating foveal schisis in the macula, and separation of the retinal layers is a typical finding on spectral-domain optical coherence tomography (SD-OCT).[1,2,3] Peripheral retinoschisis is also seen in 50% of cases, most commonly in the inferotemporal quadrant. Electroretinography (ERG) typically shows reduced b-wave and normal a-wave, indicative of a defect in the inner retinal layers.[1,2,3] Other clinical findings include white spots on the retina, thinning of the retinal vessels, dendritic appearance of the peripheral retina, and vascular sheathing, and complications such as vitreous hemorrhage and retinal detachment may occur.[1,2,3]

XLRS can manifest with highly variable clinical spectra, and even members of the same family may exhibit different clinical features and SD-OCT findings. SD-OCT is especially valuable because it reveals findings that cannot be distinguished in fundus examination and facilitates detection of the different phenotypic signs of the disease.[4] In this article, we present and discuss the different clinical and SD-OCT findings of three patients from the same family.

Case Report

Case 1

A 12-year-old male patient presented to our clinic with complaints of low vision in both eyes. His best corrected visual acuity was 20/100 in the right eye and 20/80 in the left. There was no difference in his low vision between day and night. Refraction values were +2.25 in the right and +1.25 (-1.25, 180) in the left eye. Bilateral vitreous syneresis, pigmentary changes in the peripheral retina, and a spoke wheel appearance in the macula suggesting foveal schisis were observed on dilated fundus examination (Figure 1). SD-OCT

Address for Correspondence: Sibel Doğuizi MD, Ulucanlar Eye Training and Research Hospital, Ophthalmology Clinic, Ankara, Turkey
Phone: +90 532 15375 77 E-mail: eryigits@yahoo.com **ORCID-ID:** orcid.org/0000-0001-6047-218X
Received: 07.08.2016 **Accepted:** 30.09.2016

(Spectralis; Heildelberg Engineering, Heildelberg, Germany) revealed schisis cavities in the fovea of both eyes, especially prominent in the inner nuclear layer, as well as large bilateral foveal cysts (Figure 2). Central foveal thickness (CFT) was 606 µm in the right eye and 612 µm in the left eye. Deterioration in the ellipsoid zone and external limiting membrane was also observed in the foveal regions in both eyes on SD-OCT. The patient had no systemic diseases. It was indicated in his family history that his brother and uncle also had vision impairment. The patient was diagnosed with XLRS based on the findings. The patient's other siblings and male relatives were invited for examination.

Case 2

Upon examination of the siblings (1 female, 1 male) of the first patient, the 8-year-old brother was found to have bilateral low vision. His best corrected visual acuity was 20/100 in both eyes. Refraction value was +0.75 bilaterally and anterior segment examination was normal in both eyes. Bilateral vitreous syneresis, vitreous veils, peripheral retinoschisis, and macular spoke wheel appearance suggesting foveal schisis were observed on dilated fundus examination (Figure 3). SD-OCT revealed bilateral foveal cysts, especially in the inner nuclear layer, which converged to form retinoschisis. The lesions subsided from the fovea to the periphery (Figure 4). Cysts were also observed to a much lesser extent in the outer plexiform and outer nuclear layers. CFT was 324 µm in the left eye and 456 µm in the right eye. In addition, it was observed that there was irregularity in the ellipsoid zone and external limiting membrane of the foveal region, which was more pronounced in the right eye. The patient had no systemic diseases. The patient was diagnosed with XLRS based on the findings.

Case 3

Examination of the other male members of the family revealed bilateral low vision in the 41-year-old uncle of the first two patients. It was learned that he had suffered low vision since childhood. His best corrected visual acuity was 20/200 in both eyes. Refraction value was +0.50 bilaterally and anterior segment examination was normal in both eyes. On dilated fundus examination, there was vitreous syneresis, peripheral pigmentary changes, and a weak foveal reflex in both eyes (Figure 5). Pronounced foveal atrophy was apparent in both eyes on SD-OCT (Figure 6). CFT was 127 µm in the

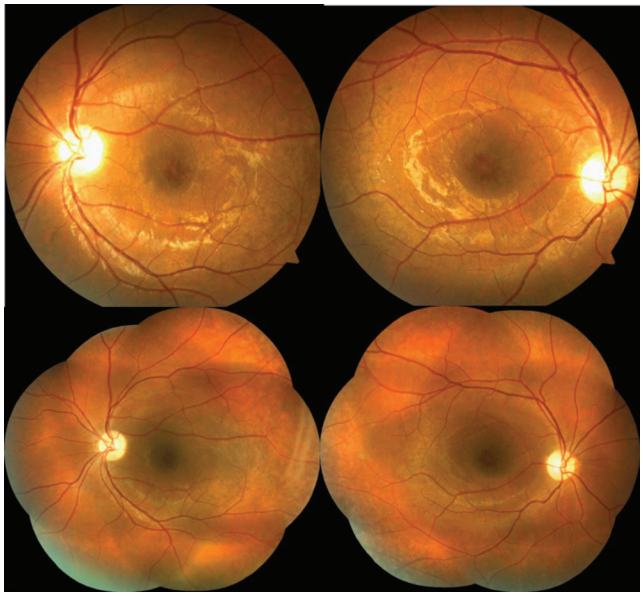

Figure 1. Case 1: Color fundus photographs of the left and right eyes showing bilateral spoke wheel appearance consistent with foveal schisis, pigmentary changes in the peripheral retina, and vitreous syneresis

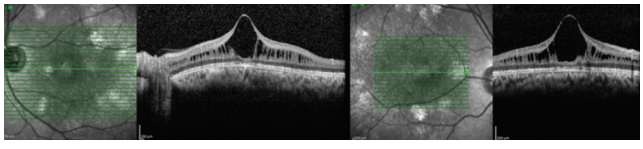

Figure 2. Case 1: Spectral-domain optical coherence tomography images of the left and right eyes showing marked schisis cavities in the fovea of both eyes, especially in the inner nuclear layer, with large bilateral foveal cysts

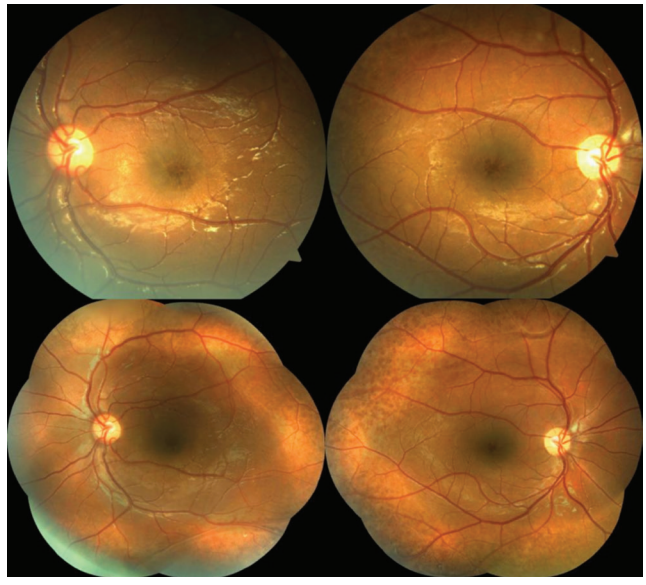

Figure 3. Case 2: Color fundus photographs of the left and right eyes showing bilateral macular spoke wheel appearance suggesting foveal schisis, vitreous syneresis, vitreous veils, and peripheral retinoschisis

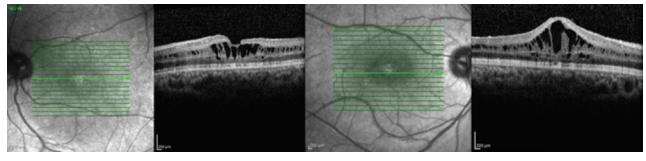

Figure 4. Case 2: Spectral-domain optical coherence tomography images of the left and right eyes showing cysts in the inner nuclear layer which converge form retinoschisis and continue decreasingly from the fovea to the periphery, with a few cysts in the external plexiform and outer nuclear layers

right eye and 125 µm in the left. It was also noted on SD-OCT that the inner retinal layers in particular could not be clearly distinguished due to severe atrophy in the foveal region. The patient had no systemic diseases. The patient was diagnosed with XLRS based on the findings.

Discussion

XLRS is an X-linked recessive retinal dystrophy characterized by splitting of the neurosensory retina into layers. The disease develops due to several different mutations of the *XLRS1* gene located in the p22 region of the X chromosome.[5] The *XLRS1* gene encodes the retinoschisis protein, which is predominantly expressed by photoreceptor and Müller cells and plays a crucial role in preserving the anatomical and functional integrity of the retina. Abnormal production of this protein due to mutation disrupts the structural integrity of the retina, leading to the formation of cysts and schisis cavities, which can develop in all retinal layers.[5]

The disease is usually detected during childhood or adolescence, but can more rarely manifest in infants with nystagmus and strabismus. Fundus examination findings of microcysts with spoke wheel appearance, especially in the foveal region, is considered the main diagnostic sign. Over the course of years, this appearance may disappear, the microcysts may converge to form large foveal cysts, or foveal atrophy may develop in more advanced stages.[3,6]

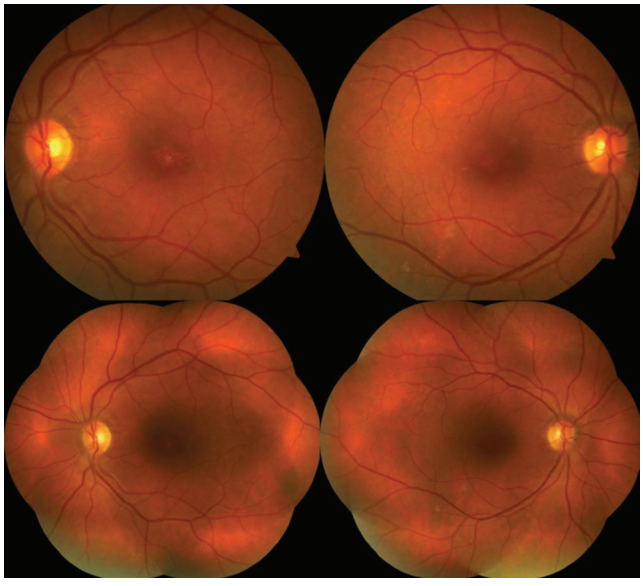

Figure 5. Case 3: Color fundus photographs of the left and right eyes showing bilateral macular atrophy, vitreous syneresis, and peripheral pigmentary changes

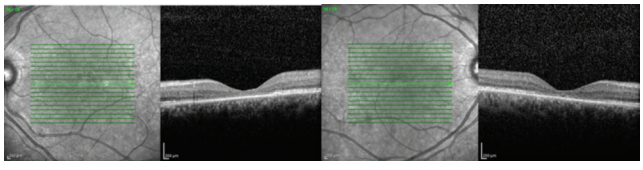

Figure 6. Case 3: Spectral-domain optical coherence tomography images of the left and right eyes showing marked bilateral foveal atrophy

Differential diagnosis of XLRS includes retinitis pigmentosa, acquired retinoschisis, Goldman-Favre syndrome, Wagner's disease, Stickler syndrome, macular dystrophies, choroidal dystrophies, and peripheral vitreoretinal degenerations. Our cases were distinguished from these diseases based on their vision levels, clinical findings, lack of comorbid systemic diseases, presence of typical macular lesions, SD-OCT findings, and hereditary pattern.

Clinical findings and ERG are important for the diagnosis of XLRS, but SD-OCT has a critical role in showing the plane of separation in the neurosensory retina and the size and extent of the schisis cavities, especially in the early stages of the disease. Clinical features and SD-OCT findings of the disease may differ between the members of the same family, as well as between the two eyes of the same patient. In addition, the characteristics of the lesions may change over time.[7] This variability is also apparent in our cases.

The most common SD-OCT finding in XLRS is extensive retinal splitting (schisis formation) in the inner nuclear layer. Less commonly, signs of splitting can also be seen in the outer nuclear and outer plexiform layers, and small cystoid changes have been reported in the nerve fiber-ganglion cell layer.[8,9,10] Similarly, in our second case, SD-OCT revealed marked schisis cavities in the fovea of both eyes, especially in the inner nuclear layer, with fewer cysts in the outer plexiform and outer nuclear layers. Although schisis cavities are typically limited to the foveal pit, they may also continue on both sides and extend across the entire posterior pole; however, in our cases they were limited to the foveal region. Recent studies of this rare disease have demonstrated that the extent of schisis is greater in the inner nuclear and outer nuclear-plexiform layers, which contradicts previous histopathological studies showing that schisis occurs mostly in more superficial retinal layers such as the internal limiting membrane and nerve fibers.[8,9,10] We believe that this discrepancy may be a result of technical limitations of the histopathological studies, and more accurate information about XLRS can be obtained using SD-OCT, which enables high-resolution *in vivo* imaging of the retina.

Our first patient exhibited large foveal cysts, which is less common in XLRS and almost always accompanied by schisis cavities in the inner nuclear layers. Large foveal cysts are thought to form when the septa between previously existing cavities rupture, and a possible association with lower visual acuity as been reported.[7,8,9] However, the visual acuity of our first patient was similar to that of our second patient. In XLRS, phenotypic SD-OCT images characterized by intraretinal schisis formation can regress over time, giving way to atrophy.[10,11,12,13] Likewise, in our study, SD-OCT revealed marked foveal atrophy in both eyes of the 41-year-old uncle of the other two siblings with XLRS. At this stage, the foveal

atrophy detected with SD-OCT is not diagnostic on its own. However, we reached the diagnosis based on the patient's nephews having XLRS, the patient's history of low vision since childhood, and the detection of pigmentary changes in the peripheral retina and vitreous changes on examination.

This study presents three cases from the same family with different clinical and SD-OCT findings. XLRS may have different clinical courses and SD-OCT findings, even among individuals in the same family. SD-OCT is a crucial, unparalleled imaging method that allows us to understand the different structural changes caused by the disease in the macula, and elucidate the levels and stages of these defects.

Ethics

Informed Consent: It was taken.

Peer-review: Externally peer-reviewed.

Authorship Contributions

Surgical and Medical Practices: Sibel Doğuizi, Mehmet Ali Şekeroğlu, Pelin Yılmazbaş, Concept: Sibel Doğuizi, Mehmet Ali Şekeroğlu, Salih Çolak, Mustafa Alpaslan Anayol, Pelin Yılmazbaş, Design: Sibel Doğuizi, Mehmet Ali Şekeroğlu, Salih Çolak, Mustafa Alpaslan Anayol, Pelin Yılmazbaş, Data Collection or Processing: Sibel Doğuizi, Mehmet Ali Şekeroğlu, Salih Çolak, Mustafa Alpaslan Anayol, Analysis or Interpretation: Sibel Doğuizi, Mehmet Ali Şekeroğlu, Salih Çolak, Mustafa Alpaslan Anayol, Pelin Yılmazbaş, Literature Search: Sibel Doğuizi, Mehmet Ali Şekeroğlu, Salih Çolak, Mustafa Alpaslan Anayol, Pelin Yılmazbaş, Writing: Sibel Doğuizi, Mehmet Ali Şekeroğlu, Salih Çolak, Mustafa Alpaslan Anayol, Pelin Yılmazbaş.

Conflict of Interest: No conflict of interest was declared by the authors.

Financial Disclosure: The authors declared that this study received no financial support.

References

1. George ND, Yates JR, Moore AT. X linked retinoschisis. Br J Ophthalmol. 1995;79:697-702.
2. Molday RS, Kellner U, Weber BH. X-linked juvenile retinoschisis: clinical diagnosis, genetic analysis, and molecular mechanisms. Prog Retin Eye Res. 2012;31:195-212.
3. Joseph E, Robertson Jr, S Martha Meyer. Hereditary vitreoretinal degenerations: Congenital hereditary retinoschisis. In: Ryan SJ, ed. Retina (1st ed). St. Louis; The CV Mosby Co; 1989:472-473.
4. Apushkin MA, Fishman GA, Janowicz MJ. Correlation of optical coherence tomography findings with visual acuity and macular lesions in patients with X-linked retinoschisis. Ophthalmology. 2005;112:495-501.
5. Sauer CG, Gehrig A, Warneke-Wittstock R, Marquardt A, Ewing CC, Gibson A, Lorenz B, Jurklies B, Weber BH. Positional cloning of the gene associated with X-linked juvenile retinoschisis. Nat Genet. 1997;17:164-170.
6. Kanski JJ, Bowling B. Hereditery Fundus Dystrophies; Juvenil X linked retinoschisis. Ken Nischal, Andrew Pearson; Clinical Ophthalmology: Systematic Approach (7th ed). Philadelphia; Elsevier Limited; 2011:15:674.
7. Xiao Y, Liu X, Tang L, Wang X, Coursy T, Guo X, Li Z. X-Linked Retinoschisis: Phenotypic Variability in a Chinese Family. Sci Rep. 2016;6:20118.
8. Gerth C, Zawadzki RJ, Werner JS, Héon E. Retinal morphological changes of patients with X-linked retinoschisis evaluated by Fourier-Domain optical coherence tomography. Arch Ophthalmol. 2008;126:807-811.
9. Gregori NZ, Berrocal AM, Gregori G, Murray TG, Knighton RW, Flynn HW Jr, Dubovy S, Puliafito CA, Rosenfeld PJ. Macular spectral domain optical coherence tomography in patients with X-linked retinoshisis. Br J Ophthalmol. 2009;93:373-378.
10. Ozdemir H, Karacorlu S, Karacorlu M. Optical coherence tomography findings in familial foveal retinoschisis. Am J Ophthalmology. 2004;137:179-181.
11. Menke MN, Feke GT, Hirose T. Effect of aging on macular fea¬tures of x-linked retinoschisis assessed with optical coherence tomography. Retina. 2011;31:1186-1192.
12. Yu J, Ni Y, Keane PA, Jiang C, Wang W, Xu G. Foveomacular schisis in juvenile X-linked retinoschisis: an optical coherence tomography study. Am J Ophthalmol. 2010;149:973-978.
13. Özdemir H, Karaçorlu S, Karaçorlu M, Şentürk F. Geç Dönem Familial Foveal Retinoskizis'de Yüksek Çözünürlüklü Optik Koherens Tomografi. Turk J Ophthalmol. 2012;42:81-83.

DOI: 10.4274/tjo.43799
Turk J Ophthalmol 2017;47:306-308

Case Report

The Diagnostic Role of Multimodal Imaging Techniques in Isolated Foveal Hypoplasia

Figen Batıoğlu, Sibel Demirel, Emin Özmert, Betül Bayraktutar, Özge Yanık
Ankara University Faculty of Medicine, Department of Ophthalmology, Ankara, Turkey

Abstract

To report a case of bilateral isolated foveal hypoplasia in which multimodal imaging was used to confirm the diagnosis. Fundus autofluorescence imaging, optical coherence tomography (OCT), and fundus fluorescein angiography were used to describe the typical findings of a patient with isolated foveal hypoplasia. Spectral domain OCT showed absence of foveal depression and persistent inner retinal layers in the fovea. Fundus autofluorescence did not reveal foveal hypoautofluorescence in the presumed foveal area. Clinical diagnosis of foveal hypoplasia may be difficult due to the subtle nature of fundus findings. Fundus autofluorescence imaging may help to diagnose these patients. Foveal hypoplasia should be considered in the differential diagnosis of absence of foveal hypoautofluorescence.

Keywords: Foveal hypoplasia, fundus autofluorescence, optical coherence tomography

Introduction

Isolated foveal hypoplasia (IFH) is a condition in which the fovea is characterized by the absence of foveal depression, pigmentation, and foveal avascular zone.[1,2,3] It may occur in isolation or in association with conditions such as albinism, aniridia, retinopathy of prematurity, achromatopsia, microphthalmus, myopia, and incontinentia pigmenti.[1,2,3,4,5] No single hereditary pattern has been established for patients with IFH. Reported cases include patients with autosomal dominant and autosomal recessive inheritance patterns as well as sporadic cases.[1,6] Some authors described the absence of genes such as *PAX6, 0CA2*, and *GPR143*, which are associated with ocular albinism in IFH.[2]

There is wide variability in clinical manifestations of the disease. In most cases, there is decreased visual acuity and an association with nystagmus, and the clinical diagnosis may be difficult due to the subtle nature of fundus findings. Optical coherence tomography (OCT) has been described as a quick and useful tool to confirm the diagnosis of IFH and a grading system based on OCT findings has been developed.[6,7] Herein, we report a case of bilateral IFH in which multimodal imaging was used to confirm the diagnosis and we describe the fundus autofluorescence (FAF) pattern.

Case Report

A 14-year old girl was referred to our department with the complaint of non-progressive reduced vision since childhood. Her family and medical history were unremarkable and she was not born prematurely. The best corrected visual acuity was 0.3 in the right eye and 0.4 in the left eye. There was no nystagmus or iris transillumination suggestive of ocular albinism in either eye. Iris and anterior chamber angle were normal with no sign of aniridia. Fundus examination revealed the absence of foveal reflex and macular pigmentation with normal appearance of optic nerve heads. Fluorescein angiography (FA) revealed the absence of capillary-free zone and the intensity of choroidal fluorescence from the macular area was similar to that from other parts of the retina. In addition, the perifoveal capillaries were abnormally close to the presumed foveal area and some

Address for Correspondence: Özge Yanık MD, Ankara University Faculty of Medicine, Department of Ophthalmology, Ankara, Turkey
Phone: +90 312 212 68 68 E-mail: oyanik05@hotmail.com **ORCID-ID:** orcid.org/0000-0002-1822-8703
Received: 04.04.2016 **Accepted:** 27.07.2016

crossed the horizontal meridian (Figure 1). Spectral domain OCT (Cirrus High Definition OCT; Carl-Zeiss Meditec) showed an absence of foveal depression and persistent inner retinal layers in the fovea (Figure 2). It also demonstrated the absence of extrusion of plexiform layers, the absence of outer segment lengthening, and the presence of outer nuclear layer widening corresponding to grade 3 foveal hypoplasia as described by Thomas et al.[7] FAF imaging did not reveal foveal hypoautofluorescence in the presumed foveal area (Figure 3).

Discussion

IFH is a rare condition in the absence of other ocular manifestations. In vitro histological examinations of foveal hypoplasia showed that the retina at the posterior pole remained at the stage of differentiation normally exhibited in the sixth month in utero.[5] Thomas et al.[7] developed a grading system according to the presence or absence of foveal pit and widening of the outer nuclear layer and lengthening of outer segment at the fovea. The grading system may also show at which stage foveal development was arrested. Our patient exhibited grade 3 foveal hypoplasia according to this system. As reported previously, capillaries which crossed the horizontal meridian and an absence of capillary avascular zone were noted on FA imaging.[1,5,8,9] However, in contrast to many other case reports, our patient did not present with nystagmus. We used multimodal retinal imaging systems for in vivo confirmation of the diagnosis of foveal hypoplasia.

Previous reports have described a FAF pattern in foveal hypoplasia.[1,9] In the present case, FAF imaging did not show the typical foveal darkening due to absence of the macular pigments and we observed similar autofluorescence at the macular area compared with peripheral parts of the fundus. We concluded that this phenomenon may be related to the amount of macular pigment in the fovea. This is supported by Charbel Issa et al.,[9] who reported that the usual foveal attenuation of

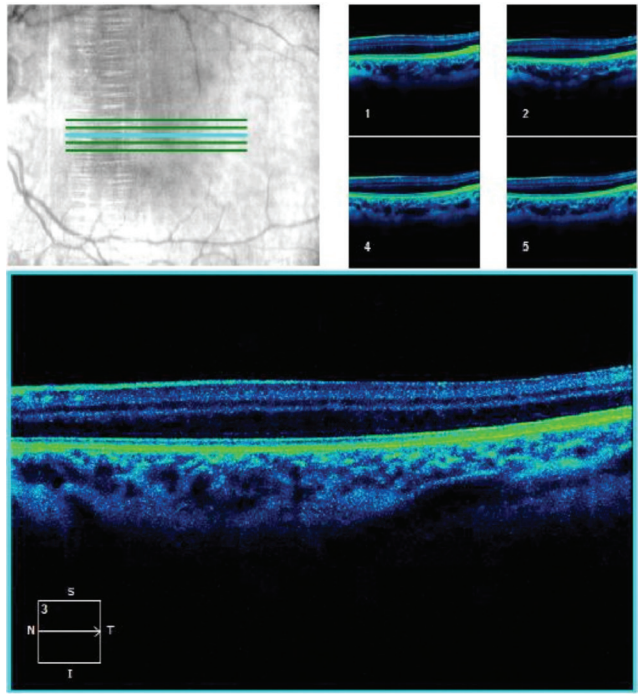

Figure 2. Spectral domain optical coherence tomography showed an absence of foveal depression and persistent inner retinal layers in the fovea

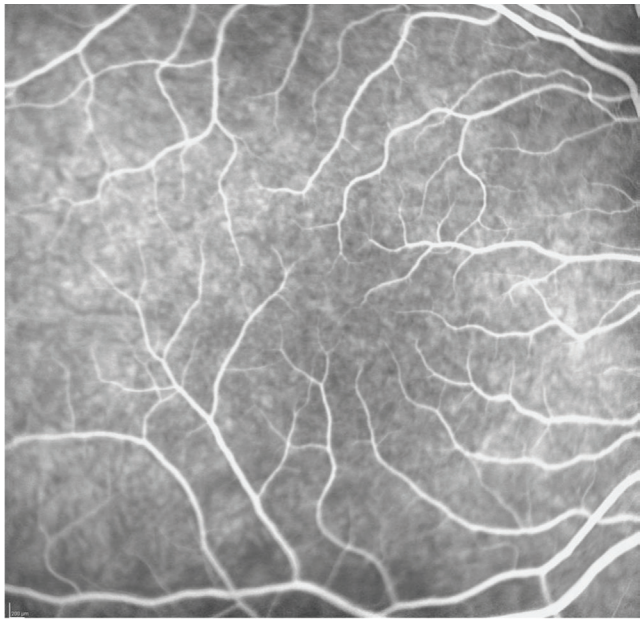

Figure 1. Perifoveal capillaries were abnormally close to the presumed foveal area, with some crossing the horizontal meridian

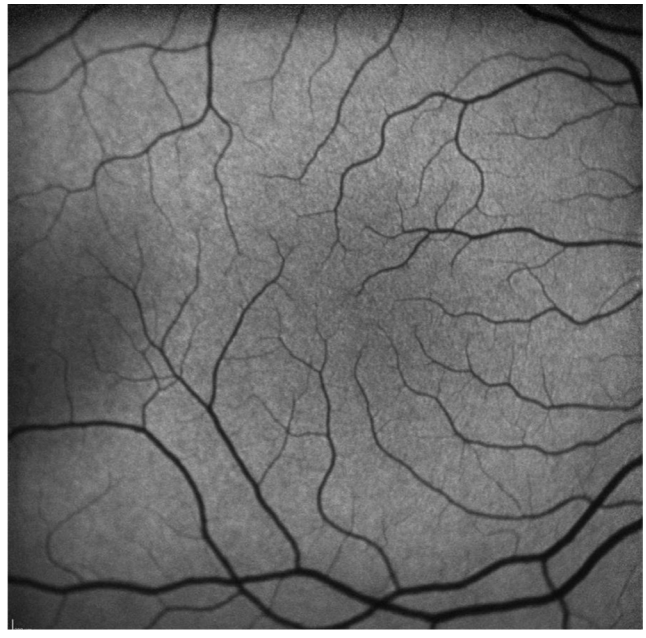

Figure 3. Fundus autofluoresce imaging did not reveal foveal hypoautofluorescence in the presumed foveal area

FAF by macular pigment is reduced in these patients. Mota et al.[1] also reported a lack of foveal darkening in one patient and only slightly reduced foveal attenuation of autofluorescence in their other foveal hypoplasia cases. However, visual acuity was better in their first patient despite a lack of normal foveal depression as well as lack of foveal darkening on FAF image. In contrast to this report, Charbel Issa et al.[9] reported that reduced foveal darkening was more pronounced in their second patient, who had worse visual acuity, and they speculated that macular pigment density correlated with the anatomical and functional integrity of the fovea in patients with foveal hypoplasia. In accordance with this previous report, this finding was prominent in our patient, who had low visual acuity and severely disorganized macular anatomy.

Although SD-OCT, a quick and non-invasive method, is helpful in the diagnosis of foveal hypoplasia,[6,7] especially in patients with decreased visual acuity, the clinical diagnosis may be difficult due to the subtle nature of fundus findings. FAF imaging may also help to diagnose these patients. Foveal hypoplasia should be considered in the differential diagnosis of absence of foveal hypoautofluorescence.

Ethics

Informed Consent: It was taken.

Peer-review: Externally peer-reviewed.

Authorship Contributions

Surgical and Medical Practices: Figen Batıoğlu, Sibel Demirel, Emin Özmert, Concept: Figen Batıoğlu, Sibel Demirel, Emin Özmert, Betül Bayraktutar, Özge Yanık, Design: Figen Batıoğlu, Sibel Demirel, Emin Özmert, Betül Bayraktutar, Özge Yanık, Data Collection or Processing: Figen Batıoğlu, Sibel Demirel, Emin Özmert, Betül Bayraktutar, Özge Yanık, Analysis or Interpretation: Figen Batıoğlu, Sibel Demirel, Emin Özmert, Betül Bayraktutar, Özge Yanık, Literature Search: Figen Batıoğlu, Sibel Demirel, Emin Özmert, Betül Bayraktutar, Özge Yanık, Writing: Figen Batıoğlu, Sibel Demirel, Emin Özmert, Betül Bayraktutar, Özge Yanık.

Conflict of Interest: No conflict of interest was declared by the authors.

Financial Disclosure: The authors declared that this study received no financial support.

References

1. Mota A, Fonseca S, Carneiro A, Magalhães A, Brandão E, Falcão-Reis F. Isolated foveal hypoplasia: tomographic, angiographic and autofluorescence patterns. Case Rep Ophthalmol Med. 2012;2012:864958.
2. Al-Saleh AA, Hellani A, Abu-Amero KK. Isolated foveal hypoplasia: report of a new case and detailed genetic investigation. Int Ophthalmol. 2011;31:117-120
3. Vedantham V. Isolated foveal hypoplasia detected by optical coherence tomography. Indian J Ophthalmol. 2005;53:276-277.
4. Querques G, Prascina F, Iaculli C, Delle Noci N. Isolated foveal hypoplasia. Int Ophthalmol. 2009;29:271-274.
5. Oliver MD, Dotan SA, Chemke J, Abraham FA. Isolated foveal hypoplasia. Br J Ophthalmol. 1987;71:926-930.
6. Saffra N, Agarwal S, Chiang JP, Masini R, Bertolucci A. Spectral-domain optical coherence tomographic characteristics of autosomal recessive isolatedfoveal hypoplasia. Arch Ophthalmol. 2012;130:1324-1327.
7. Thomas MG, Kumar A, Mohammad S, Proudlock FA, Engle EC, Andrews C, Chan WM, Thomas S, Gottlob I. Structural grading of foveal hypoplasia using spectral-domain optical coherence tomography a predictor of visual acuity? Ophthalmology. 2011;118:1653-1660.
8. McGuire DE, Weinreb RN, Goldbaum MH. Foveal hypoplasia demonstrated in vivo with optical coherence tomography. Am J Ophthalmol. 2003;135:112-114.
9. Charbel Issa P, Foerl M, Helb HM, Scholl HP, Holz FG. Multimodal fundus imaging in foveal hypoplasia: combined scanning laser ophthalmoscope imaging and spectral-domain optical coherence tomography. Arch Ophthalmol. 2008;126:1463-1465.

2017 INTERNATIONAL CONGRESSES

Euretina 2017
7-10 September 2017, Barcelona, Spain

2017 ESA/AAPOS Joint Meeting
13-16 September 2017, Porto, Portugal
http://esa2017.com

EVER 2017
27-30 September 2017, Nice, France

ESCRS
7-11 October 2017, Lisbon, Portugal
http://www.escrs.org/

An International Perspective of Pediatric Ophthalmology and Strabismus AAPOS/CAPOS Joint Meeting
12-15 October 2017, Shanghai, China

AAO
11-14 November 2017, New Orleans, LA, USA
http://www.aao.org/annual-meeting

2017 NATIONAL CONGRESSES

TOA Summer Symposium
22-24 September 2017, İzmir, Turkey

TOA 51th National Congress
24-29 October 2017, Antalya, Turkey

TURKISH
JOURNAL OF
OPHTHALMOLOGY
TJO

www oftalmoloji org

Avrupa Konutları Kale, Maltepe Mah. Yedikule Çırpıcı Yolu Sk.9.Blok No:2 Kat.1 Ofis:1 Zeytinburnu-İstanbul-Turkey
Phone: +90 212 801 44 36 -37 Fax: +90 212 801 44 39 E-mail: dergi@oftalmoloji.org

Copyright Transfer Form

Corresponding author:.....

Registered number:.....

Title of Article:.....

We, the undersigned authors, accept that the Turkish Journal of Ophthalmology bears no responsibility for the manuscript concerned prior to its acceptance to the Journal. We guarantee that the submitted paper is original, has not previously been published in any other journal, and that, in the event that it is accepted for publication, in whole or in part, the Turkish Journal of Ophthalmology has obtained all permission necessary for publication, and the original copyright form has been submitted to the responsible directorship of publication of the Turkish Journal of Ophthalmology. By signing this form, we transfer copyright of the manuscript to the Turkish Journal of Ophthalmology.

The Turkish Journal of Ophthalmology follows the criteria defined by the International Committee of Medical Journal Editors for authorship of scientific articles; we hereby acknowledge the requirement that each and every person listed in this work should have made a considerable contribution during the creation of this work (such as study design; gathering, analyzing and interpreting the data; or in the writing and scientific review of the article). By signing the Copyright Transfer Form, we hereby declare that all persons identified within the list of authors below have fulfilled the above-mentioned criteria. The authors reserve the following rights.

Note: When used as stated above, a complete reference should be given indicating that the manuscript has been published in the Turkish Journal of Ophthalmology.

1. All proprietary rights, apart form copyright, such as patent rights, etc.
2. The right to use the manuscript in whole or in part in any future work such as books and lectures, free of charge.
3. The right to copy the manuscript for personal use, provided it is not offered for sale.

All authors sign as follows

Name - Surname.....Signature..... Date .....

Name - Surname.....Signature..... Date .....

Name - Surname.....Signature..... Date .....

Name - Surname.....Signature..... Date .....

Name - Surname.....Signature..... Date .....

Name - Surname.....Signature..... Date .....

Name - Surname.....Signature..... Date .....

Name - Surname.....Signature..... Date .....

Address for Correspondence:

Phone: Fax: E-mail:

This form should be filled out completely, including original signatures, scanned and submitted electronically together with your manuscript.
If you are unable to upload the file, e-mail it as an attachment to dergi@oftalmoloji.org within three days of manuscript submission.

Distance Visual Acuity Measurements Equivalency Table

						Spatial Frequency
ETDRS Standard Line Number	**Qualitative Measurements**	**Decimal**	**Snellen**	**LogMAR**	**Angle of Resolution**	**Cycle per Degree**
-3		2.00	20/10	-0.30	0.5	60.00
-2		1.60	20/12.5	-0.20	0.625	48.00
-1		1.25	20/16	-0.10	0.8	37.50
0		1.00	20/20	0.00	1	30.00
		0.90		0.05		27.00
1		0.80	20/25	0.10	1.25	24.00
		0.70		0.15		21.00
2		0.63	20/32	0.20	1.6	18.75
		0.60		0.22		18.00
3		0.50	20/40	0.30	2	15.00
4		0.40	20/50	0.40	2.5	12.00
		0.30		0.52		9.00
5		0.32	20/63	0.50	3.15	9.52
6		0.25	20/80	0.60	4	7.50
7		0.20	20/100	0.70	5	6.00
8		0.16	20/125	0.80	6.25	4.80
9		0.13	20/160	0.90	8	3.75
10	CF from 6 m	0.10	20/200	1.00	10	3.00
11	CF from 5 m	0.08	20/250	1.10	12.5	2.40
12	CF from 4 m	0.06	20/320	1.20	16	1.88
13	CF from 3 m	0.05	20/400	1.30	20	1.50
14		0.04	20/500	1.40	25	1.20
15	CF from 2 m	0.03	20/640	1.51	32	0.94
16		0.025	20/800	1.60	40	0.75
17		0.020	20/1000	1.70	50	0.60
18	CF from 1 m	0.016	20/1250	1.80	62.5	0.48
21	CF from 50 cm	0.008	20/2500	2.10	125	0.24
31	HM from 50 cm	0.0008	20/25000	3.10	1250	0.02

Abbreviations:
CF: Counting fingers, HM: Perception of hand motions, m= meter, cm= centimeter

Equations of conversions for Microsoft Excel:
- Log10 (Decimal Acuity)= LogMAR Equivalent
Power (10; -Logmar Equivalent)= Decimal Acuity (for English version of Microsoft Excel)
Kuvvet (10; -Logmar Equivalent)= Decimal Acutiy (for Turkish version of Microsoft Excel)

Reference
Eğrilmez S, Akkın C, Erakgün T, Yağcı A. Standardization in evaluation of visual acuity and a comprehensive table of equivalent. Turk J Ophthalmol. 2002;32:132-136.

Near Visual Acuity Measurements Related Equivalency Table*														
Snellen	**20/400**	**20/320**	**20/250**	**20/200**	**20/160**	**20/125**	**20/100**	**20/80**	**20/63**	**20/50**	**20/40**	**20/32**	**20/25**	**20/20**
Decimal	0.05	0.063	0.08	0.10	0.125	0.16	0.20	0.25	0.32	0.40	0.50	0.63	0.80	1.00
Jaeger	J19	J18	J17	J16	J15	J14	J13	J11	J9	J7	J5	J3	J2	J1
Times New Roman Point	60	48	36	30	24	18	14	12	10	8	6	5	4	3
LogMAR	1.3	1.2	1.1	1.0	0.9	0.8	0.7	0.6	0.5	0.4	0.3	0.2	0.1	0.0

*Adapted from Rabbets RB: Visual acuity and contrast sensitivity. In: Rabbets RB, editör. Clinical visual optics. Edinburgh: Butterworth-Heinemann, 1998:19-61.

TURKISH JOURNAL OF OPHTHALMOLOGY

TJO

www.oftalmoloji.org

EDITORIAL

OCT (SD-OCT) to evaluate vascular changes in patients with idiopathic macular telangiectasia type 2 (MacTel 2). They report that OCTA provides data important both for understanding the pathogenesis of MacTel 2 and for patient follow-up, allowing clear observation of changes in the deep vascular plexus in early disease and choroidal neovascularization in later disease stages, unlike fundus fluorescein angiography. The authors also note that en face flow maps should be evaluated together with B-scan SD-OCT images to achieve optimal results in clinical practice (see pages 279-284).

Barut Selver et al. have reviewed the current topic of limbal stem cell failure and its treatment with stem cell transplantation. They report that blindness due to corneal vascularization and opacification arising from loss of limbal stem cell function from any primary or secondary cause accounts for about 10% of all blindness worldwide. The authors emphasize that the most effective treatment option for this pathology is to transplant tissue containing sufficient amounts of stem cells, leading to the development of various techniques to preserve and expand stem cells in culture. Of these techniques, they report that expansion of limbal biopsies as explant cultures on a biocompatible material (preferably human amniotic membrane) and the surgical transplantation of this tissue is the most successful and commonly used method (see pages 285-291).

In the first case report of this issue, Ecel et al. share the case of a 7-year-old girl who was diagnosed with asymptomatic nephropathic cystinosis when pathognomonic white crystals were detected in the cornea during a routine eye examination. Cystinosis is a metabolic disease that causes the accumulation of cystine crystals throughout the body and most commonly affects the eyes and kidneys. The authors point out that asymptomatic cystinosis can be diagnosed by anterior segment examination, especially during routine eye examination, and emphasize the important responsibility ophthalmologists have in preventing future kidney failure by enabling early treatment with cysteamine (see pages 292-295).

Swimming goggles and diving masks are necessary to resolve the refraction problem between the eye/water interface so that we can see clearly underwater. Ergözen describes a patient with subconjunctival hemorrhage associated with ocular barotrauma resulting from the use of swimming goggles during breath-hold diving, and presents preventative measures that can be taken to avoid this traumatic side effect of pressure changes while diving (see pages 296-297).

Dikkaya et al. present the fluorescein angiography, fundus autofluorescence, OCT, and electrophysiological test results in a rare case of posterior polar choroidal dystrophy. Fundus examination revealed bilateral atrophy of the retinal pigment epithelium and choriocapillaris between the vascular arcades and surrounding the optic disc, which appeared as hypoautofluorescence on fundus autofluorescence imaging. Atrophy of the choriocapillaris and outer retinal layers were evident on OCT, photopic and scotopic responses were attenuated on flash electroretinography (ERG), and responses were also minimal in pattern and multifocal ERG (see pages 298-301).

Doğuizi et al. evaluated the SD-OCT findings of three cases of X-linked juvenile retinoschisis (XLRS). XLRS is an retinal dystrophy characterized by splitting of the neurosensory retinal layers and X-linked recessive inheritance. The authors discussed the common bicycle spoke wheel appearance of the macula on fundus examination and typical SD-OCT findings of retinal splitting, emphasizing that this makes SD-OCT an important imaging method that provides more detailed information about XLRS (see pages 302-305).

In the final case report, Batıoğlu et al. present a case of bilateral isolated foveal hypoplasia in which multimodal imaging techniques were used to confirm the diagnosis. In this report, the authors indicate that clinical diagnosis of foveal hypoplasia may be difficult due to the subtle nature of fundus findings, while SD-OCT reveals loss of the foveal depression and continuity of the inner retinal layers at the fovea. They also emphasized that fundus autofluorescence imaging has emerged as an auxiliary diagnostic technique by showing loss of foveal hypoautofluorescence in the presumed foveal area (see pages 306-308).

Respectfully on behalf of the Editorial Board,

Tomris Şengör, MD